Different *EML4-ALK* fusion variants and novel *ALK* resistance mutations induce differential sensitivity to ALK kinase inhibitors

Inaugural-Dissertation

zur

Erlangung des Doktorgrades

Dr. rer. nat.

der Fakultät für

Biologie

an der

Universität Duisburg-Essen

vorgelegt von

Johannes Martin Heuckmann

aus Bergisch-Gladbach

April 2012

Die der vorliegenden Arbeit zugrunde liegenden Experimente wurden am Max-Planck-Institut für neurologische Forschung in Köln durchgeführt.

1. Gutachter: Prof. Ralf Küppers
2. Gutachter: Prof. Roman K Thomas

Vorsitzender des Prüfungsausschusses:

Prof. Shirley Knauer

Tag der mündlichen Prüfung:

12.06.2012

for Laura

Table of contents:

Abbreviations

ABL	c-abl oncogene 1
ADCY3	adenylate cyclase 3
AKT	v-akt murine thymoma viral oncogene homolog 1
ALK	anaplastic lymphoma kinase
Asp	aspartic acid
ATP	Adenosine-5'-triphosphate
BAC	bacterial artificial chromosomes
BCR	breakpoint cluster region
bp	basepair
BRAF	v-raf murine sarcoma viral oncogene homolog B1
cAMP	3'-5'-cyclic adenosine monophosphate
CDKN2A	cyclin-dependent kinase inhibitor 2A
cDNA	copy DNA
CML	chronic myelogenous leukemia
CRAF	v-raf-1 murine leukemia viral oncogene homolog 1
CREB	cAMP responsive element binding protein 1
CS	calf serum
DMEM	Dulbecco's Modified Eagle's Medium
DMSO	Dimethyl sulfoxide
DNA	Deoxyribonucleic acid
Dtk	TYRO3 protein tyrosine kinase
e.v.	empty vector
EGF	epidermal growth factor
EGFR	epidermal growth factor receptor
EML4	echinoderm microtubule associated protein like-4
ENU	N-etyl-N-nitrosourea
EphB2	ephrin receptor B2
ERBB2	v-erb-b2 erythroblastic leukemia viral oncogene homolog 2
ERBB4	v-erb-a erythroblastic leukemia viral oncogene homolog 4
ERK	mitogen-activated protein kinase 1 (MAPK)
ESRP1	epithelial splicing regulatory protein 1
FCS	fetal calf serum
FDA	U.S. Food and Drug Administration
FGFR3	fibroblast growth factor receptor 3
FISH	Fluorescence in situ hybridization
Flt-3	fms-related tyrosine kinase 3
GDP	Guanosindiphosphat
Gly	glycine
GTP	Guanosintriphosphat
GW	gateway

HSP90	heat shock protein 90kDa alpha
IL-3	interleukine-3
IMT	inflammatory myofibroblastic tumour
kDa	kilo Dalton
KIF5b	kinesin family member 5B
KIT	v-kit Hardy-Zuckerman 4 feline sarcoma viral oncogene homolog
KLC1	kinesin light chain 1
KRAS	Kirsten rat sarcoma viral oncogene homolog
LOH	loss of heterozigosity
MAP3K8	mitogen-activated protein kinase kinase kinase 8
MEK1	mitogen-activated protein kinase kinase 1 (MAP2K1)
MET	met proto-oncogene (hepatocyte growth factor receptor)
MSP-R	macrophage stimulating 1 receptor
mTOR	mechanistic target of rapamycin
MuSK	muscle, skeletal, receptor tyrosine kinase
NPM1	nucleophosmin
NRAS	neuroblastoma RAS viral (v-ras) oncogene homolog
NSCLC	non-small cell lung cancer
P/S	penicillin/streptomycin
p14ARF	protein 14 alternative reading frame
p16INK4	protein 16 inhibitor of CDK4
PBS	phosphate buffered saline
PCR	polymerase chain reaction
PDGFR	platelet-derived growth factor receptor
Phe	phenylalanine
PI3K	phosphoinositide-3-kinase
PIK3CA	phosphoinositide-3-kinase, catalytic, alpha polypeptide
PKA	protein kinase A
PTB	phosphotyrosine-binding domain
PTEN	phosphatase and tensin homolog
puro	puromycin
RAF1	v-raf-1 murine leukemia viral oncogene homolog 1
RANBP2	RAN binding protein 2
RAS	rat sarcoma viral oncogene homolog
RB1	retinoblastoma 1
RET	ret proto-oncogene
RNA	Ribonucleic acid
ROS1	c-ros oncogene 1
RPMI	Roswell Park Memorial Institute 1640 (cell culture medium)
RSV	Rous sarcoma virus
RT-PCR	reverse transcription PCR
RTK	receptor tyrosine kinase
SCLC	small cell lung cancer

SEM	standard error of the mean
SH-2	Src homology 2
SOS1	son of sevenless homolog 1
SRC	sarcoma (Schmidt-Ruppin A-2) viral oncogene homolog
TBS	tris buffered saline
TERT	telomerase reverse transcriptase
TFG	TRK-fused gene
Tie-2	TEK tyrosine kinase, endothelial
TKI	tyrosine kinase inhibitor
TP53	tumor protein p53
VEGF	vascular endothelial growth factor
WHO	World Health Organization

The international system of units (SI units) was used in this thesis.

The results of this dissertation are included in the following publications:

Heuckmann JM, Balke-Want H, Malchers F, Peifer M, Sos ML, Koker M, Meder L, Lovly CM, Heukamp LC, William Pao W, Thomas RK. Differential protein stability and ALK inhibitor sensitivity of EML4-ALK fusion variants. Clin Cancer Res. under review

Heuckmann JM, Hölzel M, Sos ML, Heynck S, Balke-Want H, Koker M, Peifer M, Weiss J, Lovly CM, Grütter C, Rauh D, Pao W, Thomas RK. ALK mutations conferring differential resistance to structurally diverse ALK inhibitors. Clin Cancer Res. 2011 Dec 1;17(23):7394-401. Epub 2011 Sep 26. PubMed PMID: 21948233.

In addition, most figures in this dissertation were used in these publications.

1 Introduction

1.1 Cancer

Cancer is one of the most deadly diseases of mankind. Even though, diseases of the cardiovascular system currently have a higher mortality rate, intensive research allowed a steady decrease of cardiovascular related mortality in the last decades. In contrast, only minimal success has been achieved in treating cancer (http://www.dkfz.de/de/krebsatlas/gesamt/mort_2.html). In the US, cancer is the leading cause of death in the population younger than 85 years (Jemal et al., 2010). However, it must be pointed out, that several cancer types (e.g. chronic myeloid leukemia) have undergone a therapeutic revolution, whereas the 5-year overall survival of other cancer types (e.g. head and neck cancer) remained almost unchanged for the last decades (Carvalho et al., 2005; Druker et al., 2006; Gambacorti-Passerini et al., 2011).

1.2 Lung cancer

1.2.1 Epidemiology

With the highest incidence rate of all cancer types, lung cancer accounts for more than 1.5 million new cases and more than 1.3 million deaths worldwide each year (http://globocan.iarc.fr/; data from 2008). Accordingly, lung cancer is the leading cause of cancer related deaths, with a five-year survival rate of only 14% (http://www.who.int/tobacco/research/cancer/en/). In 2008, almost 30,000 men and 13,000 women died from lung cancer in Germany. Here, whilst the number of lung cancer related deaths in men has decreased during the last 20 years, lung cancer related mortality in women is steadily increasing since more than 50 years (http://www.dkfz.de/de/krebsatlas/gesamt/mort_6.html). The main reason for this phenomenon is thought to be the increasing number of female smokers.

1.2.2 Histology

Lung cancer can be divided into two major subtypes based on histopathological characteristics: non-small cell lung cancer (NSCLC) and small cell lung cancer (SCLC) (Petersen, 2011).

SCLC accounts for 15-20% of all lung cancer cases and is characterized by aggressive growth and small tumor cell size. SCLC arises from airway bronchioles, but metastasizes early into other organs. Due to its aggressive growth, SCLC is usually only staged into limited disease (tumor restricted to one hemithorax and regional lymph node metastases) and extensive disease (several spatial distributed metastases) (Gustafsson et al., 2008; Travis and WHO, 2004).

NSCLC describes all types of epithelial lung cancers that are not SCLC and is divided into several subgroups, depending on the tissue of origin (Goldstraw et al., 2011).

- Adenocarcinoma, the most frequent form of NSCLC, accounts for 40-50% of all lung cancer cases. These tumors arise from epithelial cells that form the glandular tissue in the periphery of the alveoles.
- Squamous cell lung cancer, accounts for 30-35% of all lung cancer cases. Squamous cell carcinomas also arise from epithelial cells, but from those lining the main bronchus.
- Large cell carcinoma and more poorly differentiated, rare NSCLC subtypes.

NSCLC is staged by the TNM classification of malignant tumors. The composition of T (tumor size and invasiveness), N (infestation of regional lymph nodes) and M (distant metastasis) defines the tumor stage (stage 0 – IV) and the appropriate treatment (http://www.cancerstaging.org/).

1.2.3 Development

Smoking is the most important risk factor for the development of lung cancer, with 80-90% of all lung cancers being caused by tobacco smoke exposure (Khuder, 2001). Especially the development of squamous and small cell lung cancer is highly correlated with this risk factor. One likely reason for this is that these two lung cancer subtypes arise from areas in the lung highly exposed to inhaled air. Even though, smoking is the

most important risk factor for lung cancer, about 20% of adenocarcinomas develop in never-smoking patients. Thus, even in never smokers, lung cancer is the seventh leading cause of cancer death worldwide. Interestingly, these tumors use different survival signaling pathways as opposed to smoking induced tumors (Sun et al., 2007). In addition to cigarette smoke, other known carcinogens by inhalation are asbestos and Radon. If cells in the lung are exposed to higher doses of these carcinogens, somatic mutations develop. Most of these mutations can be repaired by the endogenous repair mechanisms of the cell. However, if the mutation load is too high, or if the repair mechanisms do not work properly, these mutations can persist and accumulate over time. Eventually, tumor suppressor genes or oncogenes are mutated, which can affect the behavior of the cell (as it will be discussed further below) and lead to pre-invasive lesions, invasive lesions and finally metastases (Braithwaite and Rabbitts, 1999; Brambilla and Gazdar, 2009; Herbst et al., 2008; Knudson, 1971; Noguchi, 2010). For such a development in the lung, non-transformed bronchial cells need to gain several capabilities to allow the development and maintenance of an uncontrolled growing tumor. In 2000, Douglas Hanahan and Robert Weinberg identified six essential alterations in cell physiology that collectively dictate malignant growth: “self-sufficiency in growth signals, insensitivity to growth-inhibitory (antigrowth) signals, evasion of programmed cell death (apoptosis), limitless replicative potential, sustained angiogenesis, and tissue invasion and metastasis” **(Figure 1)** (Hanahan and Weinberg, 2000). In 2011, an update was published, including two emerging

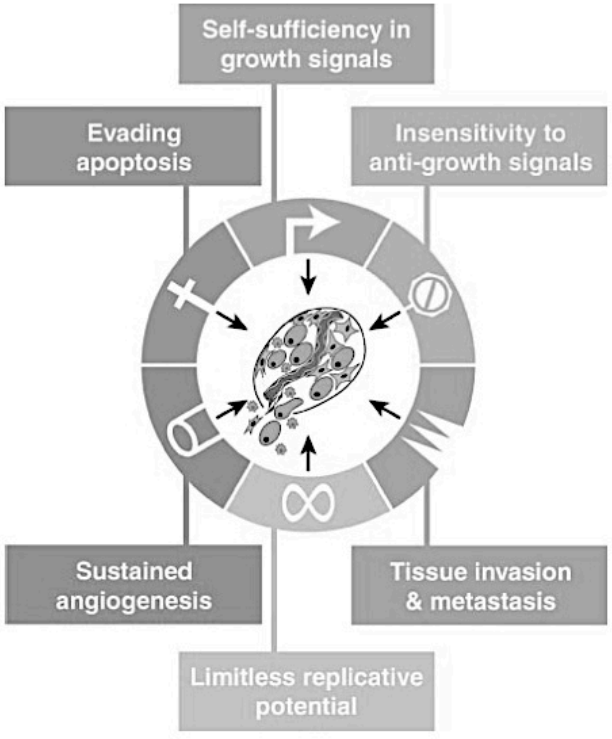

Figure 1 Set of capabilities a cancer cells needs for a completely transformed phenotype as suggested by Hanahan and Weinberg (Hanahan and Weinberg, 2000).

hallmarks, reprogramming of energy metabolism and evading immune destruction, as well as two enabling characteristics of tumor cells, namely genome instability and tumor promoting inflammation (Hanahan and Weinberg, 2011). This introduction will mainly focus on the first six hallmarks of cancer, which describe the most fundamental capabilities a cancer cell needs to acquire in order to develop a transformed phenotype.

1.2.3.1 Evading apoptosis

In the development of the human body, apoptosis is an essential mechanism to form tissues and organs (e.g. finger formation) and to sustain organ functionality (e.g. colon epithelium, T- and B-cell development etc.) (Alberts, 2002). However, apoptosis is also an important mechanism to dispose irreversibly damaged cells and can be triggered from external signals (e.g. by activation of death receptors of natural killer cells) or from internal signals (e.g. after extensive DNA damage). To prevent uncontrolled apoptosis, pro-apoptotic and anti-apoptotic proteins are tightly balanced in the normal cell. In case of an irreparable DNA damage, this balance shifts toward the pro-apoptotic proteins and thereby induces apoptosis. One of the major sentinels of the stress response is the tumor suppressor gene *TP53*. Usually locked in an inactive state in the cytoplasm, p53 becomes active upon DNA damage, hypoxia or other stress conditions. Depending on the level of DNA damage, p53 will activate the transcription of genes involved in repair mechanisms (if the damage can be fixed), or induce apoptosis (if the DNA damage is too severe to be repaired) (Kruse and Gu, 2009).

In tumor cells however, the balance of pro- and anti-apoptotic proteins is shifted towards the anti-apoptotic proteins, preventing apoptosis even in cells with a high load of DNA damage. This is often achieved by a loss of function of p53, frequently due to a mutation of the gene making TP53 the most frequently mutated gene in cancer (IARC TP53 database). In fact, 50% - 70% of NSCLC and 75% - 93% of all SCLC tumors are mutated in this gene, highlighting its importance in preventing the development of lung cancer (Herbst et al., 2008; Peifer et al., under review; Travis and WHO, 2004). Thus, even though the stress response of a damaged bronchial cell would trigger cell death, the transformed cells do not die, accomplishing the first step to become a cancer cell (Weinberg, 2007).

1.2.3.2 Self-sufficiency in growth signals

A cancer cell requires sustained chronic proliferation to form a tumor. Usually, the growth of a healthy cell is carefully controlled by growth factors secreted by neighboring cells or other tissues in the human body. After secretion, these growth factors can stimulate specific receptors on the surface or within cells. Ligand binding activates the respective receptor, triggering a cellular response specific for this growth factor (Henson and Gibson, 2006). One of the best-studied pro-proliferative pathways is the epidermal growth factor receptor (EGFR) pathway, which is activated after ligand binding to this cell surface receptor (Greulich et al., 2005; Henson and Gibson, 2006; Sharma et al., 2007). Lung adenocarcinoma cells often take advantage of this growth promoting signaling pathway by (i) uncontrolled secretion of EGFR ligands or (ii) acquiring mutations in the EGF receptor itself. In both cases the result is an uncontrolled activation of EGFR and therefore, the constitutive activation of the downstream signaling pathway (Brambilla and Gazdar, 2009; Gazdar and Minna, 2008; Greulich et al., 2005; Paez et al., 2004; Sporn and Todaro, 1980). In addition to deregulated *EGFR* signaling, mutations in *KRAS* are found in up to 40% of all adenocarcinomas of the lung, but are rare in other forms of NSCLC and SCLC (Herbst et al., 2008; Travis and WHO, 2004). Furthermore, growth-promoting mutations in the MAPK pathway, in the PI3K pathway as well as in other receptor tyrosine kinases have been described in adenocarcinomas (Ding et al., 2008; Engelman, 2007). In contrast, only a limited number of such activating mutations has been described for squamous cell carcinoma, with almost no known growth promoting mutations in SCLC (Bass et al., 2009; Peifer et al., under review; Travis and WHO, 2004; Weiss et al., 2010)

Several additional mechanisms have been described that allow tumor cells to increase the pro-proliferative signaling, without an activating mutation of an oncogene. Examples for such mechanisms are the loss of PTEN leading to the activation of the PI3K pathway and a negative feedback mechanism that induces PI3K pathway activation after pharmacological mTOR inhibition (Sos et al., 2009b; Sudarsanam and Johnson, 2010; Yuan and Cantley, 2008).

1.2.3.3 Insensitivity to anti-growth signals

As mentioned above, the growth of cells within a tissue is tightly controlled. In contrast to constantly proliferating cells as in the gut or in the skin, most cells in the human body do not proliferate after the tissue they form has developed. These cells are kept in a quiescent (G0) state by anti-growth signals, until external growth signals release the cell from these restraints. This process is controlled by tumor suppressor proteins, which negatively regulate cellular proliferation. Several tumor suppressor genes with different mechanisms of controlling proliferation have been described. One example is the retinoblastoma protein 1 (RB1), which is activated by many known external anti-growth signals, promoting its interaction with several transcription factors, and consequently altering the expression of genes that promote transition from the G0 or G1 into the S-phase of the cell cycle (Alberts, 2002; Weinberg, 2007). To evade the anti-growth signals mediated by RB1 activation, lung cancer cells universally inactivate this protein. In SCLC, *RB1* is most often inactivated by deletions or loss of function mutations. These are frequently accompanied by deletion of the remaining wild-type allele (LOH, loss of heterozygosity), making loss of *RB1* a hallmark feature of SCLC. In NSCLC, the RB1 pathway is often inactivated by inhibitory mechanisms upstream of RB1 (Knudson, 1971; Nevins, 2001; Peifer et al., under review; Travis and WHO, 2004). This can for example be achieved by loss of $p16^{INK4}$ (*CDKN2A*) activity, or the overexpression of cyclin D1 (Brambilla and Gazdar, 2009; Ding et al., 2008; Travis and WHO, 2004). *CDKN2A* is mutated in almost 40% of all lung adenocarcinomas and encodes for the RB1 and p53 regulators $p16^{INK4}$ and $p14^{ARF}$ (Brambilla and Gazdar, 2009; Ding et al., 2008).

1.2.3.4 Sustained angiogenesis

If cancer cells start to proliferate in the human body, they form a tumor mass that consists mainly of transformed cells. As soon as the tumor mass reaches the size of approximately 0.2 mm^3, the diffusion of oxygen and nutrients is not sufficient to supply the inner cells of the tumor. Therefore, new blood vessels need to pervade the tumor mass to ensure a steady nutrient and oxygen supply, a process called tumor-associated neovasculature. The best-studied growth factor to increase vascular permeability and to induce the sprouting of new blood vessels is the vascular endothelia growth factor

(VEGF) (Senger et al., 1983; Weinberg, 2007). VEGF is often secreted by cancer cells, which is thought to secure the oxygen supply of the tumor by increasing the number blood vessels penetrating the tumor mass. In lung cancer, high levels of VEGF were especially observed in non-small cell lung cancer, correlating with neovascularization within the tumor (Stefanou et al., 2004; Yuan et al., 2000). Furthermore, in NSCLC, VEGF expression has been shown to correlate with poor prognosis, arguing for an important role of VEGF in lung cancer progression (Bremnes et al., 2006; Herbst et al., 2005). However, it has been shown, that even though an inhibition of VEGF signaling decreases the number of blood vessels within the tumor and the size of the primary tumor itself, the aggressiveness of tumor cells to metastasize increases dramatically (Paez-Ribes et al., 2009). Recent findings indicate, that a combined inhibition of VEGF and MET signaling can prevent this increase in invasiveness, highlighting the importance to understand biological processes before being able to target them for the treatment of cancer (Sennino et al., 2012; Vecchiarelli-Federico et al., 2010)

1.2.3.5 Limitless replicative potential

Most cells in the human body have only a limited replication capacity. The number of possible cell divisions is defined by the length of the telomeres, which are repetitive sequences at the end of each chromosome. Each cell division leads to a loss of approximately 100 bp of telomere DNA, thus allowing the cell only a limited number of cell divisions (Counter et al., 1992). Critical shortening of the telomeres induces a DNA damage response, eventually initiating cellular senescence (losing the ability to divide) or apoptosis (Brambilla and Gazdar, 2009). To allow stem cells (cells with an unlimited replication potential; e.g. in the skin) an inexhaustible capability of cell divisions, the gene *TERT* is expressed. This gene encodes the catalytic subunit of the telomerase complex, which elongates telomeres at the end of each G2 phase and thereby prevents telomere shortening. Lung cancer cells often show an increased expression of *TERT* to prevent the telomere dependent termination of replication. A high telomerase activity has been observed in NSCLC and SCLC, allowing the tumor cells to divide indefinitely (Chen and Chen, 2011; Greider and Blackburn, 1985; Saretzki et al., 2002; Weinberg, 2007; Zhang et al., 2000).

1.2.3.6 Tissue invasion and metastasis

The three-dimensional structure of a tissue is maintained by direct interactions between the cells through adhesion proteins such as cadherins and integrins. These adhesion proteins also provide pro-survival and anti-proliferation signals, leading to the induction of apoptosis if a cell detaches from this interaction network (a process called anoikis). In the later stages of lung cancer development, tumor cells no longer depend on survival signals provided by neighboring cells. Due to the loss of E-cadherin expression, a key cell-cell adhesion molecule, these cells can leave the primary tumor mass and migrate, via the blood stream or the lymph vessel system, to any other site in the human body (Bremnes et al., 2002; Derksen et al., 2006; Kase et al., 2000). After the invasion of a distant organ, a metastasis arises, explaining the poor survival of lung cancer patients, whose tumors express low levels of E-cadherin (Bremnes et al., 2002; Fidler, 2003; Kase et al., 2000; Noguchi, 2010).

1.2.4 Treatment of lung cancer

Chemotherapy is the standard therapy for lung cancer, which, unfortunately, rarely cures the disease. Small cell lung cancer initially responds very well to chemotherapy and radiation treatment. However, almost all of these tumors develop resistance to this treatment and eventually relapse. The aggressive phenotype and the early appearance of resistance in SCLC are reflected in the five-year overall survival rate of less than 5% (Gustafsson et al., 2008). In general, compared to SCLC, NSCLC is relatively insensitive to chemotherapy. Instead, standard therapy for localized NSCLC includes surgical resection followed by chemotherapy. Unfortunately, NSCLC in advanced stages (as is the case for most diagnosed lung cancers) is already a systemic disease and cannot be surgically resected. Therefore, advanced stages are mainly treated by chemotherapy and/or radiation, although the response to these treatments is very poor (http://www.cancer.gov/cancertopics/types/lung). Depending on the stage of the tumor, five-year survival rates for NSCLC vary from almost 50% for stage IA to 1% for stage IV (www.cancer.org).

In addition to the relatively unspecific treatment options of chemotherapy and radiation, researchers have identified several genetic markers (mainly mutations) that allow a

more specific treatment of certain lung cancers. These mutations often induce the transformed state in the first place, therefore, being good markers to distinguish cancer cells from non-transformed healthy cells. In addition, several of these mutations also lead to a dependency ("oncogene addiction") of the tumor cell to the mutation-activated growth signal. Thus, inhibition of these growth signals (e.g. by a drug) induces apoptosis mainly in mutated cells. Compared to chemotherapy and radiation, side effects of these targeted therapies are less pronounced (Kwak et al., 2010; Mok et al., 2009). Unfortunately, even though a broad range of mutations has been identified so far, many transforming mutations are still unknown or cannot be specifically targeted by drugs (yet) (Herbst et al., 2008; Pao et al., 2005b).

1.3 Oncogenes and tumor suppressor genes

In 1911, Peyton Rous published a work describing a sarcoma-inducing agent found in chicken sarcomas. This agent was small (passing a fine-pore filter), was capable to multiply within the chicken tissue and induced tumors on predictable timetables (Rous, 1983). This agent later became known as the Rous sarcoma virus (RSV). The discovery of Peyton Rous allowed researchers to describe several cancer-causing viruses that were able to transform normal cells in the culture dish. More than 60 years later, Michael Bishop and Harold Varmus used a DNA probe to tag the transformation-associated viral gene in the genome of transformed cells. Surprisingly, even non-transformed chicken cells were marked by this DNA probe, with two copies per genome. This discovery revolutionized the thinking about cancer by showing that endogenous genes (proto-oncogenes) can play a role in tumor formation. Further characterization of the transforming viral oncogene *v-src* and its similar human *c-src* counterpart illustrated that minimal differences in DNA sequence are capable to convert a proto-oncogene to an transformation promoting oncogene. These discoveries paved the way for the characterization of several cellular proto-oncogenes and oncogenes in the human genome (Bishop, 1990; Varmus, 1990). After mutation of these genes, the resulting proteins gain pro-survival activity that is independent of external control and thus can induce the transformation of the cell. In addition, most oncogenes elicit an "oncogene

addicted" phenotype, describing the addiction of the tumor cell to constant activation of the respective mutated protein or signaling pathway. The most frequently mutated oncogenes in lung cancer are *EGFR*, *KRAS*, *PIK3CA*, *ERBB2* and *BRAF,* as well as translocations of *ALK, RET* and *ROS1* and amplifications of *MET* and *PDGFR* (Brambilla and Gazdar, 2009; Herbst et al., 2008; Sharma et al., 2010; Takeuchi et al., 2012).

In comparison to the activated oncogenes that act in a dominant fashion, tumor suppressor genes act as negative regulators and thereby in a recessive manner. The first tumor suppressor gene that has been discovered was the retinoblastoma gene (*RB1*), which, if mutated in both alleles, leads to the formation of retinoblastoma, a childhood eye tumor. This tumor type appears in two forms. Children without a family history of retinoblastoma usually develop a sporadic tumor in only one eye (unilateral). Children with a family history of retinoblastoma however, often develop tumors in both eyes (bilateral). In 1971, Alfred Knudsen studied the kinetics of sporadic and familial retinoblastoma and concluded, that the rate of sporadic tumors was consistent with two random genetic events, whereas the rate of familial retinoblastoma tumor development seemed to require only one single random genetic event (Knudson, 1971). Thus, children with familial retinoblastoma already carried one mutated allele of the *RB1* gene after birth, requiring only one additional mutation in the other allele for a complete loss of function of this gene. In sporadic retinoblastoma however, loss of functions for both wild-type alleles is needed for the tumor to develop. Indeed, tumor suppressor genes are either mutated in both alleles of the genome or, if only one allele is mutated, the non-mutated allele is often lost by LOH. As stated above, the RB1 pathway is also universally inactivated in lung cancer, allowing the tumor cells to escape the RB1 mediated cell cycle control.

1.3.1 Somatic mutations

Mutations describe genetic changes in the genomic DNA of a cell. These changes can be single nucleotide substitutions (point mutations), nucleotide insertions or deletions, gene fusions or genomic amplifications/deletions. If a mutation is a germ-line mutation (i.e. the mutation occurred in the germ cells), it can be detected in every cell of the

organism if transmitted to offspring. A somatic mutation however develops only in somatic cells, and is therefore not transmitted to offspring.

Several germ-line mutations have been described that increase the risk of tumor development during the lifespan of the individual. These mutations often occur in tumor suppressor genes or weak oncogenes that, even though mutated, allow the development of the organism. Other mutations might accelerate the accumulation of novel mutations (e.g. by loss of function in DNA-repair pathways) and thereby increase the risk of future cancer development (Birch et al., 2001; Ford et al., 1998; Linehan et al., 2007; Marx, 2005; Mosse et al., 2008; Thompson et al., 2005; Vasen et al., 2001).

Most cancers arise from somatic mutations, which can be defined as somatic by sequencing the tumor cells and non-transformed cells (e.g. from the skin) (Ding et al., 2008). Due to technological advances in sequencing techniques in the last decades, it is today possible to gain a comprehensive view on the genomic aberrations of cancer cells. The genomic analysis of thousands of tumors and non-transformed tissues uncovered a huge number of somatic changes in the genome of tumor cells, which, depending on tumor subtype, can vary dramatically. In general, the more the tumor cells have been exposed to carcinogens during their lifespan, the more mutations are found (Beroukhim et al., 2010; Campbell et al., 2010; Feuk et al., 2006; Peifer et al., under review; Pleasance et al., 2010). In total, several thousand mutations can be found in a tumor genome, with, depending on tumor type, only 12 to 228 causing any functional changes in proteins. If mutations outside the exome also lead to functional changes in DNA or RNA structure and thereby cause cancer is currently unknown.

Most mutations that have been found in oncogenes are restricted to certain areas or domains within the gene. A reason for this observation in kinases seems to be, that only very few amino acid changes are capable to increase the activity of the evolutionary optimized kinase. Thus, the plasticity of a kinase does not tolerate many amino acid changes without a loss in kinase activity. Tumor suppressor gene mutations however often harbor nonsense mutation (stop-codon) mutations, frame-shift mutations, or mutations that are distributed across several domains essential for a proper functioning of the protein (Harris, 1993). In either case, these mutations lead to a loss of function of the tumor suppressor. In support of this notion, frame-shift or nonsense mutations are

almost exclusively found in tumor suppressor genes (Dalgliesh et al., 2010; Ding et al., 2008; Varela et al., 2011; Yeang et al., 2008).

Although, up to 228 amino acid changing mutations are found in certain tumor types, only a few (known as “driver” mutations) lead to the transformed phenotype of the tumor cells. These “driver mutations” often occur in oncogenes and lead to an increase in protein activity that is independent of external control mechanisms. An indication for the transformation capacity of a single mutation is (i) the frequency of this mutation in tumors and (ii) *in vitro* transformation assays in the laboratory that show the transformation capacity of this mutation in an eukaryotic cell (Forbes et al., 2011; Greulich et al., 2005; Yan et al., 2009). Today, a large set of “driver mutations” across different tumor types has already been described. Careful analysis of the signaling pathways that are activated by these mutations however revealed only a limited number of pathways that seem to induce cellular transformation (Ding et al., 2008; TCGA, 2008).

1.3.2 Fusion genes

In contrast to kinases that are activated by point mutations (e.g. the L858R mutation in *EGFR*), kinases of fusion proteins are often constantly activated by a permanent homodimerization, mediated by the N-terminal fusion partner (Golub et al., 1996; McWhirter et al., 1993; Soda et al., 2007). Genomic rearrangements that lead to gene fusions can create novel proteins with new/enhanced activities. Here, the first part on the fusion gene consists of a varying number of exons from gene A and the second part of a varying number of exons from gene B. The size oft the resulting protein can vary from small (*RAF1-ESRP1*, approx. 30 kDa) to very big (*BCR-ABL*, 210 kDa) (Evans et al., 1987; Palanisamy et al., 2010). If the breakpoint leads to a frame-shift, the functionality of gene B is often compromised as it is after copy number loss or nonsense and frame-shift mutations. If the gene fusion is “in frame”, the emerging fusion protein can develop new abilities that are nonexistent in both (wild type) fusion partners.

Examples for such “in frame” fusions are translocations of *ALK*. *ALK* has been first discovered fused to nucleophosmin (NPM1) in anaplastic large-cell lymphoma, giving this gene its name (anaplastic lymphoma kinase) (Morris et al., 1994). *ALK* belongs to the insulin receptor superfamily and, in its native form, is thought to play a role in the

development and functionality of the nervous system (Palmer et al., 2009). In 2007, the first oncogenic fusion gene in lung cancer has been described, a translocation involving *ALK* (Soda et al., 2007). In lung cancer however the predominant 5'-partner of *ALK*-fusions involves echinoderm microtubule associated protein like-4 (*EML4*), with few reported cases that expressed *ALK* being fused to kinesin family member 5B (*KIF5b*), kinesin light chain 1 (*KLC1*) or the TRK-fused gene (*TFG*), which has also been described in anaplastic large-cell lymphoma (Hernandez et al., 1999; Takeuchi et al., 2009; Togashi et al., 2012). About 2-7% of lung adenocarcinomas harbor an *EML4-ALK* gene fusion, one of the first fusion genes discovered in solid tumors (Kwak et al., 2010; Soda et al., 2007). Depending on the proportion of *EML4* that is fused to the kinase domain of *ALK,* different variants develop, with variant one (v1, *EML4* exon 13 being fused to *ALK* exon 20), variant two (v2, *EML4* exon 20 being fused to *ALK* exon 20) and variants three a/b (v3a/v3b, *EML4* exon 6 being fused to *ALK* exon 20) being the most frequent fusion variants **(Figure 2)**. *EML4-ALK variant 1* is found in 33%, *EML4-ALK variant 2* in 10% and *EML4-ALK v3a/v3b* in 29% of all *EML4-ALK* positive cases (Choi et al., 2008; Sasaki et al., 2010b). All *EML4-ALK* variants harbor the coiled-coiled domain of *EML4*, which is essential for the homodimerization and thus the constitutive activation of the ALK kinase domain. In addition, almost all variants harbor exons 20-29

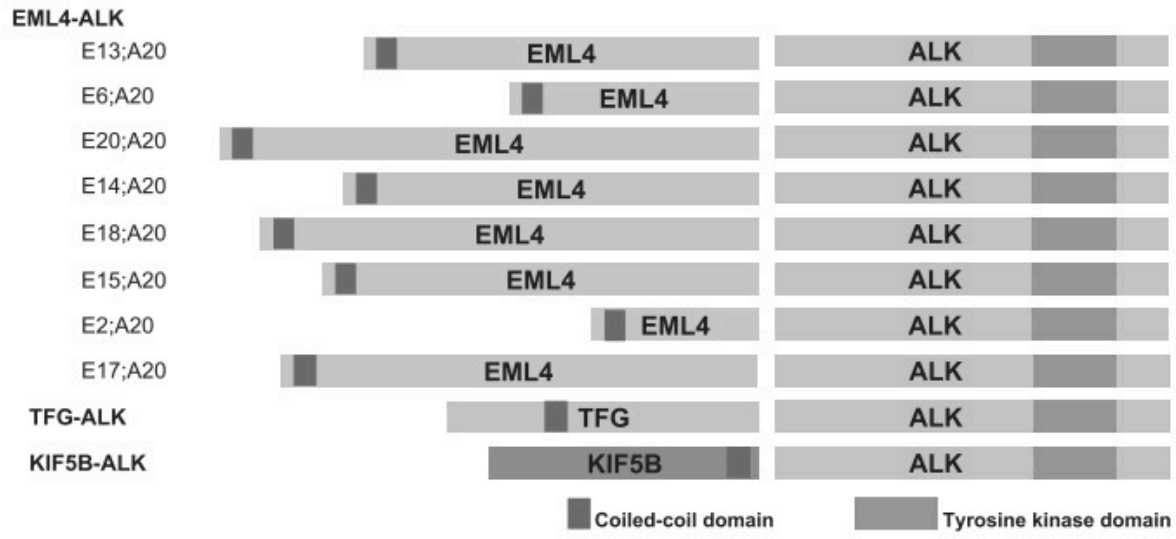

Figure 2 Schematic representation of different *EML4-ALK* variants and other *ALK* fusions that have been found in lung tumors. Domains essential for oncogenic signaling are indicated in dark gray. The nomenclature on the left refers to the respective exon in *EML4* translocated to the indicated exon in *ALK*. Figure from (Sasaki et al., 2010b).

of *ALK,* which encode the ALK tyrosine kinase domain (Doebele et al., 2012; Soda et al., 2007).

All known *EML4-ALK* fusions are oncogenic *in vitro* and/or *in vivo* and transformed cells expressing this fusion gene are sensitive to ALK kinase inhibitors (McDermott et al., 2008; Soda et al., 2007; Soda et al., 2008; Takeuchi et al., 2008). In addition to these *ALK* fusions, ALK translocations have also been described for inflammatory myofibroblastic tumors, diffuse large B-cell lymphoma and, more rarely, in breast, colon and renal cell carcinoma (Chiarle et al., 2008; Gleason and Hornick, 2008; Lin et al., 2009; Sugawara et al., 2012). Furthermore, *ALK* has also been described to be deregulated by point mutations in neuroblastoma and, rarely, in thyroid cancer (Chen et al., 2008; George et al., 2008; Janoueix-Lerosey et al., 2008; Mosse et al., 2008; Murugan and Xing, 2011; Palmer et al., 2009). These *ALK* mutations have been described to be kinase activating, and it is hoped that these *ALK* mutated tumors can (as *EML4-ALK* expressing lung tumors) be effectively treated with ALK kinase inhibitors.

1.4 Kinases

Kinases are a class of enzymes that, after activation, regulate many biological processes by transferring a phosphate group from adenosine-5'-triphosphate (ATP) to a hydroxyl group of serine, threonine or tyrosine on the substrate. The bulky and charged phosphate group alters the properties of the substrate protein by changing the conformation, charge, molecular weight and association capacity of the protein. The transfer of the phosphate group takes place in a highly conserved catalytic subunit of the protein that binds ATP and catalyzes the transfer of the terminal γ-phosphate to a kinase specific substrate. This catalytic subunit is located in a deep cleft between the N-lobe and the C-lobe of the kinase, a region defined by a conserved helix-C, a conserved sequence motif (GXGXXG) containing glycine-rich loop and an activation loop with the DFG (Asp-Phe-Gly) motif. In most kinases, a lysine residue buried in the interlobe cleft (K72 in Figure 3) and a glutamic acid in helix-C (E91 in Figure 3) arrange the ATP molecule for catalysis **(Figure 3)** (Huse and Kuriyan, 2002).

Depending on the substrate residue that is phosphorylated, kinases are subdivided in tyrosine kinases and serine/threonine kinases. Tyrosine kinases can be further subdivided into receptor tyrosine kinases and cytoplasmic kinases. Receptor tyrosine kinases transfer external signals into the cell, whereas cytoplasmatic kinases transmit and enhance signals within the cell.

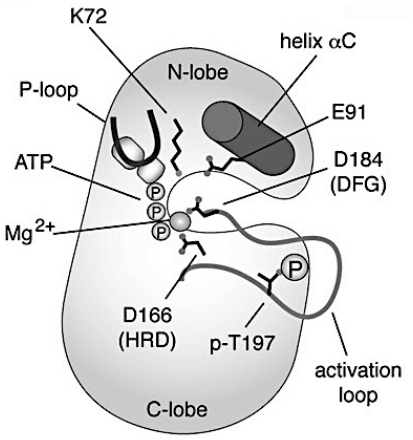

Figure 3 Schematic model of critical components of a kinase domain. The activated kinase domain of protein kinase A (PKA) is shown. Figure from (Jura et al., 2011).

Receptor tyrosine kinases (RTKs) are transmembrane proteins that bind specific ligands on the extracellular end of the receptor and transmit the signal through the plasmamembrane into the cytoplasm of the cell (e.g. *EGFR*). In the case of EGFR, the RTK can be found as inactive monomer or dimer **(Figure 4 left)**. Ligand binding to specific extracellular ligand-binding domains induces changes in the three-dimensional structure of the RTK, leading to the formation of an asymmetric dimer, which is stabilized by the association of two juxtamembrane domains. In this asymmetric dimer, the C-lobe of one kinase domain binds to the N-lobe of the other kinase domain, thereby stabilizing the active conformation of this kinase **(Figure 4 middle)** (Endres et al., 2011; Schlessinger, 2002). The activation of this kinase is defined by an inward directed formation of the DFG-motif ("DFG-in") and leads to an autophosphorylation of the C-terminus of EGFR, allowing the association of several Src homology 2 (SH-2) and phosphotyrosine-binding (PTB) domain containing downstream effector molecules **(Figure 4 right)**. These adaptor proteins then activate downstream signaling cascades by triggering the assembly of signaling complexes with additional multidomain binding partners. The intracellular multi-step transduction leads to an amplification of the initial signal which eventually results in the stimulation of cellular proliferation (Schlessinger and Lemmon, 2003). Non-receptor tyrosine kinases, or cytoplasmic kinases, are intracellular kinases, activated by specific stimuli, which are then transmitted via substrate phosphorylation to proteins downstream in the signaling pathway (e.g. *ABL1*).

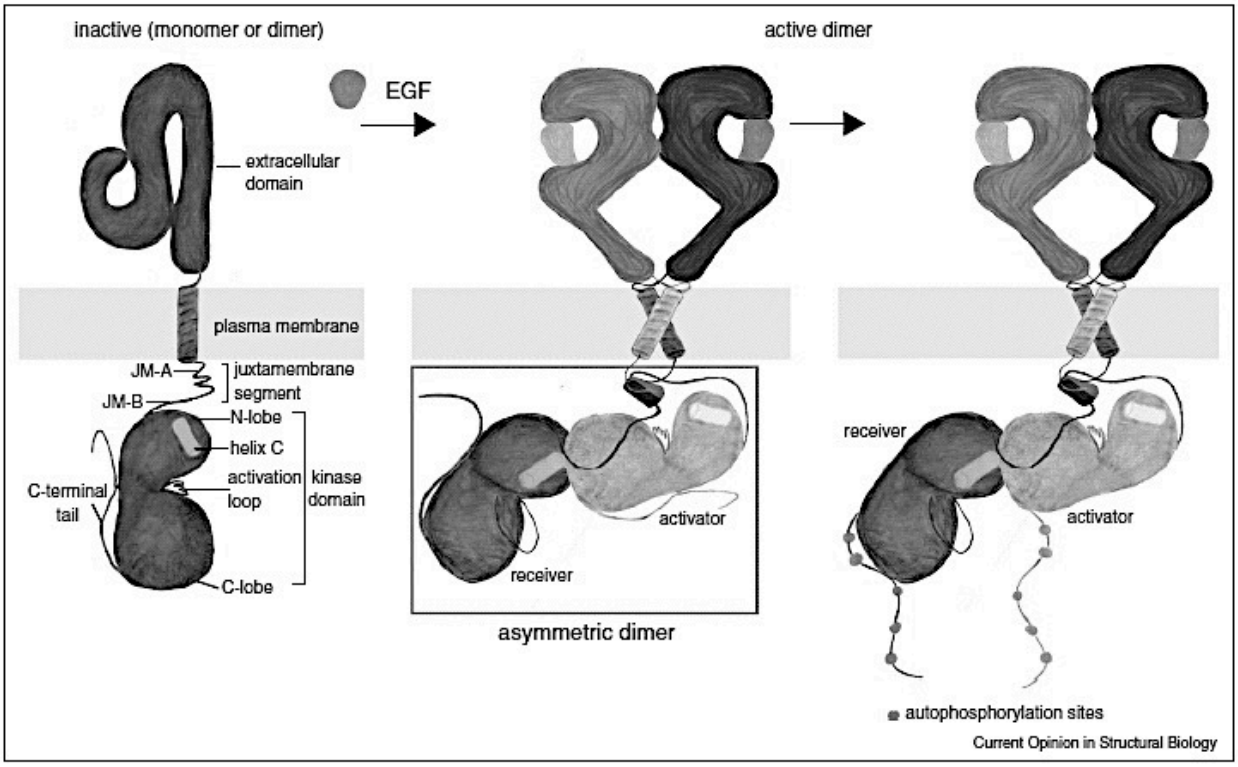

Figure 4 Schematic model of EGF receptor activation. After binding to EGF, the kinase domains of two EGFR proteins form an asymmetric dimer, which allows the autophosphorylation of the kinase (middle). Phosphorylated tyrosine residues at the C-terminal of the receptor serve as adaptor sites for several downstream signaling proteins (right). Figure from (Endres et al., 2011).

Mutations in tyrosine kinases have been found in many tumor genomes, with several of them being “driver mutations”. About 90 tyrosine kinases have been described in the human genome, with the most studied tyrosine kinases including the epidermal growth factor receptor (*EGFR*) and the Abelson tyrosine-protein kinase (*ABL1*) (Chmielecki et al., 2010; Druker et al., 2001; Lynch et al., 2004; Paez et al., 2004). In the case of *EGFR*, the most frequent mutations are deletions of amino acids 746-750 in exon 19 and point mutations in exon 21. Both mutations lead to a constant kinase activation, independently of ligand binding (Greulich et al., 2005; Yuza et al., 2007). Oncogenic activation of the Abl kinase is, in contrast to EGFR, mainly achieved by a translocation between chromosome 9 and 22 leading to the well-known “Philadelphia chromosome” (described in 1960 by Peter Nowell and David Hungerford in Philadelphia, USA). The Philadelphia chromosome is found in 95% of all chronic myelogenous leukemias (CML) as well as (to a lower extent) in acute lymphoblastic leukemia and acute myelogenous

leukemias (Kurzrock et al., 1987; Nowell and Hungerford, 1960). This translocation leads to a constant homodimerization of the fusion protein, which disrupts the autoinhibited conformation of Abl and thereby leads to a continuous activation of the tyrosine kinase (McWhirter et al., 1993; Smith et al., 2003). In EML4-ALK, the kinase domain of ALK becomes independent of ligand activation by a constant homodimerization via the coiled-coiled domain of EML4 (Mano, 2008; Soda et al., 2007). In addition to these kinases that are activated by point mutation or translocation, some RTKs are known to be transforming only by overexpression of the protein (e.g. *ERBB2* and *MET*) (Di Fiore et al., 1987; Engelman et al., 2007). Here, the higher abundance of the RTK on the cell surface is sufficient to induce dimerization and kinase activation.

1.4.1 Kinase inhibitors

Kinase inhibitors are small molecules, peptides or antibodies that inhibit the catalytic activity of a kinase. Small molecule kinase inhibitors are subdivided into three different classes, depending on the binding mode of the inhibitor to the kinase. Type-I inhibitors compete with ATP to bind to the ATP-binding pocket within the kinase domain. Most of these compounds bind to the kinase by forming hydrogen bonds with the hinge region and by hydrophobic interactions, which are usually carried out by the adenine ring of ATP. If the affinity of the small molecule to the kinase is higher than that of ATP, the molecule prevents the binding of ATP to the kinase and thereby the transfer of the phosphate group to the substrate. Thus, the activation of the signaling pathway is inhibited. Type-II inhibitors also bind to the ATP binding pocket by forming hydrogen bonds with the hinge region, but extent into a hydrophobic pocket, which emerges in a “DFG-out”

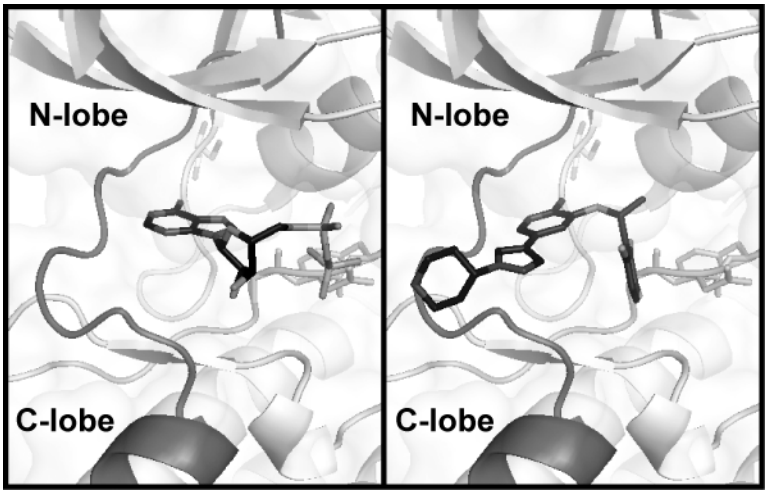

Figure 5 Crystal structure (2XP2) of the ALK kinase hinge region is shown. On the left, ADP (black sticks) is bound to the kinase; on the right, the type-II inhibitor crizotinib (black sticks) is bound to the ALK kinase domain. PyMol file was generated by Christian Grütter, TU Dortmund, Germany.

conformation and is thereby only present in the inactive kinase conformation **(Figure 5)**. Thus, Type-II inhibitors can only bind to the inactive conformation of the kinase, but have the potential to elicit higher kinase specificity due to a lower conservation of the hydrophobic ("DFG-out") pocket. Type-III inhibitors are allosteric inhibitors, which bind somewhere distant to the ATP-binding pocket. These inhibitors prevent the formation of an active kinase conformation and thereby the activation of downstream signaling proteins (Davis et al., 2011; Liu and Gray, 2006).

In 2001, imatinib was the first small molecule kinase inhibitor to receive FDA approval. Imatinib is a type-II Abl kinase inhibitor and was developed for the treatment of *BCR-ABL* expressing CML (Druker et al., 2006; Druker et al., 2001). Today, due to its "off-target" inhibition of the RTKs KIT and PDGFR, imatinib is approved for the treatment of several cancer types including gastrointestinal stromal tumors and chronic eosinophilic leukemia (Demetri et al., 2002; Piccaluga et al., 2007).

1.4.1.1 EGFR kinase inhibitors

In 2004, *EGFR* mutations were discovered in lung tumors that responded well to the EGFR inhibitor gefitinib (Lynch et al., 2004; Paez et al., 2004; Pao et al., 2004). Gefitinib and erlotinib, EGFR inhibitors with similar binding modes, are small molecules (mol. Mass ≈ 400 g/mol) that bind to the hinge region of the ATP-binding cleft and compete with ATP for binding to the active kinase domain of EGFR (Wakeling et al., 2002). As a result, these drugs induce apoptosis in cells that are dependent on constant EGFR signaling. However, $EGFR^{wt}$ signaling also exercises several non-oncogenic cellular processes. Thus, by binding to the $EGFR^{wt}$ receptor, gefitinib and erlotinib induce side effects that include skin rash and diarrhea, resulting from wild-type EGFR inhibition in the skin and gut, respectively. Depending on the specific mutation in *EGFR*, the binding affinity to gefitinib and other EGFR kinase inhibitors varies dramatically (Kancha et al., 2009; Sharma et al., 2007; Soria et al., 2011). Some of these mutations develop during the treatment with an EGFR inhibitor and thereby induce resistance (see below). To overcome resistance for some of these *EGFR* mutations, several new EGFR inhibitors with different binding modes as well as novel treatment strategies have been developed in the last years (Regales et al., 2009; Zhou et al., 2009).

1.4.1.2 ALK kinase inhibitors

Pre-clinical models for *EML4-ALK* positive tumors have shown that these cells are highly sensitive to ALK kinase inhibition (Koivunen et al., 2008; McDermott et al., 2008; Soda et al., 2007; Soda et al., 2008). Recently, a phase I/II study in advanced, *ALK* translocation positive non-small cell lung cancer (NSCLC) demonstrated strong radiographic tumor shrinkage after treatment with the type-II aminopyridine ALK kinase inhibitor crizotinib (PF02341066) (Kwak et al., 2010). Originally developed as a MET inhibitor, this drug shows relatively high binding affinities to the closely related RTK ALK. Therefore, immediately after the discovery of *EML4-ALK* translocations in lung cancers, crizotinib was used to treat these tumors (Kwak et al., 2010; Solomon et al., 2009; Timofeevski et al., 2009). In 2011, crizotinib was approved for the treatment of *EML4-ALK* positive lung cancer (FDA news release, August 26 2011). The impact of the respective fusion variant on the therapeutic efficacy of ALK inhibition is currently unknown (Sasaki et al., 2010b). However, recent studies of *EML4-ALK* positive tumors treated with crizotinib suggest a relatively heterogeneous response to this inhibitor (FDA news release, August 26 2011). Several other ALK kinase inhibitors that vary in scaffold structure, potency and selectivity, have been developed in the last years (Milkiewicz and Ott, 2010). One of these inhibitors is TAE684, a very potent type-I ALK inhibitor, which is only available for pre-clinical applications (Bossi et al., 2010; Galkin et al., 2007).

1.4.2 Resistance mechanisms

In spite of the fact that targeted therapies show promising results regarding tumor response rates and the induction of side effects, all patients that are treated with targeted therapies will eventually develop resistance. Some tumors might even express up-front resistance mechanisms that prevent compound activity from the beginning (Engelman and Janne, 2008; Mok et al., 2009; Turke et al., 2010). Resistance mechanisms are divided into *in-cis* or *in-trans* resistance, depending on the underlying mechanism of resistance.

1.4.2.1 Resistance *in-cis*

Resistance *in-cis* is defined by a structural change on the drug target (usually by a point mutation), which prevents or hinders the inhibitor to bind to its target. In *BCR-ABL* positive cells, several point mutations inducing resistance to the Abl inhibitor imatinib have been described. The most frequent resistance mutation leads to the amino acid change T315I (Shah et al., 2002). This mutation, known as the "gatekeeper" mutation, sterically impedes the binding of imatinib to the kinase domain and therefore allows the *BCR-ABL*^{T315I} expressing cells to survive. The same mechanism of resistance has been described for *EGFR* mutated lung cancer, where the "gatekeeper mutation" T790M is hampering gefitinib binding (Kobayashi et al., 2005; Paez et al., 2004; Pao et al., 2005a; Zhou et al., 2009). The threonine residues *BCR-ABL*^{T315} and *EGFR*^{T790} control the access of kinase inhibitors to a hydrophobic pocket in a recess of the kinase ATP-binding pocket, leading to the designation as "gatekeeper" residues. Notably, "gatekeeper mutations" do not interfere with the catalytic activity of the kinase, but lead to an increase in ATP affinity and are thereby transforming by themself (Azam et al., 2008). This effect, as well as the steric interaction of the bulkier isoleucine or methionine residue with the drug, induces resistance to kinase inhibitor treatment **(Figure 6)** (Kobayashi et al., 2005; Yun et al., 2008).

Most of the resistance mutations found in kinases either directly interfere with drug binding or induce a kinase conformation that impedes drug binding. However, kinase inhibitors with a different binding mode or inhibitors that do not interfere with the mutated amino acids are still capable to bind the kinase and inhibit signaling in these cells. Unfortunately, most Abl kinase inhibitors are not capable to overcome T315I induced resistance in *BCR-ABL* expressing tumors (Shah et al., 2004). However, several recent pre-clinical studies suggest the development of successful targeted therapies against these frequent "gatekeeper mutations" (Chan et al., 2011; O'Hare et al.,

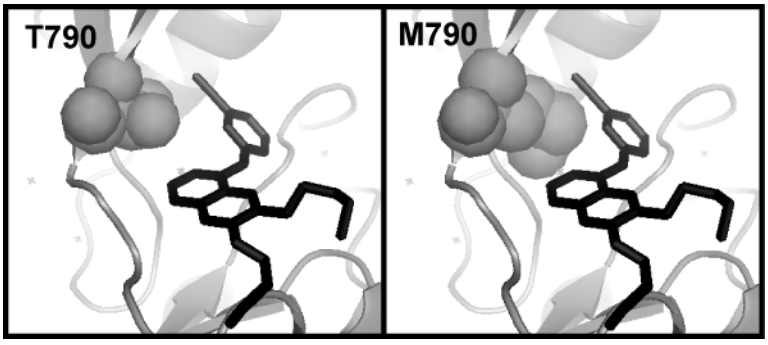

Figure 6 Crystal structure (PDB-code: 1M17) of erlotinib (black sticks) bound to EGFR^{wt} (left) and EGFR^{T790M} (right).

2009; Thomas et al., 2011; Zhou et al., 2009). In addition to new drug scaffolds with different binding modes, several studies suggest a combination treatment with drugs targeting essential downstream signaling proteins of the respective oncogenic pathway (Engelman and Settleman, 2008; Shimizu et al., 2012; Sos et al., 2009a). However, in the case of an *EML4-ALK* xenograft model, the combined treatment of PI3K and MEK inhibitors did not result in significant tumor regression (Chen et al., 2010)

1.4.2.2 Resistance *in-trans*

Resistance mechanisms *in-trans* are not found on the targeted protein itself. Here, another genetic event (i.e. mutation/fusion/amplification/overexpression of another gene) leads to the observed resistant phenotype. The most prominent example for *in-trans* resistance are *MET* amplifications in *EGFR* mutated tumors, leading to resistance to EGFR inhibition. In this case, MET signaling can substitute for the EGFR signaling that is lost due to kinase inhibition, and thereby prevent the induction of apoptosis (Engelman et al., 2007; Turke et al., 2010). Other examples for *in-trans* resistance have been found in $BRAF^{V600E}$ mutated tumors treated with PLX4032 (a BRAF inhibitor). Here, resistance can be induced by the overexpression of *COT* or *PDGFRβ* and activating mutations in *MEK1* or *NRAS* (Emery et al., 2009; Johannessen et al., 2010; Nazarian et al., 2010)

2 Objective of this study

EML4-ALK positive lung cancers can be effectively treated with ALK tyrosine kinase inhibitors (Kwak et al., 2010). However, the response rate and the individual duration of response are very heterogeneous. Furthermore, acquired resistance limits the efficacy of ALK inhibitors, but only few resistance mutations have been described (Choi et al., 2010; Katayama et al., 2011; Sasaki et al., 2010a; Zhang et al., 2011).

To analyze mechanisms that influence the sensitivity to ALK kinase inhibition, three major questions were addressed in this study:

1. Do different *EML4-ALK* variants respond differently to ALK kinase inhibition?

To address this question, different *EML4-ALK* variants as well as other *ALK* fusion genes were expressed in Ba/F3 and NIH3T3 cells and analyzed for protein stability and sensitivity to ALK and heat shock protein 90 (HSP90) inhibitors.

2. Which mutations in *EML4-ALK* can induce resistance to ALK kinase inhibitors?

To find novel resistance mutations in *EML4-ALK*, different methods for accelerated random mutagenesis were applied on *EML4-ALK* expressing Ba/F3 cells. In addition, two structurally diverse ALK kinase inhibitors were used to define specific sensitivity patterns for each resistance mutation and each inhibitor.

3. Which additional mechanisms of resistance can develop in *EML4-ALK* expressing cells after long-term treatment with ALK kinase inhibitors?

To analyze resistance mechanisms after long-term ALK inhibitor treatment, an *EML4-ALK* expressing human cell line was exposed to increasing concentrations of ALK inhibitor for 6 month. Resistant clones were then genetically analyzed to define possible resistance mechanisms.

In summary, this work aims to decipher genetic variations in *EML4-ALK* expressing cells that influence the sensitivity to ALK kinase inhibitors. Hopefully, these findings will lead to a better understanding of resistance in *EML4-ALK* positive tumors and help to enhance tumor control in the future.

3 Materials and Methods

3.1 Chemicals, Enzymes and solutions

Chemicals were purchased from CarlRoth and Sigma-Aldrich, enzymes were purchased from Fermentas and Invitrogen. Cell culture reagents were purchased from PAA.

3.2 General DNA/RNA procedures

Standard procedures such as polymerase chain reaction (PCR), gel electrophoresis, restriction enzyme digestion, DNA ligations and bacterial transformations were carried out according to the manufacturers protocol. Mini-preparations of plasmid DNA were performed using the NucleoSpin mini-kit (Machery Nagel), midi-preparations were performed using the NucleoBond Xtra Midi EF kit (Machery Nagel). If not stated otherwise, sequencing was performed at the Cologne Center for Genomics (CCG) using standard dideoxy-sequencing.

RNA was isolated using TRIZOL-reagent (Invitrogen) following the manufactures protocol. Therefore, 1 µg of RNA was transcribed into cDNA using the Superscript II reverse transcriptase (Invitrogen, #18064). 100 ng of cDNA were used to amplify the gene of interest (*SOS1-ADCY3*). After enzymatic digestion, the cDNA was ligated into the pBabe-puro backbone and transformed into chemically competent DH5α bacteria.

3.3 cDNA and plasmids

pMA-3FLAG-*EML4-ALK v1/v2/v3b* and *KIF5b-ALK* cDNAs were synthesized at GeneArt. All *EML4-ALK* cDNAs and the *KIF5b-ALK* cDNA were cloned into the retroviral pBabe-puro backbone. pDONR-*EML4-ALK v3a* and *NPM1-ALK* were synthesized at GeneScript and cloned into the retroviral pBabe-puro gateway (GW) backbone. Site directed mutagenesis was performed following the manufactures protocol (Stratagene) to generate pBabe-puro *EML4-ALK v3a* from pBabe-puro *EML4-ALK v3b*, pBabe-puro *EML4-ALK del223* from pBabe-puro *EML4-ALK v3a,* pBabe-puro *EML4-ALK del346* and *702* from pBabe-puro *EML4-ALK v2.* In addition, site directed mutagenesis was

performed to integrate the following point mutations:

pBabe-puro *EML4-ALK v1 F1174L*

pBabe-puro *EML4-ALK v1 L1196M*

pBabe-puro *EML4-ALK v1 D1203N*

pBabe-puro GW *EML4-ALK v3a F1174L*

pBabe-puro GW *EML4-ALK v3a L1196M*

pBabe-puro GW *EML4-ALK v3a G1269S*

pBabe-puro GW *EML4-ALK v3a L1198P*

3.4 Oligonucleotides

Oligonucleotides were purchased from Eurofins MWG Operon.

Primers used to sequence from the pBabe-puro backbone into the cloned cDNA (from 5' to 3')
pBb5' CTTTATCCAGCCCTCAC
pBb3' ACCCTAACTGACACACATTCC

Primers used to sequence pBabe-puro GW *EML4-ALK* cDNA (from 5' to 3')
EA_F_393 TCTCATTCTAATGATCAAAGTCCACA
EA_R_951 CCTGTTCAGAGCACACTTCAGG
EA_R_1440 GATTTCCCATAGCAGCACTCC
EA_F_1355 CTGTGCCATGCTGCCAGT
EA_F_2007 CCAACGTACGGCTCCTG
EA_R_2097 GACAGTACAGCTTCCCTCCAG
ALK_R_493 GCTGAGATTGAACTGGAGCA
ALK_F_417 CAGTTGGTGCTGGAGCTG
ALK_F_986 CAAGCACACCATCCTGAGTC
ALK_R_1078 GCAGCTGGGCAATGTACC
ALK_F_1488 CACACTCCTCAATGGCAGGT
ALK_R_1554 GGACATCAGTGGTACTGAGCAATAG
ALK_R_2124 CACCTCCACGCTCAGGTT
ALK_F_2578 GACTGGAGAATAACTCCTCGGTTC
ALK_R_2636 ATCATTCCAGCCACCTCCA
ALK_F_2955 AACTGCAGTCACTGTGAGGTAGAC

Primers used to sequence pBabe-puro *EML4-ALK* cDNA (from 5' to 3')
EA_WP25F GCCGAATTCTGATGGCTTC
EA_WP 417F AAAGAGGAAAGCCACAGCAA
EA_WP 952F CACACCGACTGCGTGAAG
EA_WP 1389F TACGAGAAGCCCAAGTTCGT
EA_WP 1950F GACTTCCACCCTAGCGGAAC
EA_WP 2416F TCAGCGATCTGAAAGAGGTG
EA_WP 2922F CCCGGGACATCTACAGAGC
EA_WP 3437F TACAACAAGCTCTGGCAAGG
EA_WP 283R TGGTGATGCAGCTCATGG
EA_WP 787R GTCCGGATGTCGTCGTAGTT
EA_WP 1266R ACCACCTCGTTGGTGGTCT
EA_WP 1800R CCTGCACCTCAATCTGGAAG
EA_WP 2303R CTGCAGTTCTTGGTGCTTCC
EA_WP 2784R GTGCAGCAGGTCCAGCAT
EA_WP 3288R GGCGGTGTTGATCACGTC
EA_WP 3784R CTAGAGGGTTCCAGCAGCAG

Primers used for *EML4-ALK* site-directed mutagenesis (from 5' to 3')
F1174L_F_WP_SDM AAGCCCTGATCATCAGCAAGTTAAACCACCAGAAC
F1174L_R_WP_SDM GTTCTGGTGGTTTAACTTGCTGATGATCAGGGCTT
L1196M_F_WP_SDM CCCCGGTTCATCCTGATGGAACTGATGGCTG
L1196M_R_WP_SDM CAGCCATCAGTTCCATCAGGATGAACCGGGG
L1198P_F_WP_SDM CATCCTGCTGGAACCGATGGCTGGAGGCG
L1198P_R_WP_SDM CGCCTCCAGCCATCGGTTCCAGCAGGATG
G1269S_F_WP_SDM GAGTGGCCAAGATCAGCGACTTCGGCATG
G1269S_R_WP_SDM CATGCCGAAGTCGCTGATCTTGGCCACTC
D1203N_F_WP_SDM CTGATGGCTGGAGGCAACCTGAAGTCCTTCC
D1203N_R_WP_SDM GGAAGGACTTCAGGTTGCCTCCAGCCATCAG
EA_V5A_WP_F_SDM AAAGCGTGTCCAGCATACCGGCGGAAGCAC
EA_V5A_WP_R_SDM GTGCTTCCGCCGGTATGCTGGACACGCTTT
V2_DEL299-346_F_SDM GCTGTTCAACTACGAGGATAGCGTGACCCTGA
V2_DEL299-346_R_SDM TCAGGGTCACGCTATCCTCGTAGTTGAACAGC
V2_DEL299-702_F_SDM GCTGTTCAACTACGAGGTGGTGTCCGAGAACG
V2_DEL299-702_R_SDM CGTTCTCGGACACCACCTCGTAGTTGAACAGC
EA_3B_DEL224-234F ATCATCAACCAGGCCTACCGGCGGAAGCAC
EA_3B_DEL224-234R GTGCTTCCGCCGGTAGGCCTGGTTGATGAT

Primers used to amplify *EML4-ALK* for deep sequencing (from 5' to 3')
EA_F1_454amp_adapt CGTATCGCCTCCCTCGCGCCATCAGACGAGTGCGTGATCCCAGTGTGGTGGTACAT
EA_R1_454amp_adapt CTATGCGCCTTGCCAGCCCGCTCAGACGCTCGACACTTGCTTTCTGGAGTTTGTCTGT
EA_F2_454amp_adapt CGTATCGCCTCCCTCGCGCCATCAGACGAGTGCGTCCTCTTCACAACCTCTCCAAA
EA_R2_454amp_adapt CTATGCGCCTTGCCAGCCCGCTCAGACGCTCGACATCCTGTTCAGAGCACACTTCAG
EA_F3_454amp_adapt CGTATCGCCTCCCTCGCGCCATCAGACGAGTGCGTCTGCAAGTGGCTGTGAAGAC
EA_R3_454amp_adapt CTATGCGCCTTGCCAGCCCGCTCAGACGCTCGACAGAGAAAAGATTTCCCATAGCAG
EA_F4_454amp_adapt CGTATCGCCTCCCTCGCGCCATCAGACGAGTGCGTCAGACACATGGTCCTTTGGAG
EA_R4_454amp_adapt CTATGCGCCTTGCCAGCCCGCTCAGACGCTCGACACGAAGGAGGGTTGGACTG
EA_F5_454amp_adapt CGTATCGCCTCCCTCGCGCCATCAGACGAGTGCGTGGACACGTGAATATGGCATTC
EA_R5_454amp_adapt CTATGCGCCTTGCCAGCCCGCTCAGACGCTCGACACCTAACTGACACACATTCCACAG

Primers used to sequence *EML4-ALK* deep sequencing amplicons by dideoxy sequencing (from 5' to 3')
454amp_seq_F CCCTCGCGCCATCA
454amp_seq_R GCTGGCAAGGCGCATA

Primers used to amplify *SOS1-ADCY3* (from 5' to 3')
SOS_5_amp CAGGGATCCATGCAGGCGCAGCAG
ADCY3_3_amp CAGGAATTCTCAGGAGTTGTCCACCACCT

Primers used to sequence verify the cloned *SOS1-ADCY3* cDNA (from 5' to 3')
ADCY3_F_37 TGCCCTACGAGTTTTTCAGC
SOS-ADCY3_F_276 GCAATAGCTGATGCCCAATC
SOS-ADCY3_F_704 GCCCTTTGTCTCCAATTCAA
SOS-ADCY3_F_1280 ATACCACCAGCTGCGGATTA
SOS-ADCY3_F_1758 GCACCAGCTTCCTCAAAGTC
SOS-ADCY3_F_2275 AGAAGCTTGTGGCCTTCTCA
SOS-ADCY3_F_2770 ACTACTTCTCCCGCCACGTA
SOS-ADCY3_F_3275 CATGAAGGATACGCTCACCA
SOS-ADCY3_R_125 GATGAACTTGCCCCTGGAC
SOS-ADCY3_R_603 TGGAAGGCTCTTCGTCAGTT
SOS-ADCY3_R_1130 GAACTGCTGCTGGTCCTTCT
SOS-ADCY3_R_1613 AAACTCCCCTTTCAGGCAGT
SOS-ADCY3_R_2096 CTCCTTCTCCACCGAGTAGC
SOS-ADCY3_R_2594 CCAGGCATAGAGGTTGATGG
SOS-ADCY3_R_3108 TGGGATTGTCCAGGAGAGAG
SOS-ADCY3_R_3596 GGGGAAGGTGGCTAGCTTAT

3.5 Cell lines

NIH3T3, HEK293T and H3122 cells were purchased from ATCC, Ba/F3^{wt} and Ba/F3$^{BCR-ABL}$ cells were a kind gift from Nikolas von Bubnoff.

NIH3T3 cells were cultured in DMEM high glucose (Gibco) supplemented with 10% calf serum (CS) and 100 U/ml penicillin/streptomycin (P/S). Ba/F3 cells were cultured in RPMI (Gibco) supplemented with 20% fetal calf serum (FCS) and 100 U/ml penicillin/streptomycin. HEK293T cells were cultured in DMEM high glucose (Gibco) supplemented with 10% fetal calf serum (FCS) and 100 U/ml penicillin/streptomycin, H3122 cells were cultured in RPMI (Gibco) supplemented with 10% fetal calf serum (FCS) and 100 U/ml penicillin/streptomycin. All adherend cells were routinely passaged at approximately 80% of confluence. Therefore, culture medium was removed, cells were washed with 5 ml of cold PBS and incubated in 2 ml Trypsin/EDTA until cells were detached. Trypsin was inactivated by the addition of 10 ml of culture medium and cells

were plated or diluted accordingly.
Suspension cells were passaged by appropriate dilution of the cell/medium suspension. All cells were incubated at 37 °C and 5% CO_2.
For long-term storage, cells were harvested, centrifuged for 5 minutes at 200 g and 4 °C before resuspending the cells in growth medium with 10% DMSO. After slowly cooling down to -80 °C, cells were moved to liquid nitrogen (-196 °C) the next day.

3.6 Compounds

Compounds were purchased from Selleck Chemicals, AxonMedchem or extracted from tablets and diluted in DMSO. PF02341066 describes a racemix mixture, whereas crizotinib represents only the active R-enantiomer of PF02341066. Bortezomib was a kind gift from Nina Reinart.

3.7 Virus production

$8*10^5$ HEK293T cells were plated on a 6 cm dish in DMEM + 10% FCS without P/S and incubated over night at 37 °C. The next day, cells were transfected with retroviral plasmids. Therefore, 12 µl of TransIT were added dropwise to 400 µl of Opti-Mem. In a separate tube, 4 µg of pBabe-puro expression plasmid were mixed with 4 µg of pCL-eco packaging plasmid in 400 µl of Opti-Mem. After 5 minutes of incubation, both tubes were mixed carefully and incubated at room temperature for 20 minutes. After incubation, Trans-IT/plasmid mixture was added dropwise to HEK293T cells. The next day, medium was removed and changed to DMEM + 30% FCS with P/S. After 24 hours, medium was collected and cells were cultured again for 24 hours with fresh medium. The next day, both collected supernatants were mixed, centrifuged at 300 g for 5 minutes, filtered through a 0.45 µm filter to remove cellular debris and frozen in aliquots at -80 °C.

3.8 Stable cDNA expression

Ba/F3 cells were thawed and cultured in RPMI + 20% FCS + 10 ng/ml IL-3 (R&D Systems; 403-ML-050). After 48 hours, $4*10^6$ proliferating cells were transferred into a 25 cm^2 flask, with 5 ml total medium, 10 ng/ml IL-3, 8 µg/ml polybrene and 1 ml retroviral supernatant. Cells were incubated for 24-48 hours before adding 2 ml of fresh medium (20% FCS, no IL-3) with 4 µl puromycin (3 mg/ml). 96 hours post-transduction, cells were centrifuged at 200 g for 5 minutes and resuspended in 6 ml fresh medium (20% FCS) with 3 µl puromycin (3 mg/ml). After 2-3 weeks, oncogene-expressing cells started to proliferate and were expanded and frozen in liquid nitrogen for long-term storage.

3.9 Soft agar assay

3.9.1 Preparation of bottom agar

Agarose Type IX ultra low (Sigma Aldrich) was prepared as a 2% stock using ddH_2O. Agar was heated to 95 °C for at least 30 minutes using a thermoblock, allowed to cool down to approximately 60 °C before adding equal volumes of 2x DMEM medium with 20% FCS and 2% P/S to the agar to get a final 1% agar/DMEM solution. 50 µL of this mixture were then added into each 96-well and allowed to solidify at 4 °C for 10 minutes.

3.9.2 Preparation of top agar

For top agar preparation, a stock solution of 1.2% was prepared in the same manner as described for the bottom agar, but cooled down slowly to 40 °C before use. NIH3T3 cells were detached by trypsine before cell numbers were determined using the Z2-coulter counter from Beckman Coulter. For each 96-well, 2000 cells were mixed with the 0.6% agar/DMEM solution and plated in 50 µl of cell/agar suspension on top of the previously prepared, pre-warmed bottom agar 96-well plate. To ensure top agar solidification, the plates were placed at 4 °C for 10 minutes and incubated at 37 °C in a humidified incubator for 14-28 days. During incubation time, the medium was carefully

changed when appropriate. After colony formation, pictures of each well were taken using the Scanalyzer imaging system (Lemnatec).

3.10 Whole cell lysates, protein extraction and quantification

Cells were washed with cold PBS and lysed in lysis buffer (20 mM Tris-HCl (pH 7.5), 150 mM NaCl, 1 mM Na_2EDTA, 1 mM EGTA, 1% Triton X-100 2.5 mM sodium pyrophosphate, 1 mM beta-glycerophosphate, 1 mM Na_3VO_4, 1 µg/ml leupeptin, 1 mM PMSF, complete Protease Inhibitors Cocktail and Phosphatase Inhibitors Cocktail Set II). After 15 minutes of incubation on ice, lysates were centrifuged at 22,000 g for 20 minutes at 4 °C. Supernatant was collected and protein concentrations were measured using the BCA Protein Assay (ThermoScientific). Cell lysates were stored at -20 °C.

3.11 Discontinuous SDS polyacrylamide gel electrophoresis

Proteins were separated on Novex® 4-12% Tris-Glycin polyacrylamide gel (Invitrogen) by electrophoresis. 5x Laemmli buffer (5x SDS sample buffer: 250 mM Tris (pH 6.8), 50% glycerol, 5% β-mercaptoethanol, 10% SDS and 0.05% bromophenol blue) was added to 50 µg of protein before denaturing each sample at 95°C for 10 minutes. Electrophoresis was performed in SDS running buffer (192 mM Glycin, 25 mM Tris-HCl, 0.1% SDS) at 100V in XCell SureLock Gel Chambers (Invitrogen). PageRuler™ Plus Prestained Protein Ladder (Fermentas) was used as a standard.

3.12 Immunoblotting

Electrophoresis separated proteins were transferred from the polyacrylamide gel to a nitrocellulose membrane using the XCell-II Blot Module (Invitrogen) and 1x transfer buffer (25 mM Tris-HCl, 192 mM Glycin, 20% methanol). The transfer was performed for three hours at 25 V. After transfer, membranes were blocked in 5% skimmed milk in TBS-T (50 mM Tris-HCl, 150 mM NaCl, pH 7.4, 0.05% Tween-20) before over night incubation at 4 °C with primary antibodies in 5% milk in TBS-T. The following antibodies were used: p-AKT Ser473, total AKT, p-ERK, total ERK, pALK Tyr1604 and pALK

Tyr1278/1282/1283 (Bossi et al., 2010) from Cell Signaling, Actin from MP Biomedical and total ALK from Bethyl Laboratories. Secondary HRP conjugated antibodies were purchased from New England Biolabs (NEB) and diluted 1:3000 in 5% milk TBS-T before incubation with the membrane for 30 minutes at room temperature. After incubation, the membrane was washed three times with TBS-T at room temperature. X-ray films and ECL solution were purchased from GE Healthcare and used according to the manufacturer´s instructions. Immunoblot signal intensities were measured using ImageJ (1.42q).

The human phosphor-receptor tyrosine kinase array (R&D Systems) was performed according the manufacturer´s instructions

3.13 Immunohistochemistry

NIH3T3 cells stably expressing the respective *EML4-ALK* cDNAs were seeded with 60% confluence on 22 mm diameter glass slides. The next day, slides were removed from the culture dish, membranes were stabilized in PBS + 3 mM $MgCl_2$ and fixed in 4% PFA for 15 minutes before incubation in PBS + 0.2% TritonX for 5 minutes to rehydrate the slides. Primary anti-ALK antibody was diluted 1:1000 in TBS-T + 1% BSA. Slides were incubated with the primary antibody in a humified chamber for 1 hour at room temperature. FITC-labeled secondary antibody was diluted 1:800 in TBS-T + 1% BSA plus 1:1000 DAPI. After three washing steps in TBS-T, glass slides were incubated with secondary antibody for 45 minutes in a dark humified chamber. After again three washing steps, slides were washed in Ethanol and dried in the dark for 45 minutes before covering slides on coverslips with SlowFade Gold (Invitrogen). Pictures were taken on an Aristoplan machine (Leica/Leitz Microsystems) using a 400-fold magnification.

3.14 Viability assays

Ba/F3 cells were counted using the Z2-coulter counter from Beckman Coulter. 20,000 cells were plated into each well of a sterile 96-well microtiter plate using a multichannel

pipette. The next day, compounds were added in serial dilutions. Cellular viability was determined after 96 hours of treatment by measuring cellular ATP content using the CellTiter-Glo Assay (Promega). Luminescence was measured on a Mithras LB 940 Plate Reader (Berthold Technologies). GI_{50} values were determined using the following R package (Frommolt and Thomas, 2008).

3.15 Generation of ALK inhibitor resistant H3122 cells

H3122 cells were seeded at ~70% confluence in 6-well dishes in RPMI with 10% FBS. PF02341066 was added at a starting concentration of 30 nM, and cells were treated with fresh drug-containing medium every ~72 hours. Drug concentrations were increased as soon as the cells reached ~90% of confluence. The concentration of PF02341066 was increased until a final concentration of 3 µM was achieved. The resulting polyclonal resistant cells (designated as H3122 PR) were maintained in RPMI with 10% FCS containing 3 µM PF02341066 or 1.5 µM crizotinib.

3.16 Trypan-blue staining

Ba/F3 cells expressing the indicated *EML4-ALK* cDNA were treated with ALK kinase inhibitors for 48 hours. Cells were resuspended and diluted 1:1 with trypan-blue before being transferred to a Neubauer-Chamber were trypan blue negative (viable) and positive (dead) cells were counted under the light microscope.

3.17 Mutagenesis screens

To generate randomly mutated pBabe-puro GW EML4-ALK v3a plasmids, a saturation mutagenesis screen was performed as has been described previously (Azam et al., 2003; Emery et al., 2009). Therefore, mismatch-repair-deficient E.coli (strain XL1-Red, Stratagene) were transformed with the *EML4-ALK* cDNA and propagated for 48 or 72 hours. Plasmids were isolated and expanded in XL1-Blue bacteria. Isolated plasmids were packaged in retroviruses followed by infection of Ba/F3 cells as described above. 24 hours after infection, cells were cultured in the absence of IL-3 and presence of ALK

kinase inhibitor (750 nM/ 1000 nM/ 1500 nM of PF02341066) to only allow proliferation of resistant clones with an active kinase. Surviving cells were expanded before the isolation of genomic DNA. Mutant inserts were recovered by PCR using the primers stated above. The amplified *EML4-ALK* fragments were pooled and sequenced on a GS Flex instrument at the Cologne Center for Genomics (CCG). The raw data was aligned and visualized by IGV.

In a second mutagenesis screen, *EML4-ALK*-expressing Ba/F3 cells were treated with N-ethyl-N-nitrosourea (ENU; 100 µg/ml) over night to induce random mutations in the cells genomes. After 24 hours of incubation, cells were centrifuged, washed in PBS and cultured in the presence of the ALK inhibitor (750 nM/ 1000 nM/ 1500 nM of PF02341066) to select for resistant and viable clones. Again, genomic inserts were PCR-amplified and sequenced as described above.

To differentiate the clonal origin of the two resistance mutations found, dideoxy sequencing was performed for each polyclonal resistant clone separately.

3.18 Structural modeling

Resistance mutations were modeled into ALK (PDB-codes: 2XP2 (crizotinib) and 2XB7 (TAE684) by Daniel Rauh, using PyMol software (Schroedinger).

3.19 Mass spectrometry

After rigorous vortexing, 30 µl of Protein A/G agarose breads were mixed with 5 µg of anti-ALK antibody (Bethyl laboratories) and 500 µl of cold PBS. After 4 hours of incubation on a rotating shaker at 4 °C, beads were washed three times with cold PBS before adding 500 µg of whole cell lysate and subsequent incubation on a rotating shaker over night at 4 °C. The next day, beads were washed three times, mixed with 30 µl Laemmli buffer and run on a polyacrylamide gel as indicated above. After protein separation, the polyacrylamide gel was stained with coomassie solution for protein visualization. Each lane was cut out and analyzed by mass spectrometry at the CMMC bioanalytic service in Cologne.

3.20 RNA-sequencing

After RNA extraction and cDNA library construction, cDNAs were sheared and fragments were size-selected to a fragment length range of 300 - 400 base pairs using a bioanalyzer. cDNA fragments were then loaded into separate flow-cell lanes on an Illumina Genome Analyzer II. 41,570,899 fragments of 95-mer reads were obtained, leading to ~7.6 gigabases of total sequence. First, duplicate pair reads and low-quality reads were discarded, leading to 37,836,347 distinct reads. The achieved mean sequence coverage of the annotated transcriptome was approximately 30x. Data analysis was performed using Velvet+Oases for *de novo* assembly (Zerbino and Birney, 2008; Zerbino and Schulz, unplublished data). Reconstructed transcripts were then compared to given transcript annotations to recover gene fusion events. In addition, potential fusion transcripts were identified by recurrent conflicts in the assignment of pair-end reads to only one gene.

3.21 In silico domain search

Protein domains were searched using **S**imple**M**odular**A**rchitecture**R**esearch**T**ool (http://smart.embl-heidelberg.de/)

4 Results

4.1 Differential protein stability and ALK inhibitor sensitivity of *EML4-ALK* fusion variants

4.1.1 *EML4-ALK* variants transform NIH3T3 cells

EML4-ALK translocations lead to a fusion protein whose kinase is, due to its persistent homodimerization, constantly activated. Depending on the breakpoint between *EML4* and *ALK*, different variants develop that differ in size of the fusion transcript.

In order to analyze the transformation capacity of different *EML4-ALK* variants, the most frequent variants were cloned into the retroviral pBabe-puro backbone and used for retroviral transduction of NIH3T3 cells. These murine fibroblasts spontaneously immortalized after serial subcultivation, exhibit a hypertriploid karyotype but do not show a transformed phenotype (Jainchill et al., 1969; Todaro and Green, 1963). After plating NIH3T3 cells into a layer of soft-agar, non-transformed NIH3T3 cells stop dividing. If, however, an oncogene is expressed in these cells, the lack of a polar surface does not inhibit cell division anymore. Thus, the transformed NIH3T3 cells become insensitive to anti growth signals, leading to colony formation in soft agar (Hanahan and Weinberg, 2000). After plating NIH3T3 cells expressing *EML4-ALK v1*, *v2* and *v3a* in soft agar, all variants formed similar numbers of colonies, indicating comparable transformation capacities in NIH3T3 cells **(Figure 7)** (Chen et al., 2008; Greulich et al., 2005).

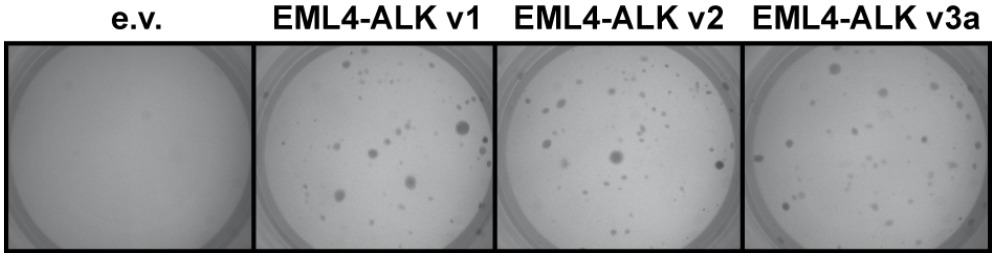

Figure 7 NIH3T3 cells transduced with pBabe empty vector (e.v.) or the indicated *EML4-ALK* variant were plated in soft agar. Pictures were taken after 14 days of incubation using a Scanalyzer imaging system (Lemnatec).

4.1.2 *EML4-ALK* variants induce differential sensitivity to ALK kinase inhibition

In order to test, whether different *EML4-ALK* fusion variants show differential sensitivity to ALK kinase inhibitors, the Ba/F3 cell line model was used. These murine pre-B-cells are dependent on constant interleukin-3 (IL-3) stimulation for cell survival. To prevent rapid induction of apoptosis, Ba/F3^{wt} cell culture medium is usually supplemented with 10 ng/ml of exogenous IL-3. Oncogenes (e.g. oncogenic RTKs) can substitute for the essential IL-3 signaling, and thereby render the cells IL-3 independent. Thus, the expressed oncogenes prevent the induction of apoptosis and make these cells independent of external growth signals (Hanahan and Weinberg, 2000). This cell line model has been used extensively to monitor transformation capacity and kinase inhibitor sensitivity of several *EGFR* mutations (Jiang et al., 2005; Yuza et al., 2007).

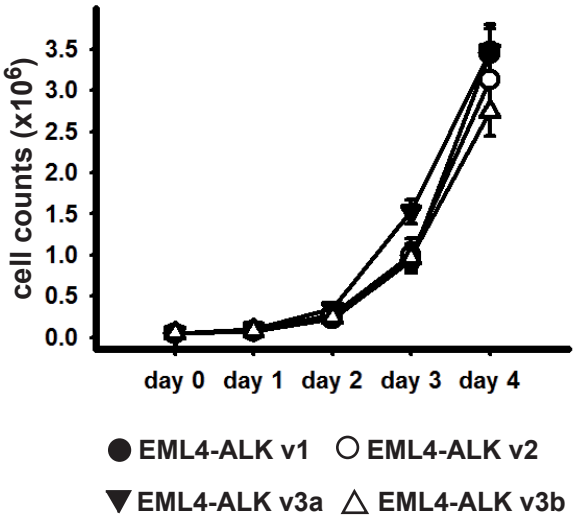

Figure 8 Ba/F3 cells expressing the indicated *EML4-ALK* variants were plated at equal cell numbers at day 0. Cell counts were determined at each of the following 4 days, error bars indicate SEM.

Again, virus particles were generated for all *ALK* fusion genes and used to transduce Ba/F3^{wt} cells. Stable expression of *EML4-ALK v1*, *v2*, *v3a* and *v3b* rendered Ba/F3 cells independent of IL-3, thus, as expected, all variants showed transforming capacity. In addition, all cells expressing different *EML4-ALK* variants showed similar proliferation rates **(Figure 8)**.

To analyze the sensitivity of each variant to ALK kinase inhibition, fusion gene expressing cells were plated into 96-well plates and treated with increasing concentration of the aminopyridine ALK inhibitor crizotinib (PF02341066). After incubation for 96 hours, the ATP content in each well was measured using an ATP-dependent luminescence reaction (cell titer glow, Promega). *EML4-ALK* variants *v1* and *v3b* showed no significant differences in sensitivity, represented by the half-maximal growth inhibitory concentration ("GI_{50} values") (GI_{50s} 470 nM, **Figure 9**). Interestingly, Ba/F3 cells expressing the longest and

the shortest of the four *EML4-ALK* variants (i.e. *v2* and *v3a*) showed considerable differences in crizotinib sensitivity (GI_{50} 150 nM and 1000 nM respectively). To test, whether this phenotype was restricted to this specific ALK inhibitor, the same set of cells was treated with the structurally different diaminopyrimidine ALK inhibitor TAE684 **(Figure 9)**. Here, the same pattern of sensitivity was observed, with *v2* being the most

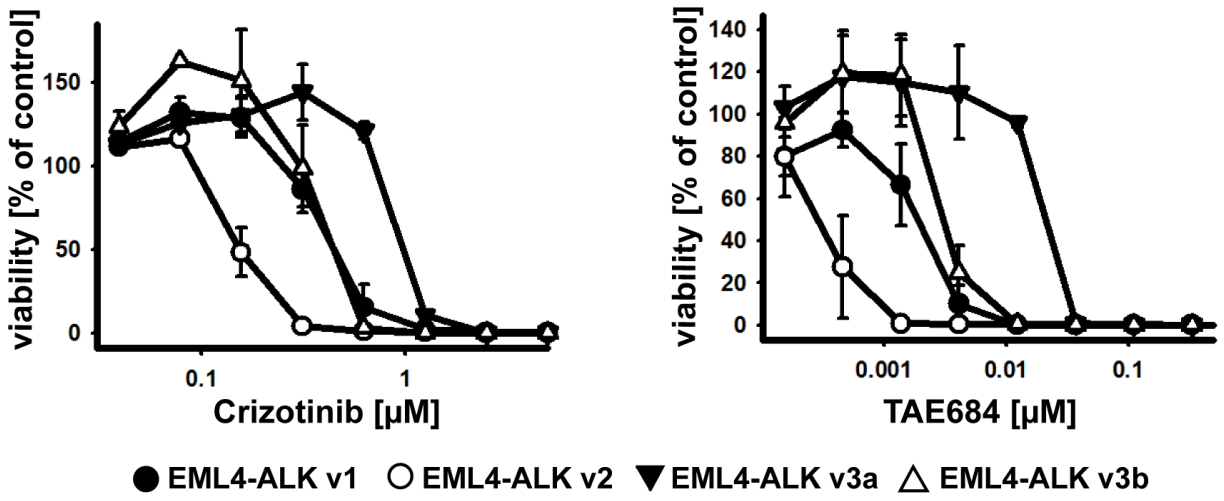

Figure 9 Ba/F3 cells expressing the indicated *EML4-ALK* variants were treated with increasing concentrations of crizotinib (left) or TAE684 (right). Viability was determined after 96 hours of treatment by measuring the ATP content in each well. Viability is expressed as a function of compound dose and ATP-content, relative to the DMSO-treated control. Each data point represents the mean of three independent experiments with triplicate measurements, error bars indicate SEM.

sensitive (GI_{50} 0.3 nM) and *v3a* the most resistant (GI_{50} 24 nM) variant of *EML4-ALK*. These findings show, that different *EML4-ALK* variants elicit differential sensitivity to ALK kinase inhibition, independent of the binding mode of the inhibitor to the kinase. Even though both inhibitors bind to the hinge region of the kinase, the three dimensional expansion into the ATP-binding pocket differs for both compounds **(Figure 10)**.

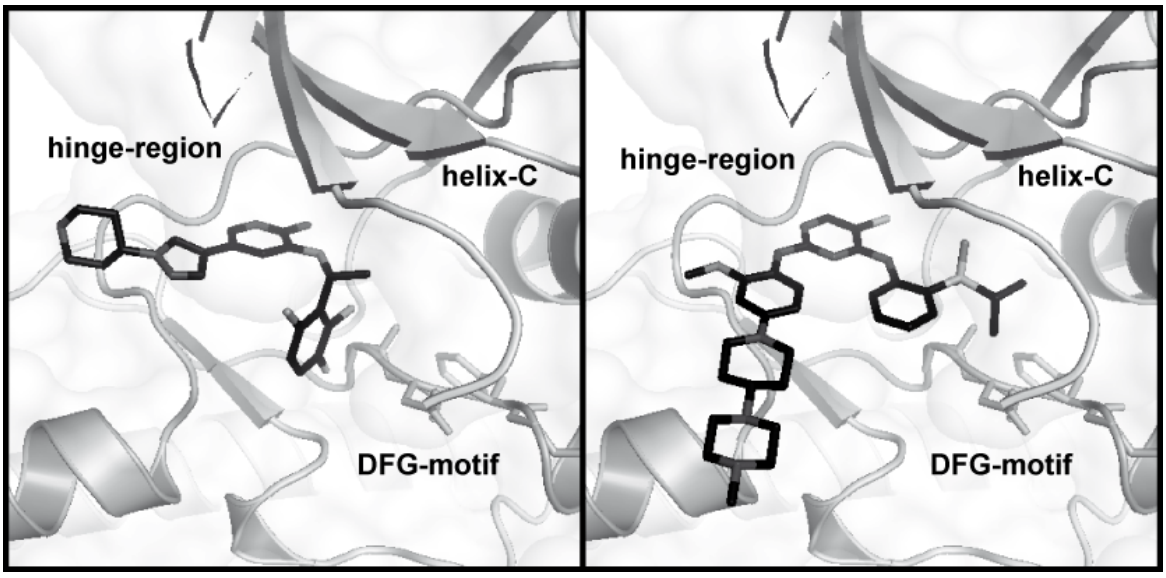

Figure 10 Crystal structures showing crizotinib (left) and TAE684 (right) bound to the kinase domain of ALK. Both compounds are shown as black sticks, the hinge-region, helix-C and DFG-motif are labeled. PyMol file was generated by Christian Grütter, TU Dortmund, Germany.

One possible explanation for the differences in sensitivity could be a differential accessibility of the inhibitors to the ATP-binding pocket of the kinase. Even though both variants harbor the same proportion of *ALK*, the three dimensional arrangement of the fusion protein might vary depending on the proportion of *EML4* that is fused to *ALK,* thereby hindering inhibitor binding. To test this hypothesis, *EML4-ALK v2* and *v3a* expressing Ba/F3 cells were treated with increasing concentrations of crizotinib and lysed after 1 hour of treatment. Proteins were separated on a polyacrylamide gel before immunoblotting was performed to monitor ALK phosphorylation. As has already been shown for another ALK kinase inhibitor, no differences in ALK phosphorylation were observed for concentration from 300 to 3000 nM of crizotinib **(Figure 11)** (Lovly et al., 2011).

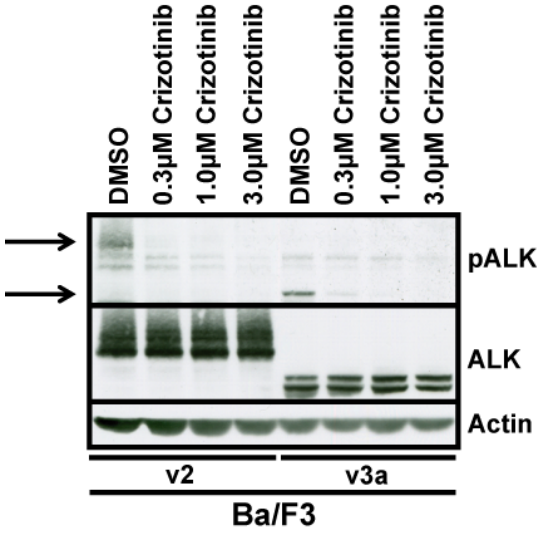

Figure 11 *EML4-ALK v2* and *v3a* expressing Ba/F3 cells were treated with the indicated concentrations of crizotinib for 1h. Whole cell lysates were stained for pALK, ALK and actin by immunoblotting.

To verify these results in an independent cell line model, ALK phosphorylation was monitored in NIH3T3 cells expressing *EML4-ALK variants 2* and *3a* respectively. NIH3T3 cells expressing the respective variants were seeded on 6-well dishes and treated the next day with increasing concentrations of crizotinib for 1 hour. Again, immunostainings did not show any differences in ALK phosphorylation at crizotinib concentrations from 300 to 3000 nM **(Figure 12 A)**. Treatment with lower doses of crizotinib supported this finding, showing a dose dependent inhibition of ALK phosphorylation between 30 and 300 nM of crizotinib. Consistent with previous findings, crizotinib treatment led to a dose dependent decrease in ERK phosphorylation, whereas no changes in AKT phosphorylation were observed **(Figure 12 B)** (Takezawa et al., 2011). In addition, the same pattern of phosphorylation was shown for *EML4-ALK v1* **(Figure 12 C)**. Thus, the binding capacity of crizotinib to the ATP-binding pocket does not seem to be altered in the three *EML4-ALK* variants studied.

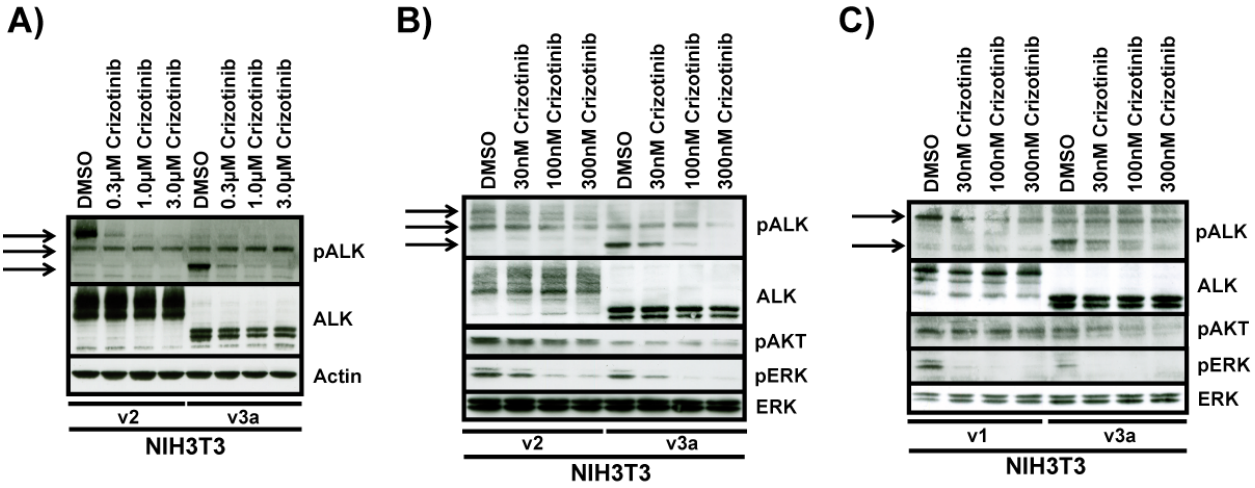

Figure 12 A/B/C NIH3T3 cells expressing the indicated *EML4-ALK* cDNAs were treated with the indicated concentrations of crizotinib for 1 hour. Whole cell lysates were stained for pALK, ALK, pAKT, pERK and ERK or actin as loading control. Black arrows indicate the respective EML4-ALK variant (top, bottom) or unspecific staining (central).

4.1.3 *EML4-ALK* variants show differences in intracellular distribution

All *EML4-ALK* variants studied harbor exon 20 to exon 29 of *ALK,* which are fused to different breakpoints within the *EML4* gene **(Figure 2, Figure 13)**. Thus, the proportion of *EML4* that is fused to *ALK* is probably responsible for the observed differences in inhibitor sensitivity **(Figure 9, Figure 13)**.

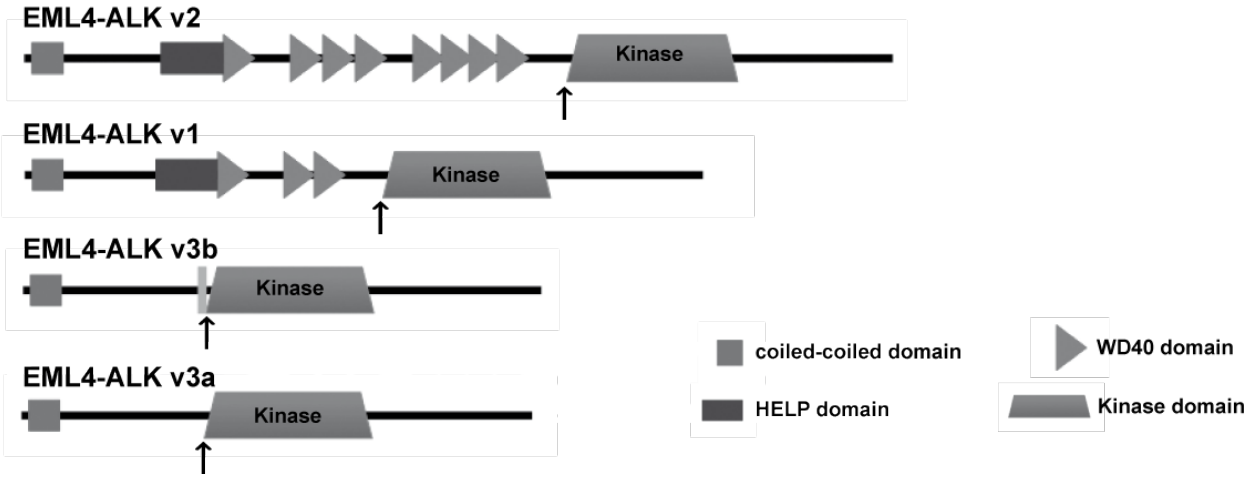

Figure 13 Schematic presentation of *EML4-ALK variants 1*, *2*, *3a* and *3b.* The breakpoint between *EML4* and *ALK* is indicated with a black arrow. The additional 33-bp sequence derived from intron 6 of *EML4* that differentiates *v3b* from *v3a* is shown as a light gray box.

Even though the exact function of EML proteins is unknown, it is believed that these proteins represent a class of microtubule destabilizers (Pollmann et al., 2006). At the N-terminal of the EML4 protein, a coiled-coiled domain is located which is essential for the oncogenic capacity of EML4-ALK (Soda et al., 2007). At the C-terminal end of the coiled-coiled domain, a HELP domain is followed by nine WD40 domains. It is thought, that the HELP domain of EML4 mediates tubulin binding (Pollmann et al., 2006), while WD40 domains are involved in a wide range of cellular functions (Xu and Min, 2011). In order to analyze the intracellular localization of different EML4-ALK variants, NIH3T3 cells expressing *EML4-ALK v1*, *v2*, *v3a* were stained for ALK by immunohistochemistry. EML4-ALK variants 1 and 2, both containing a HELP domain, were mainly abundant in the cytoplasm **(Figure 14)**. Variant 3a, which lacks the HELP domain, was equally distributed throughout the cytoplasm and the nucleus, suggesting, that the HELP domain retains the fusion protein in the cytoplasm **(Figure 13, Figure 14)** (Pollmann et al., 2006). However, since variant 1 and variant 2 showed the same intracellular

localization, but showed differences in sensitivity, the intracellular distribution does not seem to highly influence the sensitivity to ALK kinase inhibitors.

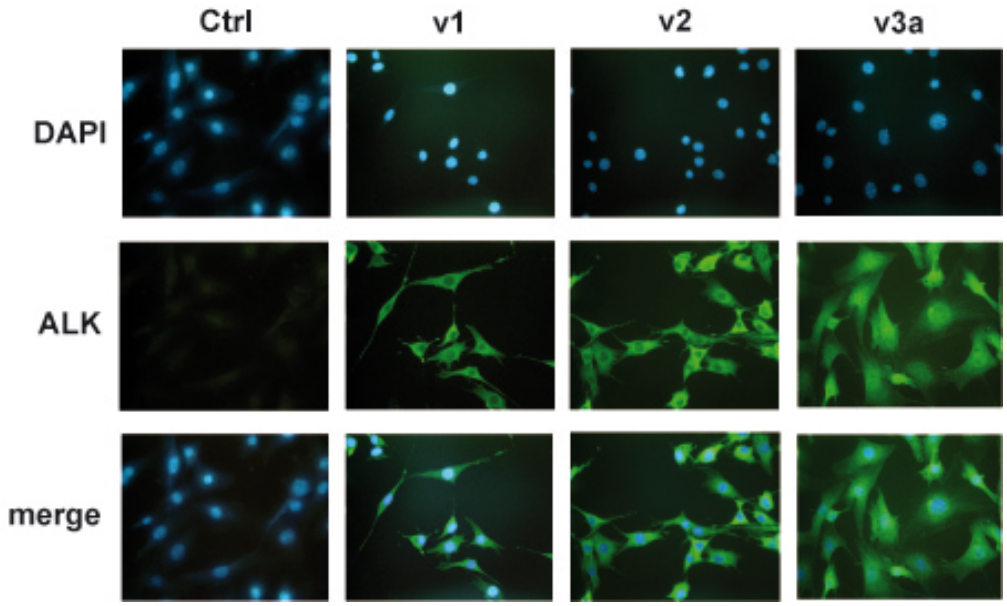

Figure 14 NIH3T3 cells expressing the indicated *EML4-ALK* variants were fixed on glass slides and stained for total ALK (FITC) and nuclei (DAPI). Pictures were taken at 400-fold magnification.

4.1.4 EML4-ALK v2 and v3a interact with HSP90 proteins

As shown in Figure 13, an additional structural difference between EML4-ALK variant 2 and variant 3a is the number of WD40 domains. These domains are one of the most prevalent domains in eukaryotic proteins and are thought to arise from genetic duplications. They form β-propeller like structures that allow the formation of a wide range of protein-protein and protein-DNA interactions. However, these interactions, and therefore also potential binding partners, are difficult to predict (Xu and Min, 2011). To analyze if the WD40 domains in EML4-ALK v2 promote interactions with specific binding partners, immunoprecipitations of EML4-ALK v2 and v3a were performed **(Figure 15)**.

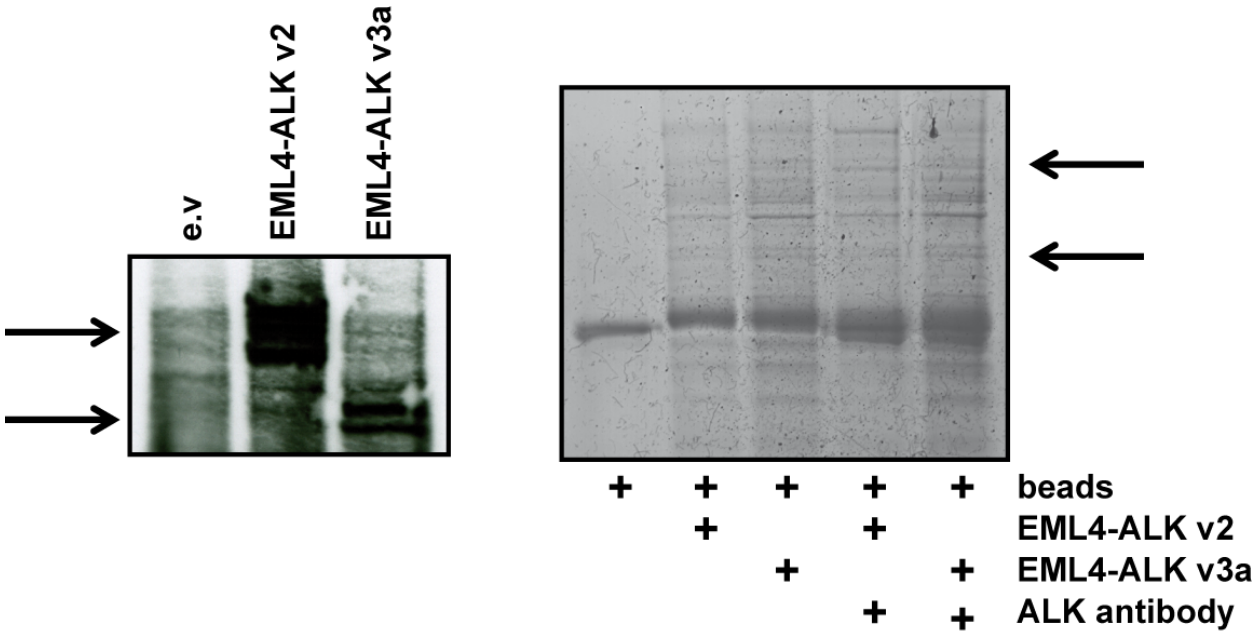

Figure 15 NIH3T3 cells transduced with pBabe empty vector, *EML4-ALK v2* or *EML4-ALK v3a* were lysed to perform immunoprecipitations of ALK. First, total ALK protein levels were stained on a nitrocellulose membrane to control proper precipitation of ALK (left). Second, immunoprecipitated proteins were separated on a polyacrylamide gel, stained with coomassie (right) and subsequently analyzed by mass-spectometry. Arrows indicate the respective EML4-ALK fusion variant.

Pulled proteins were analyzed by mass-spectrometry for interacting proteins. As has been described previously, high amounts of HSP90 proteins were found to be associated to both variants. This interaction potentially explains the described dependency of *EML4-ALK* expressing cells to HSP90 chaperonage (Katayama et al., 2011; Normant et al., 2011). However, negative controls consisting of beads and lysates only also yielded some HSP90 peptides, arguing for an unspecific binding of HSP90 proteins to the agarose-beads. The only protein that was found in immunoprecipitations and not in controls was AMPD2 (an AMP deaminase). However, no robust differences between v2 and v3a were observed **(Table 1, page 51)**.

Table 1 Immunoprecipitated proteins are listed for both EML4-ALK variants. EML4-ALK proteins are highlighted in light gray, proteins that were only found in ALK immunoprecipitations are highlighted in dark gray. Proteins that were also found in antibody negative controls are shown with a white background.

Lysates NIH3T3 EML4-ALKv2 + beads + antibody	Lysates NIH3T3 EML4-ALKv3a + beads + antibody
ALBU_HUMAN Serum albumin	ALBU_HUMAN Serum albumin
ALBU_MOUSE Serum albumin	ALBU_MOUSE Serum albumin
ALK_HUMAN ALK tyrosine kinase receptor	ALK_HUMAN ALK tyrosine kinase receptor
ALK_MOUSE ALK tyrosine kinase receptor	AMPD2_HUMAN AMP deaminase2
AMPD2_HUMAN AMP deaminase2	AMPD2_MOUSE AMP deaminase2
AMPD2_MOUSE AMP deaminase2	CH60_HUMAN 60kDa heat shock protein, mitochondrial
EMAL4_HUMAN Echinoderm microtubule-associated protein-like 4	CH60_MOUSE 60kDa heat shock protein, mitochondrial
EMAL4_MOUSE Echinoderm microtubule-associated protein-like 4	EF2_HUMAN Elongation factor 2
HS90B_HUMAN Heat shock protein HSP90-beta	EF2_MOUSE Elongation factor 2
HS90B_MOUSE Heat shock protein HSP90-beta	ENPL_HUMAN Endoplasmin
HSP7C_HUMAN Heat shock cognate 71kDa protein	ENPL_MOUSE Endoplasmin
HSP7C_MOUSE Heat shock cognate 71kDa protein	GRP78_HUMAN 78kDa glucose-regulated protein
K1C10_HUMAN Keratin, type I cytoskeletal 10	GRP78_MOUSE 78kDa glucose-regulated protein
K1C10_MOUSE Keratin, type I cytoskeletal 10	HS90A_HUMAN Heat shock protein HSP90-alpha
K22E_HUMAN Keratin, type II cytoskeletal 2 epidermal	HS90A_MOUSE Heat shock protein HSP90-alpha
K2C1_HUMAN Keratin, type II cytoskeletal 1	HS90B_HUMAN Heat shock protein HSP90-beta
K2C1_MOUSE Keratin, type II cytoskeletal 1	HS90B_MOUSE Heat shock protein HSP90-beta
K2C5_MOUSE Keratin, type II cytoskeletal 5	HSP7C_HUMAN Heat shock cognate 71kDa protein
K2C8_MOUSE Keratin, type II cytoskeletal 8	HSP7C_MOUSE Heat shock cognate 71kDa protein
	K1C10_HUMAN Keratin, type I cytoskeletal 10
	K1C10_MOUSE Keratin, type I cytoskeletal 10
	K22E_HUMAN Keratin, type II cytoskeletal 2 epidermal
	K2C1_HUMAN Keratin, type II cytoskeletal 1
	K2C1_MOUSE Keratin, type II cytoskeletal 1
	KPYM_HUMAN Pyruvate kinase isozymes M1/M2
	KPYM_MOUSE Pyruvate kinase isozymes M1/M2
	MYH9_HUMAN Myosin-9
	MYH9_MOUSE Myosin-9

4.1.5 ALK inhibitors induce a dose dependent EML4-ALK protein degradation

Since no differences in ALK phosphorylation were observed after 1 hour of treatment, longer crizotinib treatments were performed to analyze potential feedback mechanisms that re-activate kinase activity. Therefore, immunoblotting was performed using lysates of *EML4-ALK* expressing NIH3T3 cells that were treated for 24 hours with ALK inhibitor. Interestingly, treatment with 1 µM or 3 µM of crizotinib led to a reduction of total ALK protein in *variant 2* expressing cells. In contrast, in *variant 3a* expressing cells total ALK levels were only reduced at 3 µM crizotinib, but not at 1 µM drug concentrations **(Figure 16 A)**. To confirm this effect in another cell line, the same assay was repeated using Ba/F3 cells. Here, again, the dose-dependent effect of ALK degradation was much more pronounced for variant 2 compared to variant 3a **(Figure 16 B)**. Treatment of

these cells with 1 µM of TAE684 for 24 hours also induced degradation of variant 2, but not of variant 3a **(Figure 16 C)**. Thus, ALK kinase inhibition induces a fusion variant dependent degree of EML4-ALK protein degradation after long-term treatment.

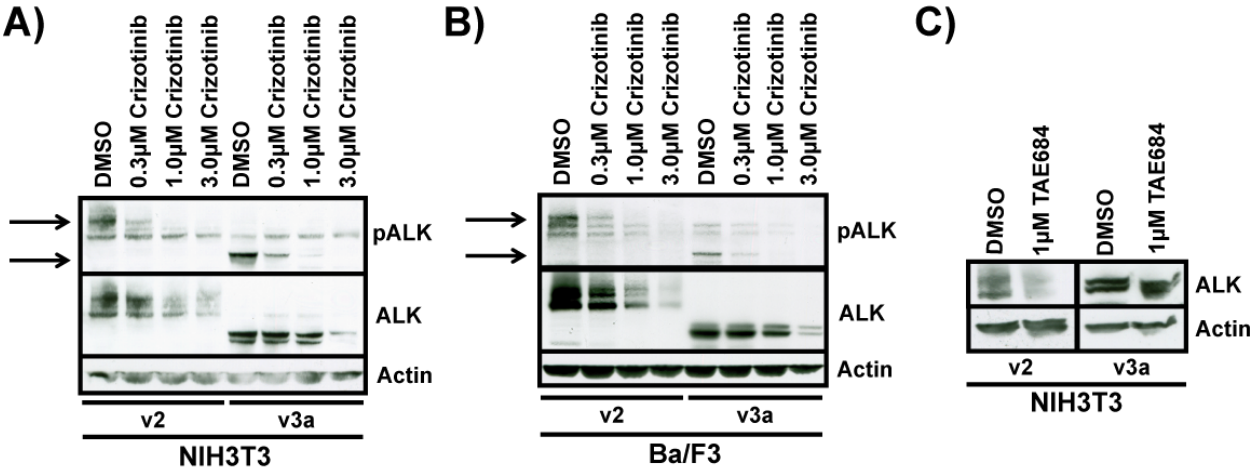

Figure 16 NIH3T3 cells (**A/C**) or Ba/F3 cells (**B**) expressing the indicated *EML4-ALK* cDNAs were treated with increasing concentrations of crizotinib (**A/B**) or TAE684 (**C**). After 24h of treatment, lysates were prepared and analyzed for pALK, ALK and actin protein levels by immunoblotting.

4.1.6 Crizotinib induced EML4-ALK degradation is proteasome independent

Most proteins are degraded in the cytosolic proteasome machinery. To test, whether the observed degradation of *EML4-ALK* is mediated by the proteasome, Ba/F3 cells expressing different *EML4-ALK variants* were first treated with increasing concentrations of the proteasome inhibitor bortezomib. Viability measurements in cells expressing *EML4-ALK variants 2* and *3a* revealed no differences in sensitivity. However, in both cases, addition of exogenous IL-3 into the medium was not capable to rescue this phenotype, indicating an *EML4-ALK* unrelated toxicity of bortezomib in these cells **(Figure 17 A)**. To circumvent this problem, *EML4-ALK* expressing NIH3T3 cells were treated with 3 µM crizotinib, 100 nM bortezomib or both compounds combined for 24 hours. In this setting, a proteasome dependent degradation of EML4-ALK should lead to increased ALK levels in the bortezomib treated cells and should rescue the crizotinib induced degradation in crizotinib + bortezomib treated cells. Interestingly, the inhibition of proteasomal activity did not increase the protein levels of EML4-ALK

compared to DMSO treated cell, nor did it rescue the crizotinib-induced EML4-ALK degradation in the combination treatment. This finding implies a proteasome independent degradation of EML4-ALK in these cells **(Figure 17 B)**.

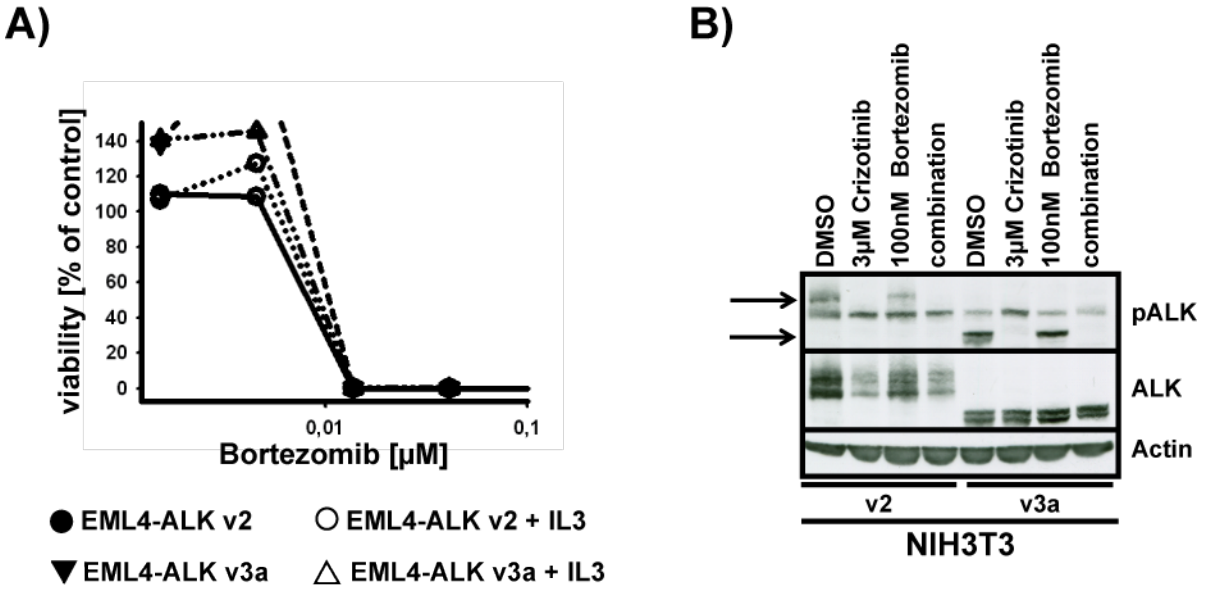

Figure 17 A Ba/F3 cells expressing the indicated *EML4-ALK* variants were treated with increasing concentrations of bortezomib. Viability was determined after 72 hours of treatment and is expressed as a function of compound dose and ATP-content, relative to DMSO-treated controls. **B** NIH3T3 cells expressing the indicated *EML4-ALK* cDNAs were treated with 3 µM crizotinib, 100 nM bortezomib or both compounds combined. After 24 hours of treatment, whole cell lysates were prepared and analyzed for pALK, ALK and actin protein levels by immunoblotting.

4.1.7 EML4-ALK variants show differences in protein stability

In order to analyze the basal protein stabilities of the different fusions, *EML4-ALK* expressing Ba/F3 and NIH3T3 cells were treated with 50 µg/ml or 100 µg/ml of cycloheximide for 24 hours respectively. Cycloheximide is an inhibitor of the protein biosynthesis, thereby uncovering differences in the half-life of proteins. Immunoblotting after DMSO and cycloheximide treatment showed remarkable differences in total ALK levels. The most pronounced difference of total ALK protein was observed between untreated and treated cells expressing EML4-ALK variant 2. EML4-ALK variant 1 showed an intermediate difference in protein levels, whereas EML4-ALK variant 3a showed almost no reduction in total ALK protein levels after treatment **(Figure 18 A/B)**.

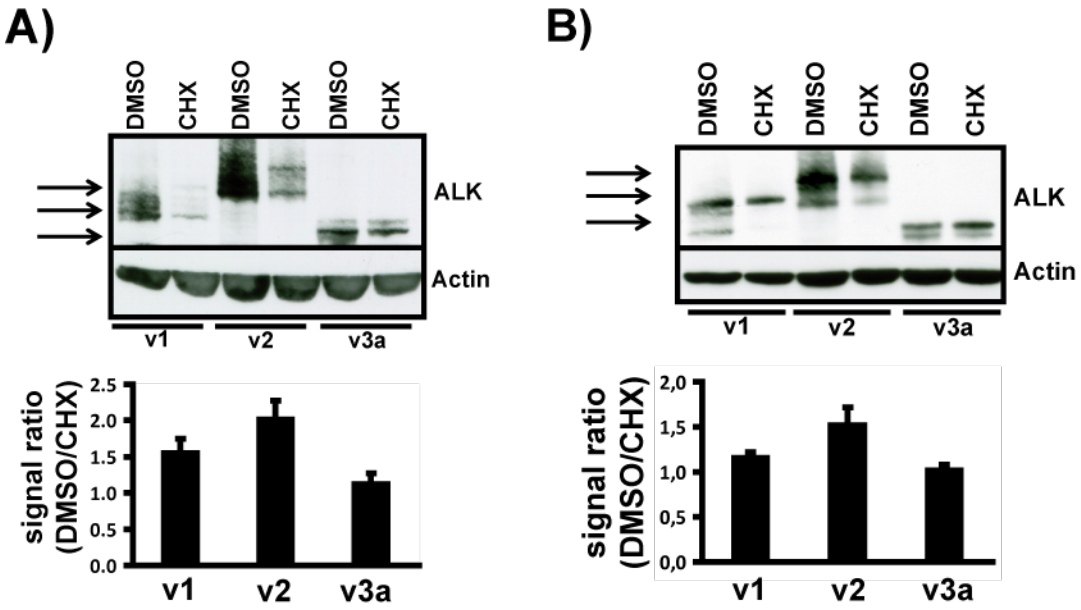

Figure 18 *EML4-ALK* expressing Ba/F3 (**A**) or NIH3T3 (**B**) cells were treated with DMSO or cycloheximide for 24 hours. Whole cell lysates were stained for total ALK (top). Signal intensity of each staining was analyzed using ImageJ software. Signal ratios of DMSO/CHX are shown for each *EML4-ALK* variant as an average of three independent experiments, error bars indicate SEM (bottom).

Thus, the proportion of EML4 that is fused to ALK, strongly influences the stability of the fusion protein. This effect might also play a role in the drug binding induced degradation of the protein as well as the differences in ALK kinase inhibitor sensitivity **(Figure 9, Figure 16)**. Interestingly, even though *EML4-ALK v3b* was more sensitive to ALK inhibitor treatment compared to *v3a*, protein levels after treatment with cycloheximide did not vary significantly, indicating that ALK kinase inhibitor sensitivity is not a direct consequence of the different protein stabilities in these cells **(Figure 19)**.

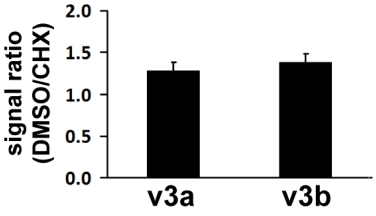

Figure 19 Total ALK signal intensity ratios after cycloheximide treatment of Ba/F3 are shown for *EML4-ALK v3a* and *v3b*. Error bars indicate SEM.

4.1.8 Artificial *EML4-ALK* deletion mutants modify ALK inhibitor sensitivity

To evaluate the effect of *EML4* on the degradation kinetics of EML4-ALK fusion proteins and on the kinase inhibitor sensitivity of *EML4-ALK* expressing cells, site directed

mutagenesis was performed on different *EML4-ALK variants* to generate artificial deletion constructs. With *variant 2* being the longest and least stable variant **(Figure 13, Figure 18)**, deletions at the 5' end of *EML4-ALK* might increase basal protein stability and decrease ALK inhibitor sensitivity. *Variant 2* was used as a template to remove amino acids 299-346 to generate variant *del346* (lacking the first WD40 domain next to the HELP domain) or 299-702 to generate variant *del702* (lacking the first seven WD40 domains). *Variant 3a* was used to remove amino acids 61-223, generating variant *del223* which is similar to EML4-ALK *variant 5* **(Figure 20 A)**. Importantly, all deletion constructs maintained the coiled-coiled domain of EML4, essential for continuous ALK kinase activation (Soda et al., 2007). As expected, all of the deletion constructs transformed Ba/F3 cells, however, depending on the respective deletion, a distinct sensitivity pattern was observed after treatment with ALK kinase inhibitors. Ba/F3 cells expressing *EML4-ALK del346* were as sensitive as *variant 2* expressing cells **(Figure 20 B)**. By contrast, Ba/F3 cells expressing *del702* were much more resistant to kinase inhibition compared to cells expressing *variant 2*, being almost as resistant as cells expressing *variant 3a* **(Figure 20 B)**. *EML4-ALK del223* expressing cells showed no significant differences in crizotinib sensitivity, indicating that the region of amino acids 61-223 does not influence the sensitivity of the *EML4-ALK* variants to kinase inhibition. Even though *EML4-ALK v3a* and *del223* were the most resistant ALK fusion genes tested, both variants were still more sensitive to ALK inhibition compared to *BCR-ABL* expressing Ba/F3 **(Figure 20 C)**.

4.1.9 *EML4-ALK* deletion mutants show differences in protein stability

Treatment of Ba/F3 cells expressing *EML4-ALK del346* and *del702* with cycloheximide, revealed striking differences in protein stability. Here, EML4-ALK del346 seemed slightly less stable compared to EML4-ALK v2, whereas the deletion in *EML4-ALK del702* increased protein stability dramatically **(Figure 20 B)**. Cells expressing *EML4-ALK del223* displayed no degradation of the fusion protein after 24 hours of cycloheximide treatment, supporting the notion that amino acids 61-223 in EML4 do not seem to have a high impact on the protein properties **(Figure 20 C)**.

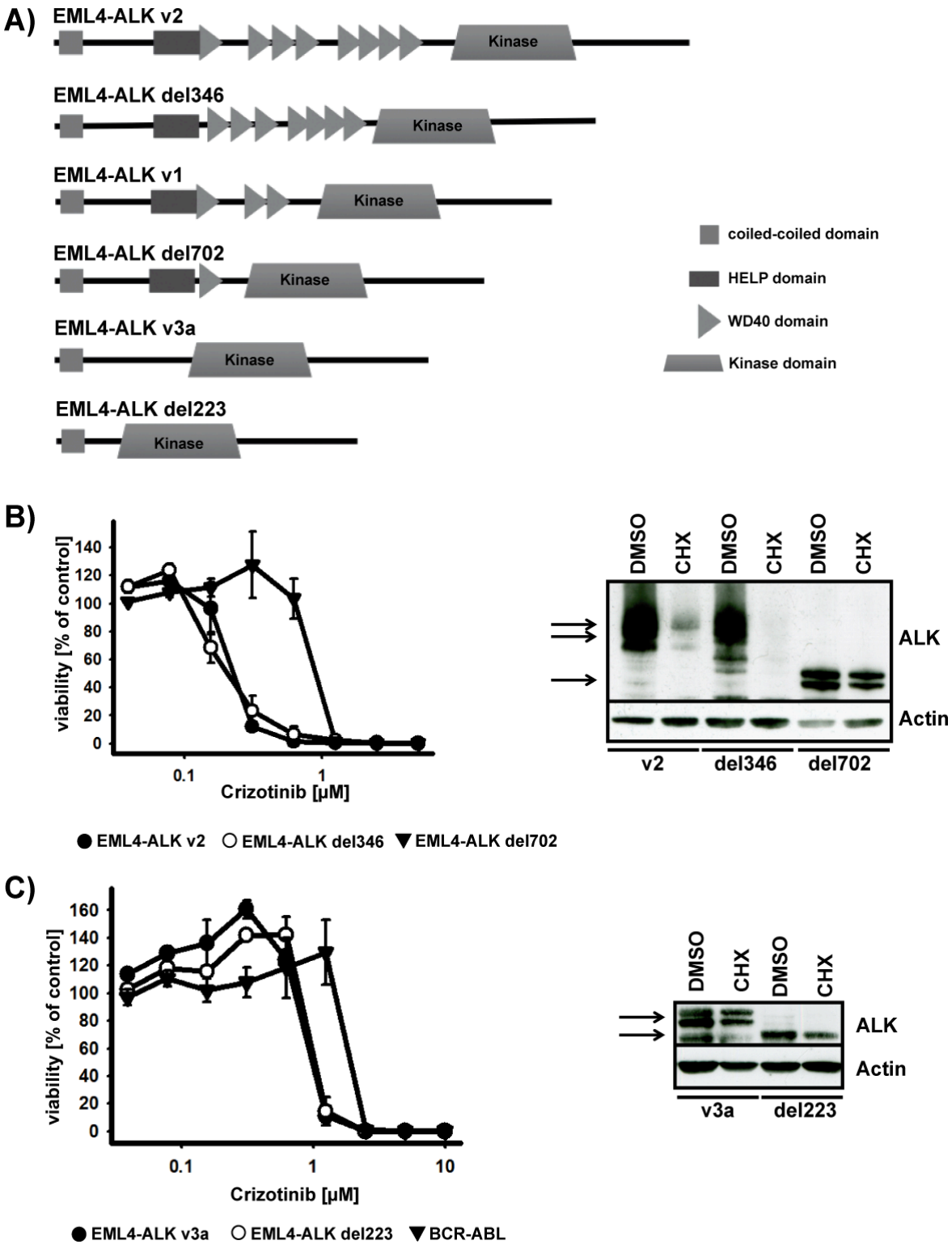

Figure 20 A Schematic presentation of *EML4-ALK v1, v2 and v3a as well as* the deletion constructs *EML4-ALK del346, del702* and *del223.* **B/C** Ba/F3 cells expressing the indicated *EML4-ALK* deletion variants were treated with increasing concentrations of crizotinib before viability was determined after 72 hours. Each data point represents the mean of three independent experiments with triplicate measurements, error bars indicate SEM (left). Whole cell lysates from Ba/F3 cells expressing the indicated *EML4-ALK* deletion variants were prepared after 24 hours treatment with DMSO or 50 µg/ml cycloheximide and stained for total ALK levels by immunoblotting (right).

Overall, these findings indicate that variations in *EML4* can, depending on the affected amino acids, highly influence the overall stability of the EML4-ALK fusion protein. Furthermore, these findings might, to some extend, also translate into the differences in sensitivity to ALK kinase inhibition.

4.1.10 *EML4-ALK* variants induce differential sensitivity to HSP90 inhibition

As stated above, previous publications have shown that *EML4-ALK* expressing cells are sensitive to HSP90 inhibition. Treatment with HSP90 inhibitors leads to a decrease of total ALK protein levels and thereby induces cytotoxicity in *EML4-ALK* expressing cells. Importantly, this effect is independent of ALK inhibitor resistance mutation status (Chen et al., 2010; Katayama et al., 2011; Normant et al., 2011). To explore if different *EML4-ALK* variants induce differential sensitivity to HSP90 inhibition, Ba/F3 cells expressing *EML4-ALK variants 2* and *3a* were treated with increasing concentrations of 17-DMAG, an ansamycin antibiotic derivative. Ba/F3 cells expressing *variant 2* were 2-fold more sensitive to HSP90 inhibition compared to Ba/F3 cells expressing *variant 3a* (GI_{50}s of 115 nM and 226 nM respectively). It must be mentioned, that Ba/F3 cells expressing *EML4-ALK v3a* were almost as sensitive as the IL-3-supplemented control, indicating that other HSP90 clients, and not only the EML4-ALK v3a degradation itself, induced the detected reduction in viability **(Figure 21 A)**. To confirm these results, the synthetic HSP90 inhibitor AUY922 was used to treat *EML4-ALK v2* and *v3a* expressing cells. Here, the same pattern of sensitivity was observed. However, the high intrinsic sensitivity of IL-3-treated cells to this HSP90 inhibitor made these experiments difficult to interpret (compare *EML4-ALK v2* + IL-3 with *EML4-ALK v3a* and *EML4-ALK v3a* + IL-3, **Figure 21 B**). Interestingly, cells expressing *EML4-ALK variant 1* were slightly more sensitive to HSP90 treatment compared to cells expressing *variant 2* **(Figure 22 A)**. These findings show, that ALK kinase inhibitor sensitivity and the intrinsic stability of the fusion protein alone do not predict the sensitivity to HSP90 inhibitors **(**compare **Figures 9, 18, 21** and **Figure 22)**. However, the intrinsic protein stability seems to impact the

dependency on HSP90 chaperonage, since no difference in HSP90 inhibitor sensitivity was observed for Ba/F3 cells expressing *EML4-ALK v3a* and *v3b* **(Figure 22 B)**.

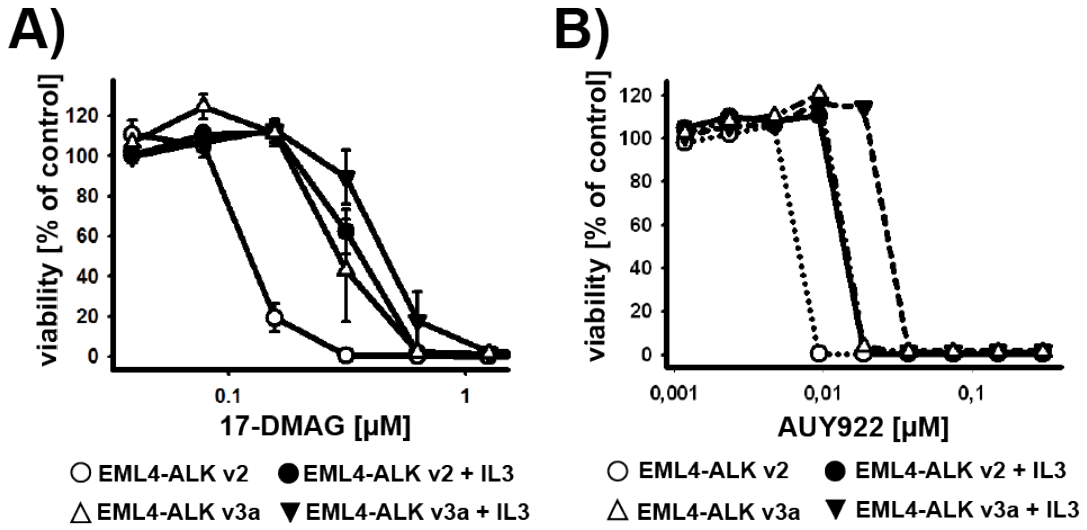

Figure 21 Ba/F3 cells expressing the indicated *EML4-ALK* variants were treated with increasing concentrations of 17-DMAG (**A**) or AUY922 (**B**). Viability was determined after 72 hours and is expressed as a function of compound dose and ATP-content, relative to the DMSO-treated controls. Each data point shows the mean of three independent experiments with triplicate measurements, error bars indicate SEM.

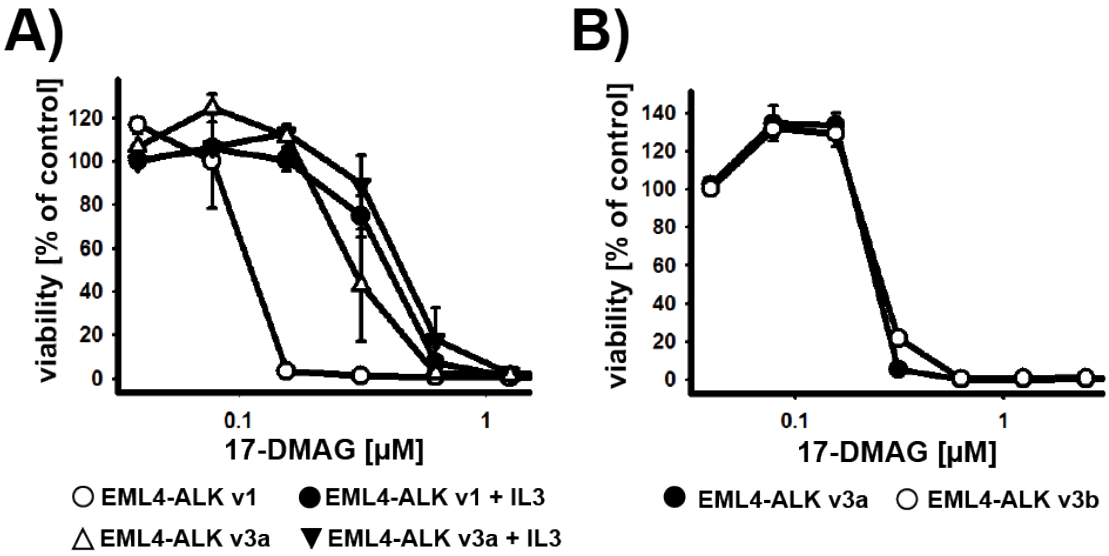

Figure 22 A/B Ba/F3 cells expressing the indicated *EML4-ALK* variants were treated with increasing concentrations of 17-DMAG. Viability was determined after 72 hours and is expressed as a function of compound dose and ATP-content, relative to the DMSO-treated controls. Each data point shows the mean of three (**A**) or two (**B**) independent experiments with triplicate measurements, error bars indicate SEM.

4.1.11 Inhibitor sensitivity and protein stability of other ALK fusions

To analyze the effect of the N-terminal fusion partner on kinase inhibitor sensitivity and protein stability in other *ALK* fusion genes, Ba/F3 cells expressing *KIF5b-ALK* and *NPM1-ALK* were generated **(Figure 23 A)**. Both fusion genes rendered Ba/F3 cells IL-3 independent, as has been described previously (Galkin et al., 2007; Morris et al., 1994; Takeuchi et al., 2009). After treatment with crizotinib, Ba/F3 cells expressing *KIF5b-ALK* were as sensitive as cells expressing *EML4-ALK v2.* Ba/F3 cells expressing *NPM1-ALK* showed a sensitivity pattern similar to *EML4-ALK v1* and *v3b* **(Figure 23 B)**. After treatment with cycloheximide, KIF5b-ALK and NPM1-ALK showed a similar degree of degradation, even though the sensitivity to crizotinib varied substantially **(Figure 23 C)**. EML4-ALK v2 and v3a were again the two fusion proteins with the lowest and highest protein stability respectively. Hence, a correlation between ALK kinase inhibitor sensitivity and overall protein stability only seems to apply for EML4-ALK fusion proteins, with the exception of EML4-ALK v3b.

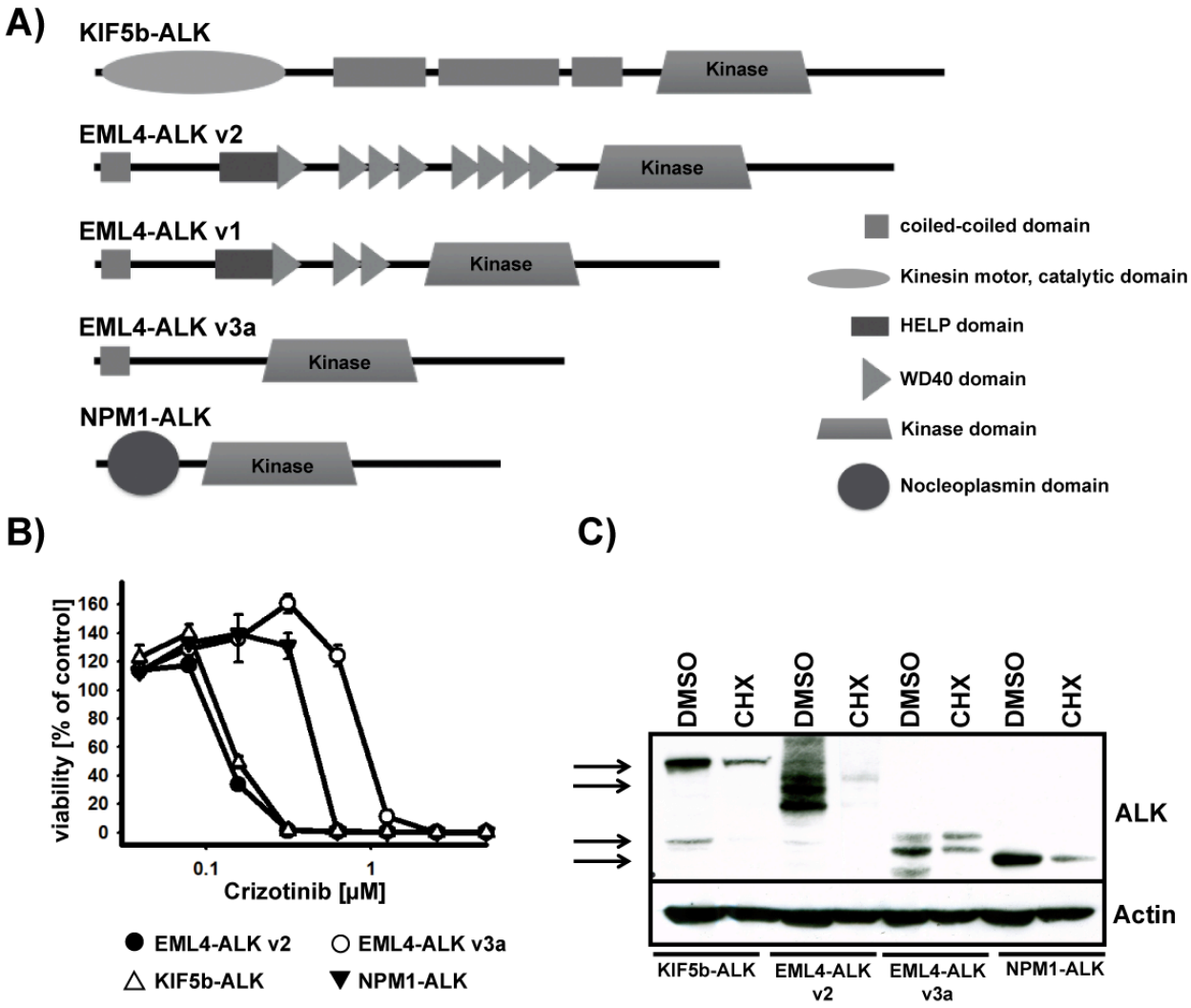

Figure 23 A Schematic presentation of *EML4-ALK variants, KIF5b-ALK* and *NPM1-ALK*. **B** Ba/F3 cells expressing the indicated *ALK* fusion genes were treated with increasing concentrations of crizotinib. Viability was determined after 72 hours and is expressed as a function of compound dose and ATP-content, relative of the DMSO-treated control. Each data point shows the mean of two independent experiments with triplicate measurements, error bars indicate SEM. **C** Ba/F3 cells expressing the indicated *ALK* fusion genes were treated with DMSO or 50 µg/ml cycloheximide for 24 hours. Whole cell lysates were prepared and stained for total ALK by immunoblotting.

4.1.12 Synergistic effects after combined ALK and HSP90 inhibitor treatment

Treatment of *EML4-ALK v1* and *EML4-ALK v2* expressing Ba/F3 cells with HSP90 or ALK inhibitors revealed different sensitivity patterns for these two inhibitors respectively. Thus, sensitivity to ALK and HSP90 inhibition seems to be mediated by different

mechanisms and might therefore lead to an additive effect in a combined treatment. To test this hypothesis, *EML4-ALK v1, v2* and *v3a* as well as *KIF5b-ALK* and *BCR-ABL* expressing Ba/F3 cells were treated with increasing concentrations of one of the two inhibitors alone or both compounds combined, each at the same concentration. Strikingly, in all *ALK* fusion-gene expressing cells, treatment with increasing concentrations of crizotinib or 17-DMAG alone was less cytotoxic compared to the combined treatment **(Figure 24 A)**. Further analysis using an algorithm generated by Martin Peifer et al. revealed a synergistic effect in all *ALK* fusion-gene expressing cells, but not in *BCR-ABL* expressing Ba/F3 cells **(Figure 24 B)** (Peifer et al., 2010). The combined compound concentration leading to the highest synergistic effect varied depending on the respective fusion gene. In *EML4-ALK v2* and *KIF5b-ALK* expressing cells, the highest synergy was observed at 80 nM of crizotinib and 17-DMAG, whereas the highest synergy in *EML4-ALK v3a* expressing cells was observed at 160 nM of each inhibitor. GI_{50} values for the combined treatment, calculated under the assumption that both compounds are equally concentrated, were 1.2- to 2.3-fold lower in these cells compared to the single drug GI_{50} of the more potent compound **(Table 2, ratio 1, page 61)**. For unknown reasons, combination treatment in *EML4-ALK v1* expressing cells induced the lowest synergy in all *ALK* fusion-gene expressing cells **(Figure 24 A/B)**. Interestingly, the higher the ratio between the higher and the lower GI_{50} value of single HSP90 and ALK inhibitor treatments, the lower the synergy after combination treatment **(Table 2, ratio 2, page 61).** As expected, *BCR-ABL* expressing cells did not show any synergistic cytotoxic effects after the combined treatment of HSP90 and ALK inhibitors. Here, only the effect of HSP90 inhibition reduced cellular viability, which could not be enhanced by ALK kinase inhibition **(Figure 24 A)**.

Table 2 GI_{50} values (nM) of crizotinib, 17-DAMG or an equal combination of both compounds in Ba/F3 cells expressing different fusion genes.

	crizotinib	17-DMAG	combination	ratio 1	ratio 2
EML4-ALK v1	309	69	56	1.23	4.48
EML4-ALK v2	129	115	55	2.09	1.12
EML4-ALK v3a	713	226	124	1.82	3.15
KIF5b-ALK	145	205	63	2.30	1.41
BCR-ABL	1880	147	126	1.17	12.79

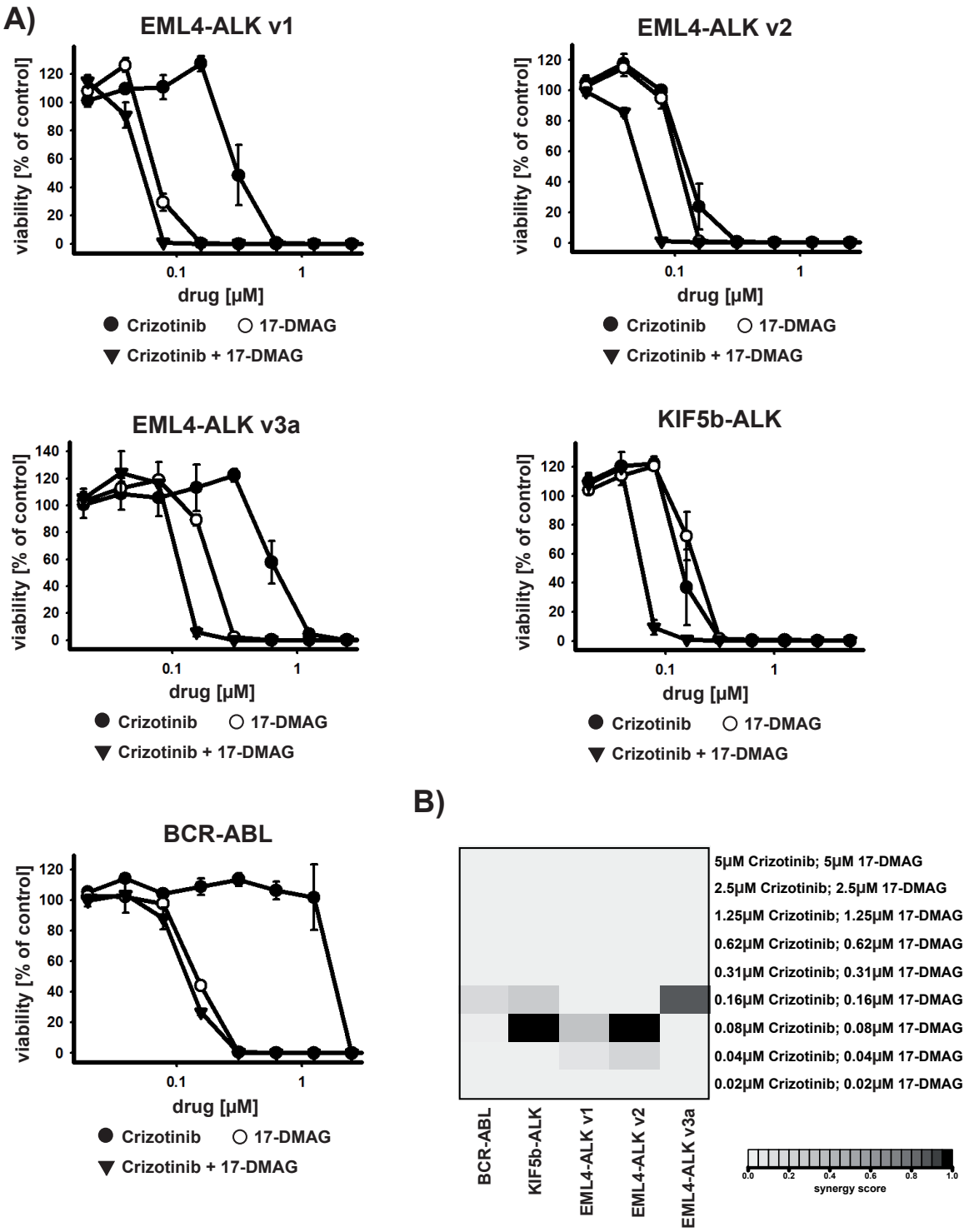

Figure 24 A Ba/F3 cells expressing the indicated fusion genes were treated with increasing concentrations of crizotinib, 17-DMAG or both compounds combined (at equal concentrations). Viability was determined after 96 hours and is expressed as a function of compound dose and ATP-content relative to the DMSO-treated control. Each data point shows the mean of two independent experiments with triplicate measurements, error bars indicate SEM. **B** Viability data was analyzed for synergy and visualized as a heatmap.

Thus, different *ALK* fusion genes show differences in protein stability and induce differential sensitivity to ALK and HSP90 inhibitors, which might explain some of the heterogeneous responses to crizotinib treatment in the clinic. Furthermore, combining ALK and HSP90 inhibitors results in synergistic cytotoxicity in *ALK* fusion gene expressing cells

4.2 Different *EML4-ALK* mutations confer various levels of resistance to structurally diverse ALK kinase inhibitors

4.2.1 Known crizotinib resistance mutations are highly sensitive to TAE684

In 2010, a L1196M "gatekeeper mutation" has been reported in an *EML4-ALK* positive patient that has been treated with crizotinib for 5 month before relapse (Choi et al., 2010). Furthermore, the same mutation has been described one year later in an experimentally raised crizotinib resistant *EML4-ALK* positive cell line (Katayama et al., 2011). In the case of L1196M, as it is known for many other "gatekeeper mutations", the bulky methionine side chain is thought to interfere with inhibitor binding (Choi et al., 2010). However, structural modeling of this mutation suggested that a structurally unrelated ALK kinase inhibitor, like the diamino-pyrimidine scaffold of TAE684, should still be able to bind the mutated kinase (Galkin et al., 2007). In addition to this "gatekeeper mutation", another mutation, F1174L, has been described in a patient with an inflammatory myofibroblastic tumour (IMT) (Butrynski et al., 2010; Sasaki et al., 2010a). This patient has been treated with crizotinib, but showed disease progression. Sequencing of the tumor revealed the F1174L mutation in the kinase domain of the translocated *ALK*, which has been previously described as a kinase-activating mutation in neuroblastoma (Chen et al., 2008; George et al., 2008; Janoueix-Lerosey et al., 2008; Mosse et al., 2008; Sasaki et al., 2010a). Thus, the activating nature of the F1174L mutation decreases the sensitivity to the type-II kinase inhibitor crizotinib, which only

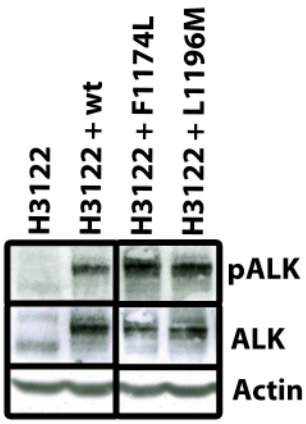

Figure 25 Whole cell lysates from H3122 cells expressing the indicated *EML4-ALK* cDNAs were stained for protein levels of pALK, ALK and Actin (Heuckmann et al., 2011).

binds to the inactive kinase conformation of ALK. The type-I kinase inhibitor TAE684 however, binds to the active kinase conformation of ALK and thus, should be able to overcome resistance mediated by this mutation (Galkin et al., 2007). To test these hypotheses, both mutations were expressed in the *EML4-ALK v1* positive NSCLC cell line H3122 **(Figure 25)**. At that time, the purified R-enantiomer crizotinib was not commercially available, which is why the racemic mixture (PF02341066) was used. As expected, both mutations induced resistance to PF02341066 **(Figure 26)**. More precisely, *EML4-ALK*^{F1174L} only induced resistance at lower concentrations of PF02341066, but was sensitive to higher compound concentrations. The L1196M mutation also induced resistance to high concentrations of PF02341066. After treating these cells with TAE684, both mutants were highly sensitive to kinase inhibition, with the F1174L expressing cells being exceptionally sensitive **(Figure 26)**.

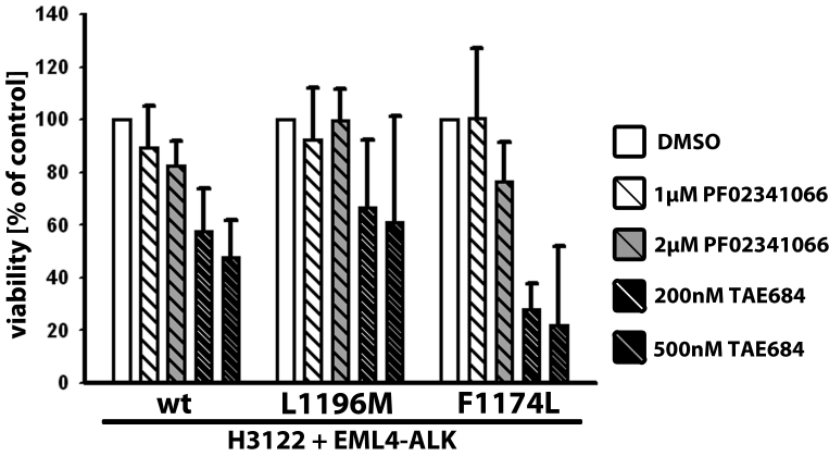

Figure 26 *EML4-ALK* cDNA expressing H3122 cells were treated with PF02341066 or TAE684. After 96 hours of treatment, viable and dead cells were counted using trypan-blue (Heuckmann et al., 2011).

4.2.2 Novel crizotinib resistance mutation increases ALK kinase activity

To validate these finding in an independent cell line model, both mutated fusion genes were expressed in Ba/F3 cells and treated with increasing concentrations of both compounds. In addition to the two resistance mutations described above, another mutation, G1269S (located adjacent to the DFG-motif of the kinase), was expressed in these cells. Structural modeling of this mutation, performed by Daniel Rauh and colleagues, suggested a steric clash with PF02341066, but not with TAE684 **(Figure 27)**. Immunoblotting of these mutated fusion proteins showed an increased basal ALK phosphorylation in *EML4-ALK*^{F1174L} and *EML4-ALK*^{G1269S} expressing cells, but not in *EML4-ALK*^{L1196M} expressing cells **(Figure 28 A)** (Choi et al., 2010; Sasaki et al., 2010a). As expected, the expression of F1174L led to a slight increase in resistance, whereas the mutations L1196M and G1269S induced a high level of resistance to PF02341066

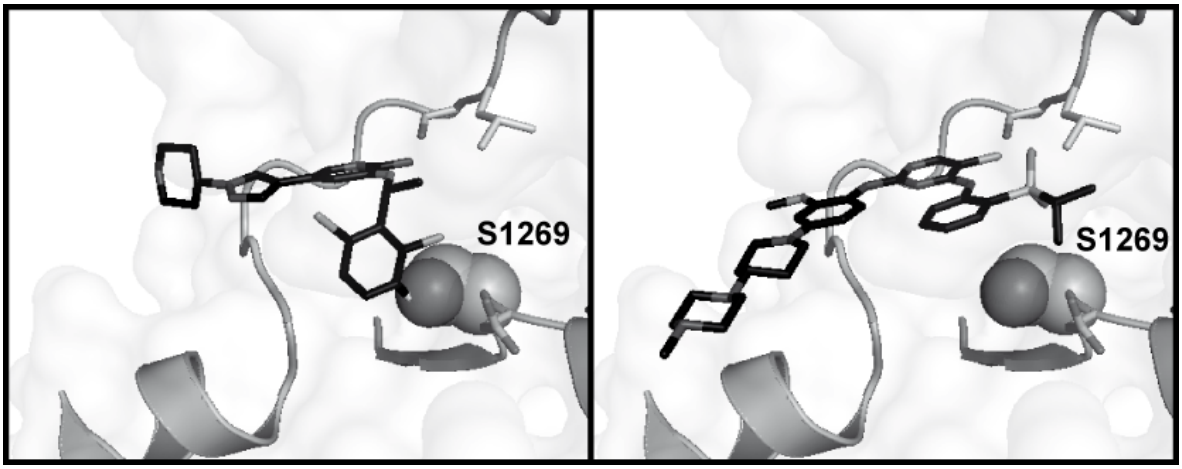

Figure 27 Crystal structures of ALK bound to PF02341066 (left) and TAE684 (right). Serine residue 1269 is shown as sphere to highlight steric hindrance induced by the G1269S mutation. PyMol file was generated by Chritian Grütter, TU Dortmund, Germany.

(Figure 28 B). Again, all resistance mutations were sensitive to treatment with TAE684, with the activating mutations (*EML4-ALK*^{F1174L} and *EML4-ALK*^{G1269S}) being extremely sensitive compared to *EML4-ALK*^{wt} and *EML4-ALK*^{L1196M} **(Figure 28 C)**. In line with these findings, the phosphorylation of ALK in these mutants was completely abolished after treatment with 30 nM TAE684, but remained unchanged after treatment with up to 2.5 µM of PF02341066 **(Figure 29)**.

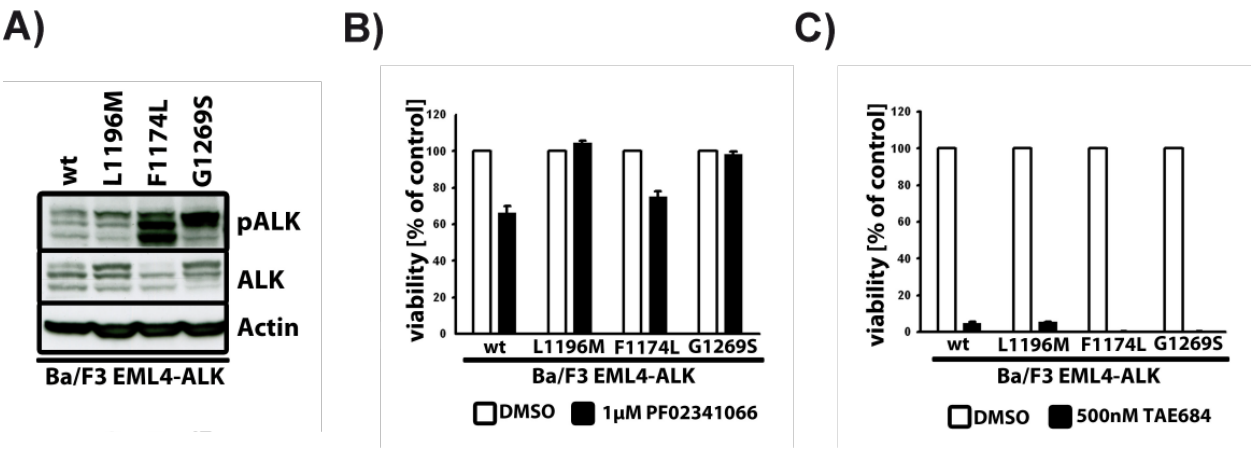

Figure 28 A Whole cell lysates of Ba/F3 cells expressing the indicated *EML4-ALK* cDNAs were stained for pALK, ALK and Actin protein levels. **B/C** Ba/F3 cells expressing the indicated mutations of *EML4-ALK* were treated with PF02341066 (**B**) or TAE684 (**C**). After 48 hours of treatment, viable and dead cells were counted using trypan-blue, error bars indicate SEM of three independent experiments (Heuckmann et al., 2011).

Thus, kinase-activating mutations (F1174L and G1269S) can induce resistance to the type-II inhibitor PF02341066, which can be overcome by TAE684 due to its ability to bind the active kinase conformation. Structural modeling of TAE684 bound to G1269S mutated ALK however suggests that an amino acid larger than serine might, due to steric hindrance, be able to induce resistance to TAE684 **(Figure 27)**. Steric hindrance is also the proposed resistance mechanism for the L1196M mutation and PF02341066. Here, TAE684 is able to overcome the induced resistance by a different binding mode that prevents the approximation to the M1196 residue (Choi et al., 2010; Katayama et al., 2011).

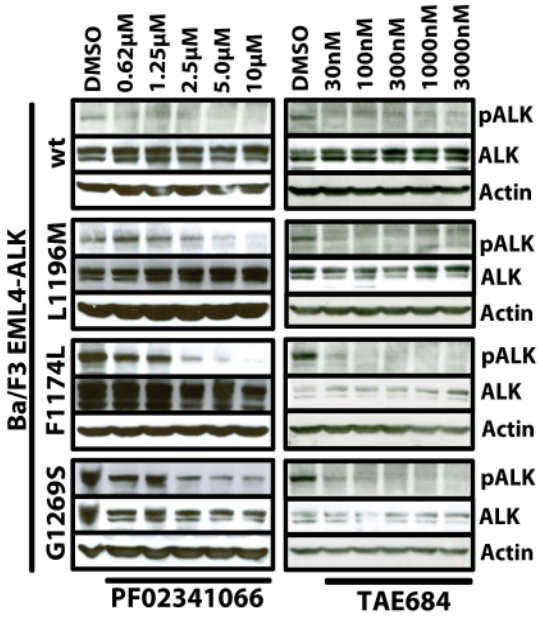

Figure 29 Ba/F3 cells expressing the indicated *EML4-ALK* mutations were treated with PF02341066 (left) or TAE684 (right). ALK phosphorylation was monitored by immunoblotting after 6 hours of treatment (Heuckmann et al., 2011).

4.2.3 Novel *EML4-ALK* resistance mutations induce resistance to crizotinib and TAE684

In order to discover additional *ALK* resistance mutations, two functional saturation mutagenesis screens were performed (Azam et al., 2003; Emery et al., 2009). First, *EML4-ALK v3a* cDNAs were randomly mutagenized by propagation in repair-deficient *E.coli*. The harvested cDNAs were used to generate virus particles for Ba/F3 cell transduction (Yuza et al., 2007). After transduction, cells were cultured without exogenous IL-3, but with different concentrations of PF02341066 (750 nM, 1000 nM, 1500 nM) to select for cells with (i) an active ALK kinase and (ii) an ALK kinase that is resistant to PF02341066 kinase inhibition **(Figure 30)**. Resistant cells were expanded and genomic DNA was isolated for massively parallel picoliter reactor pyrosequencing-by-synthesis sequencing of the *EML4-ALK* fusion gene (Thomas et al., 2006). The most predominant mutations were L1198P (49%) and D1203N (12%), two novel resistance mutations **(Figure 31 A)**.

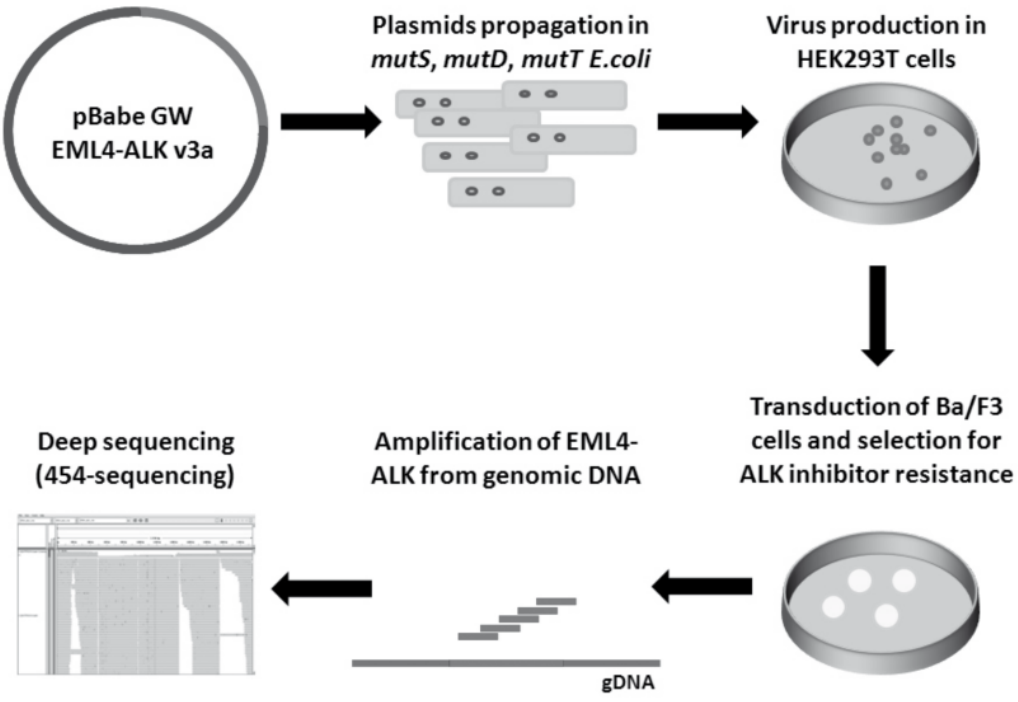

Figure 30 Schematic presentation of the “saturated mutagenesis” screen (Heuckmann et al., 2011).

Interestingly, both mutations induced resistance not only to PF02341066 (*v3a* wt GI_{50}: 1.5 µM; L1198P GI_{50}: 3.4 µM; D1203N GI_{50}: 3.4 µM), but also to TAE684 (*v3a* wt GI_{50}: 56 nM; L1198P GI_{50}: 624 nM; D1203N GI_{50}: 604 nM) **(Figure 31 B)**. To verify these findings, the respective mutations were introduced into the *EML4-ALK*^{wt} plasmid by site

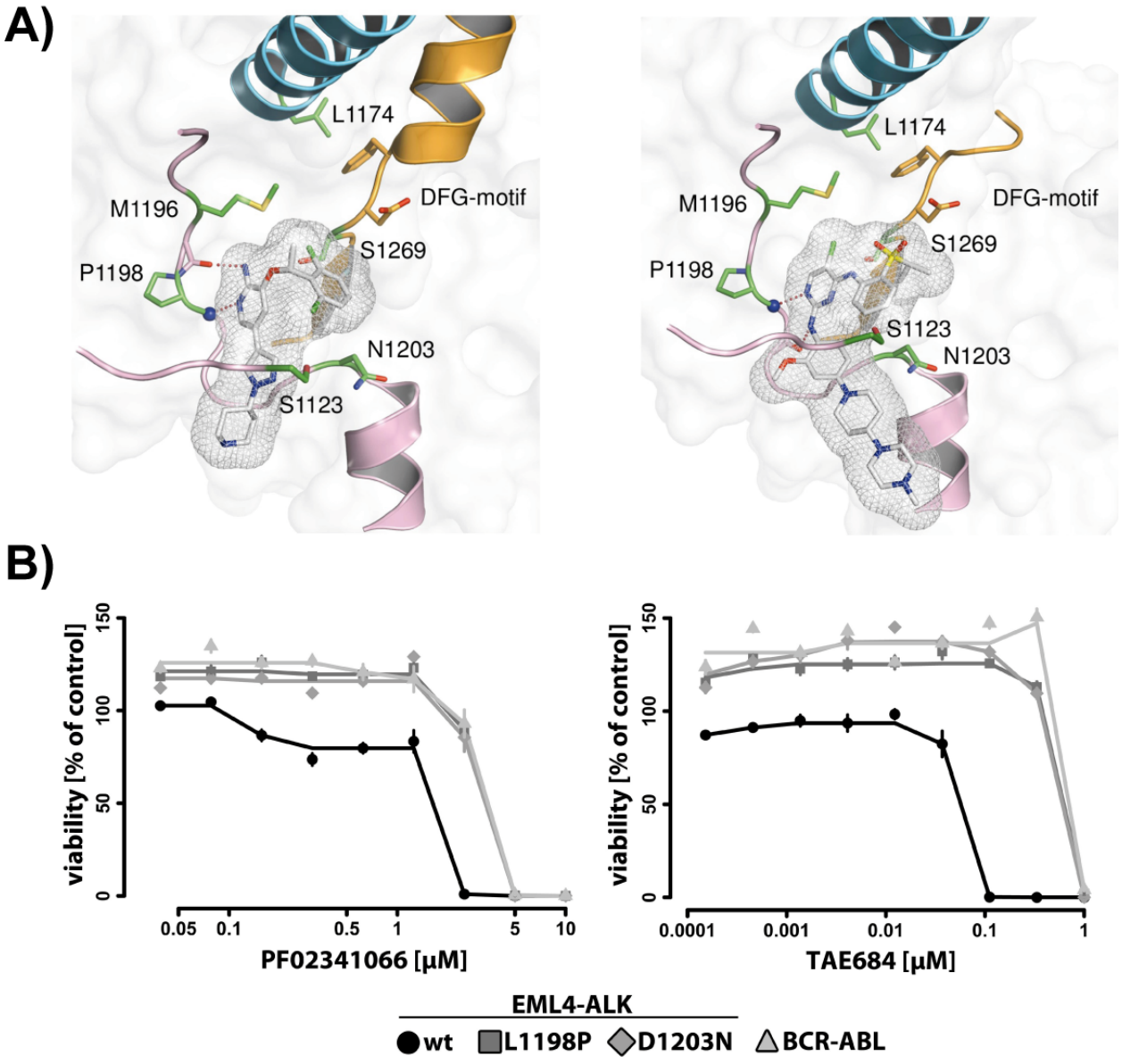

Figure 31 A Crystal structures showing PF02341066 (left) and TAE684 (right) bound to ALK. Amino acids that confer resistance to ALK inhibitors if mutated are indicated (G1123S, F1174L, L1196M, L1198P, D1203N, G1269S) (picture by Christian Grütter, TU Dortmund, Germany) **B** Polyclonal Ba/F3 cultures expressing the indicated resistance mutations were treated with increasing concentrations of PF02341066 (left) or TAE684 (right). Viability was determined after 96 hours of treatment and is expressed as a function of compound dose and ATP-content relative to DMSO-treated controls (Heuckmann et al., 2011).

directed mutagenesis to ensure the expression of only one mutation per clone. *EML4-ALK*^{L1198P} expressing Ba/F3 cells showed a general increase in kinase activity, thereby explaining the resistance to PF02341066 **(Figure 32 A)**. Counting of viable cells after ALK kinase inhibitor treatment using trypan-blue confirmed the previous results **(Figure 32 B)**. Furthermore, resistance by L1198P was characterized by stable ALK phosphorylation at concentrations up to 2.5 µM of PF02341066 and 300 nM of TAE684 **(Figure 32 C)**. The same applied for the resistance mutation D1203N, even though this effect was less pronounced. Furthermore, the D1203N mutation did not increase the basal kinase activation, showing that increased kinase activation is not the resistance mechanisms to PF02341066 for this mutation **(Figure 33 A/B)**.

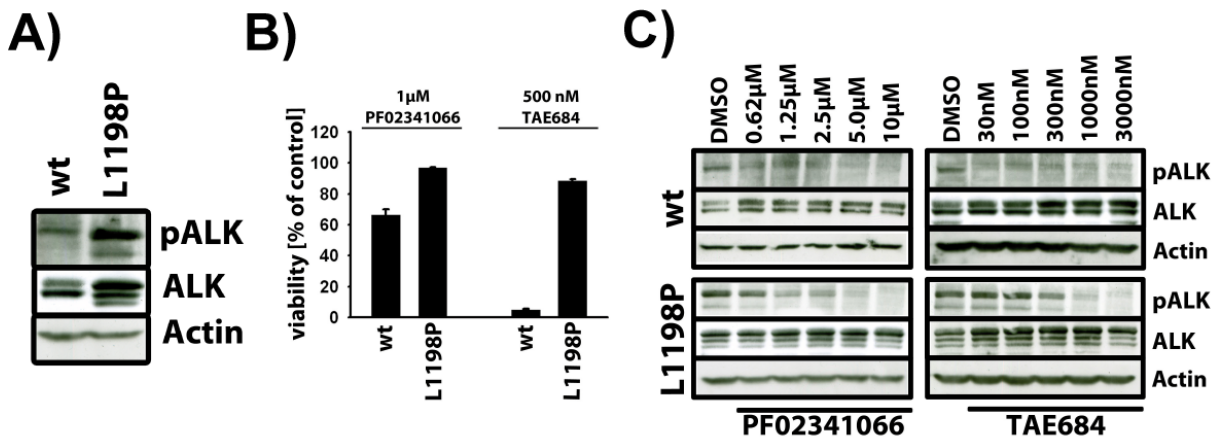

Figure 32 A *EML4-ALK*^{wt} and *EML4-ALK*^{L1198P} expressing Ba/F3 cells were lysed and stained for phosphorylation of ALK. **B** *EML4-ALK*^{wt} and *EML4-ALK*^{L1198P} expressing Ba/F3 cells were treated with 1 µM of PF02341066 or 500 nM of TAE684 respectively. Viable cells were counted using trypan blue after 48 hours of treatment. **C** Ba/F3 cells stably expressing *EML4-ALK*^{wt} or *EML4-ALK*^{L1198P} were treated with increasing concentrations of ALK inhibitor. Whole cell lysates were stained for ALK phosphorylation. Actin was used as loading control (Heuckmann et al., 2011).

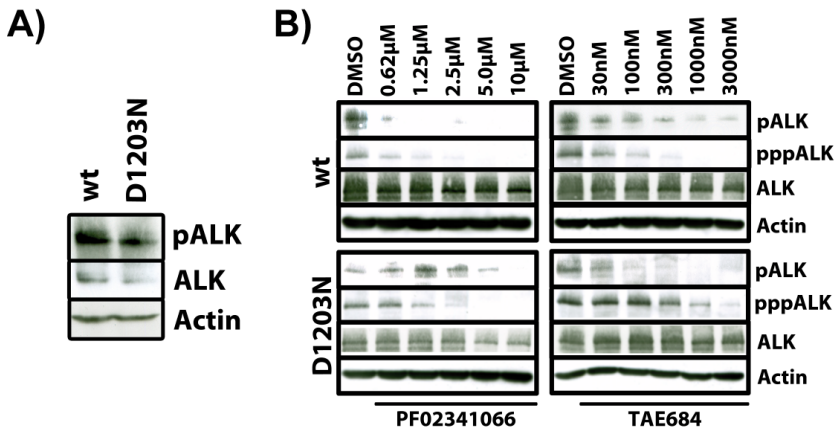

Figure 33 A *EML4-ALK*^{wt} and *EML4-ALK*^{D1203N} expressing Ba/F3 cells were lysed and stained for phosphorylation of ALK. **B** Ba/F3 cells stably expressing *EML4-ALK*^{wt} or *EML4-ALK*^{D1203N} were treated with increasing concentrations of ALK inhibitor. Whole cell lysates were stained for ALK phosphorylation. Actin was used as loading control (Heuckmann et al., 2011).

To verify these findings in an orthogonal mutagenesis screen, *EML4-ALK* expressing Ba/F3 cells were treated with the chemical mutagen N – etyl – N - nitrosourea (ENU) (Bradeen et al., 2006). After ENU treatment, cells were cultured in different concentrations of PF02341066 (750 nM, 1000 nM, 1500 nM) until resistant clones emerged **(Figure 34)**. Here again, most of the resistant cells expressed the L1198P mutations and showed a high degree of resistance to treatment with PF02341066 and TAE684 **(Figure 35)**.

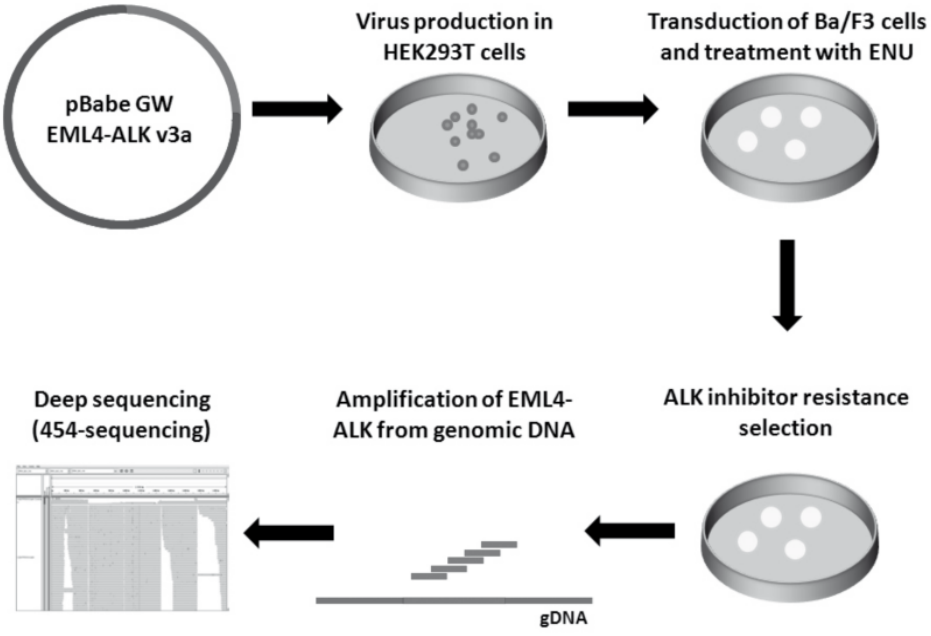

Figure 34 Schematic presentation of the N-ethyl-N-nitrosourea mutagenesis screen (Heuckmann et al., 2011).

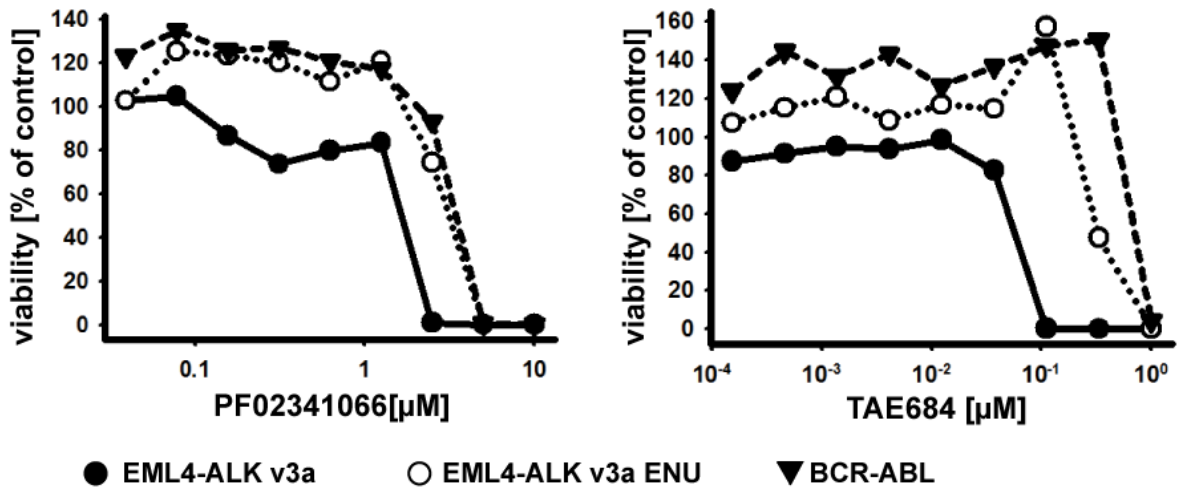

Figure 35 ALK inhibitor resistant *EML4-ALK* expressing Ba/F3 cells that emerged after ENU treatment were incubated with increasing concentrations of PF02341066 (left) or TAE684 (right). Viability was measured after 96 hours of treatment and is expressed as a function of compound dose and ATP-content, relative to DMSO-treated controls.

In reference to the differential ALK kinase inhibitor sensitivity observed for different *EML4-ALK* variants, the L1198P mutation was introduced into *EML4-ALK v2.* As expected, treatment of *EML4-ALK v2* and *EML4-ALK v2*^{L1198P} expressing Ba/F3 cells with TAE684 revealed a dramatic increase in resistance of the mutated cells **(Figure 36)**. Thus, depending on the sensitivity of the wild type *EML4-ALK* variant, the L1198P mutation can induce a more than 100-fold increase in resistance (here; *EML4-ALK v2*^{wt}: GI_{50} 0.15 nM, *EML4-ALK v2*^{L1198P}: GI_{50} 190 nM)

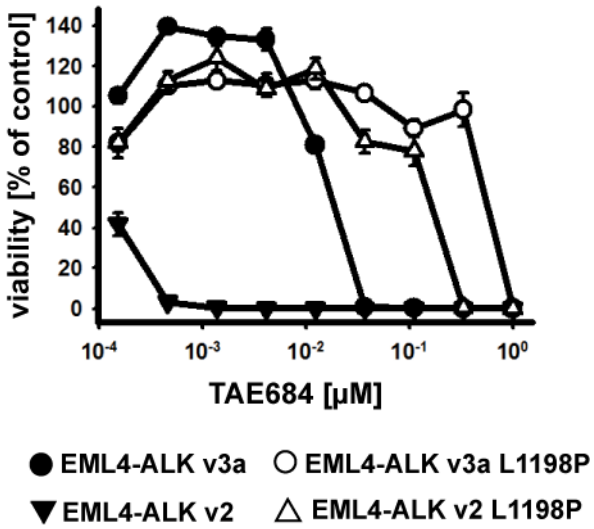

Figure 36 Ba/F3 cells expressing the indicated *EML4-ALK* cDNAs were treated with increasing concentrations of TAE684. Viability is shown as a function of compound dose and ATP-content, relative to DMSO-treated controls. Error bars indicate SEM.

4.2.4 Mechanisms of resistance in L1198P mutated ALK

To explain the resistance phenotype induced by *EML4-ALK*^{L1198P}, Daniel Rauh and colleagues performed structural modeling of L1198P in the crystal structure of ALK. Most *in-cis* resistance mutations that are known today shift the kinase

equilibrium towards a higher kinase activity (e.g. F1174L mutations in *ALK*) or show direct contact with the inhibitor (e.g. T790M mutations in *EGFR*). The L1198P mutation is localized in the hinge region of the kinase, a region where ATP, PF02341066 and TAE684 bind. Leucine 1198 lies between two residues that form key hydrogen bonds to the backbone of PF02341066, and are therefore essential for inhibitor binding **(Figure 31 A)**. One of these residues, E1197, forms hydrogen bonds to K1267 and R1181 **(Figure 37)**. This interaction has recently been described as “molecular brake”, by shifting the equilibrium of the kinase into the more inactive state. This interaction network is proposed to be a common mechanism to regulate kinase activation (Chen et al., 2007). Even though leucine 1198 does not directly participate in this hydrogen

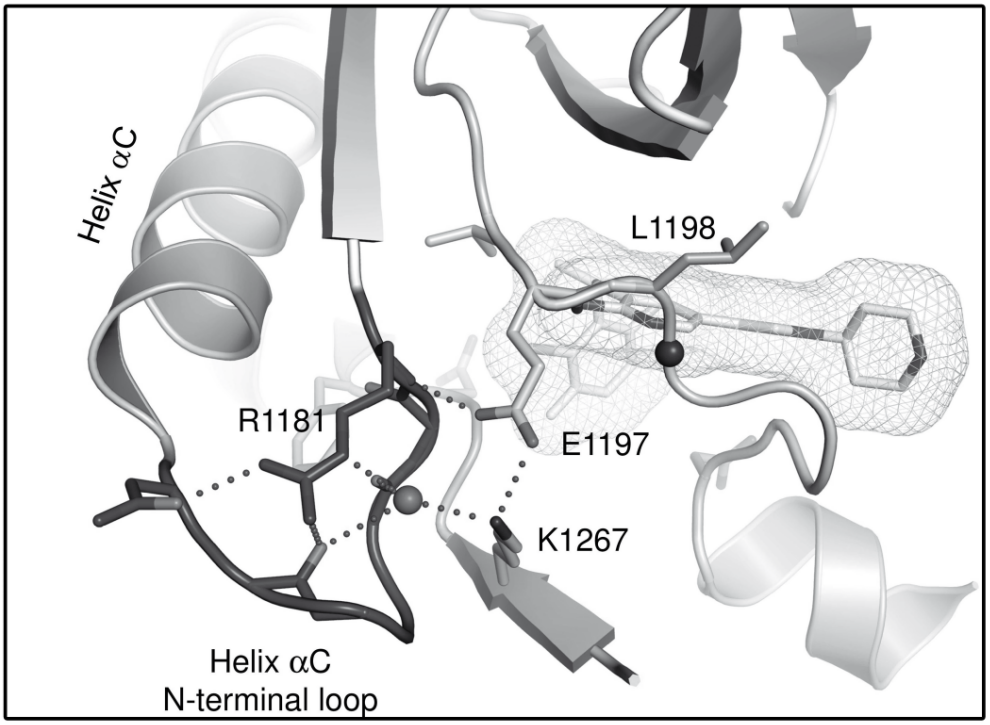

Figure 37 Crystal structure of PF02341066 bound to the ALK kinase domain. The side chain of E1197 forms hydrogen bonds with K1267 at the N-terminal end of a loop segment that is connected to the activation loop. These interactions form the “molecular brake” that might be perturbed in L1198P mutated kinases. Picture by Christian Grütter, TU Dortmund, Germany (Heuckmann et al., 2011).

network, it is known that proline residues can perturb the three dimensional arrangement of protein backbones (MacArthur and Thornton, 1991). Thus, the L1198P mutation might destroy the hydrogen network of the neighboring residues by changing

the protein backbone. This perturbation of the “molecular brake” could then lead to the increase of basal kinase activity that was observed in L1198P mutated cells, a mechanism to induce resistance to PF02341066 **(Figure 31, Figure 32)**. In addition, crystal structures of ALK and TAE684 show, that the methoxy-group of TAE684 binds into a small cavity between the hinge region and the N-lobe of the kinase **(Figure 38)** (Bossi et al., 2010; Galkin et al., 2007). As mentioned above, the L1198P mutation should perturb the three dimensional arrangement of the protein backbone and might therefore disturb TAE684 binding **(Figure 38)**.

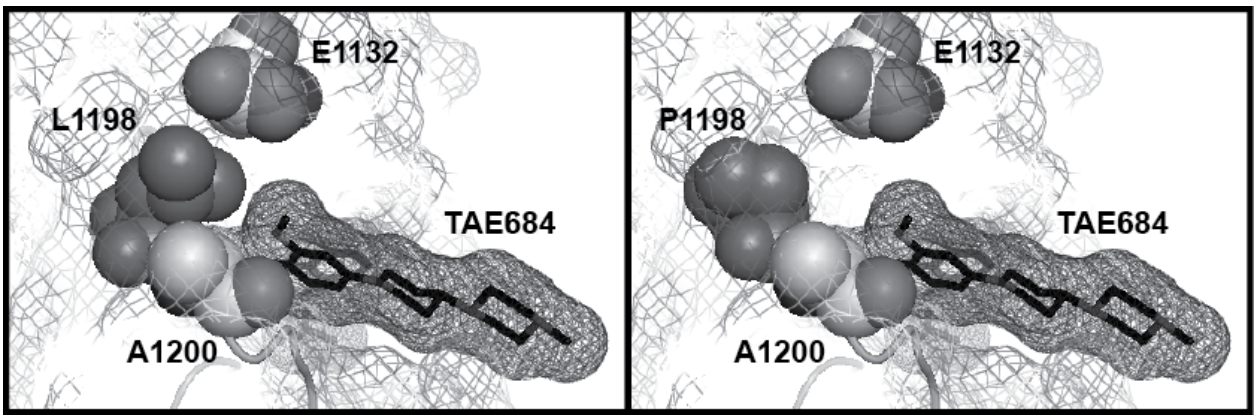

Figure 38 Crystal structure of TAE684 (black sticks) bound to the ALK kinase domain (PDB-code: 2XB7). The surface of the kinase and the compound are indicated as gray mesh. Amino acids forming a cavity that interacts with the methoxy-group of TAE684 are shown as spheres and labeled accordingly. L1198 (left) and P1198 (right) are shown as dark gray spheres.

4.2.5 Mechanisms of resistance in D1203N mutated ALK

The D1203N mutation lies at the lip of the ATP pocket and is in close proximity to both ALK inhibitors studied **(Figure 31 A)**. However, the aspartatic acid and asparagine side chains point away from the inhibitors and towards the solvent, making a steric interaction as mechanism of resistance highly unlikely. In addition, the D1203N mutation does not increase the basal kinase activity. Thus, the mechanism of resistance for this mutation is currently unknown. However, a recent study from Katayama et al. found a G1202R mutation in an *EML4-ALK* positive, but crizotinib resistant tumor which induced resistance to crizotinib and TAE684 in a cellular model (Katayama et al., 2012). Hence, mutations at this specific region of ALK seem to mediate resistance to both ALK kinase inhibitors tested.

Thus, resistance induced by the mutations F1174L, L1196M and G1269S can be overcome by ALK inhibitors that bind to the active kinase conformation (type-I inhibitors) or that avoid interference with certain amino acid side chains (Sun et al., 2010). Furthermore, two novel resistance mutations (L1198P and D1203N) were shown to induce resistance to PF02341066 and TAE684, in the case of the L1198P mutation, most likely due to an increase in kinase activity and structural alterations of the kinase that hamper compound-kinase interactions.

4.3 Overexpression of a novel fusion gene in ALK inhibitor resistant H3122 cells

4.3.1 ALK kinase inhibitor resistant H3122 cells

All resistance mechanisms described so far were defined by point mutations within the *ALK* kinase domain. However, several tumors have been shown to develop gene amplifications (e.g. *MET* amplifications in *EGFR* mutated tumors) or other genetic events (e.g. aberrant splicing of *BRAF* in *BRAF* mutated cells) as resistance mechanisms (Engelman et al., 2007; Poulikakos et al., 2011; Turke et al., 2010). In order to analyze potential resistance mechanisms in *EML4-ALK* expressing cells in an unbiased fashion, H3122 cells were cultured with steadily increasing concentrations of PF02341066. H3122 cells express *EML4-ALK variant 1* and have a GI_{50} of ≈ 1 µM if treated with PF02341066. After starting with 30 nM of PF02341066, drug concentrations were steadily increased as soon as cell became 90% confluent, up to concentrations of 3 µM (designated as H3122 PR). At the same time, H3122 cells were treated with increasing concentrations of TAE684, up to concentrations of 1 µM (designated as H3122 TR). Viability measurements after treatment with increasing concentrations of PF02341066 showed a shift in GI_{50} values up to 6 µM, including the H3122 TR clone **(Figure 39)**. Interestingly, all polyclonal H3122 PR clones also showed a high degree of resistance to TAE684 with a shift of GI_{50} values from 18 nM up to 10 µM **(Figure 39)**. Thus, cross-resistance developed in all resistant H3122 clones, independently of the

inhibitor used to establish the cells. Sequencing of the complete *ALK* kinase domain in all of these clones did not reveal any mutations, indicating a resistance mechanism *in-trans*.

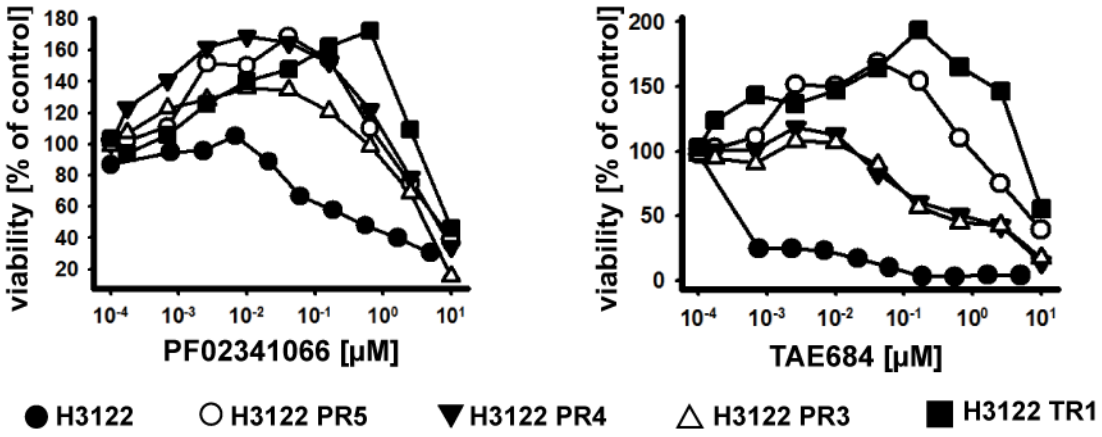

Figure 39 H3122 and ALK inhibitor resistant H3122 clones were treated with increasing concentrations of PF02341066 (left) or TAE684 (right). Viability is shown as a function of compound dose and ATP-content, relative to DMSO-treated controls.

4.3.2 Co-occurring fusion genes in the *EML4-ALK* positive H3122 cell-line

To search for the novel “driver lesion” that induces resistance to ALK inhibition in these cells, RNA was isolated from the sensitive (H3122) and the resistant (H3122 PR1) cells to perform RNA-seq. As expected, the *EML4-ALK variant 1* fusion transcript was detected in both clones with the same coverage (31-fold). In addition, a novel fusion gene, *SOS1-ADCY3,* was detected and further validated by RT-PCR. Surprisingly, the resistant and the sensitive H3122 clones expressed this fusion gene with identical coverage (32-fold), indicating that this fusion was not acquired in the ALK inhibitor resistant cells. Furthermore, the similar mRNA levels of *EML4-ALK* and *SOS1-ADCY3* show that transcriptional changes in the expression of these fusion genes are not responsible for the resistant phenotype **(Figure 40)**.

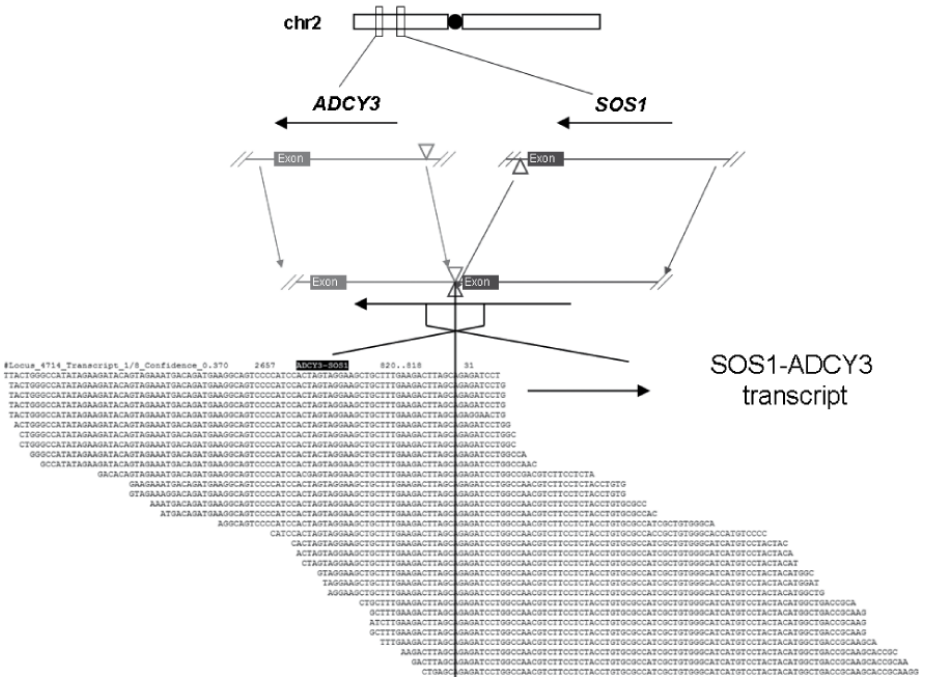

Figure 40 Schematic representation of the fusion transcript of *SOS1-ADCY3* and the location of each gene on chromosome 2. Below, breakpoint spanning reads from RNAseq are shown. (data generated by Lynnette Fernandez-Cuesta, Max-Planck-Insitute for neurological research, Cologne, Germany).

The *SOS1-ADCY3* transcript consists of the first seven exons of *SOS1* and exon 2-21 of *ADCY3*. To confirm the gene fusion on a genomic level, Roopika Menon designed a break-apart FISH assay. Therefore, a green- and a red-labeled bacterial artificial chromosome (BAC) are used for hybridization at the centromeric and telomeric end of each gene respectively. On a non-translocated chromosome, both dyes map close to each other, leading to a yellow (mixed green and red) light signal. If a translocation occurs, both probes map to more distant locations on the chromosome (or on different chromosomes), leading to a separate green and red signal **(Figure 41 A)**. Sometimes, a loss of one of the signals may happen, as it has been the case for the *SOS1* and *ADCY3* probes in H3122 cells, thereby confirming translocations of these two genes **(Figure 41 A/B)**. Furthermore, a fusion assay (combining a *SOS1* and an *ADCY3* probe) confirmed the genomic fusion of these two genes **(Figure 41 B)**. In order to determine if the generation of *SOS1-ADCY3* was genetically linked to *EML4-ALK*, a double-fusion assay including FISH probes for *ADCY3* and *ALK* was established. Here, the finding that each of the *ADCY3* and *ALK* FISH assays generated a single green

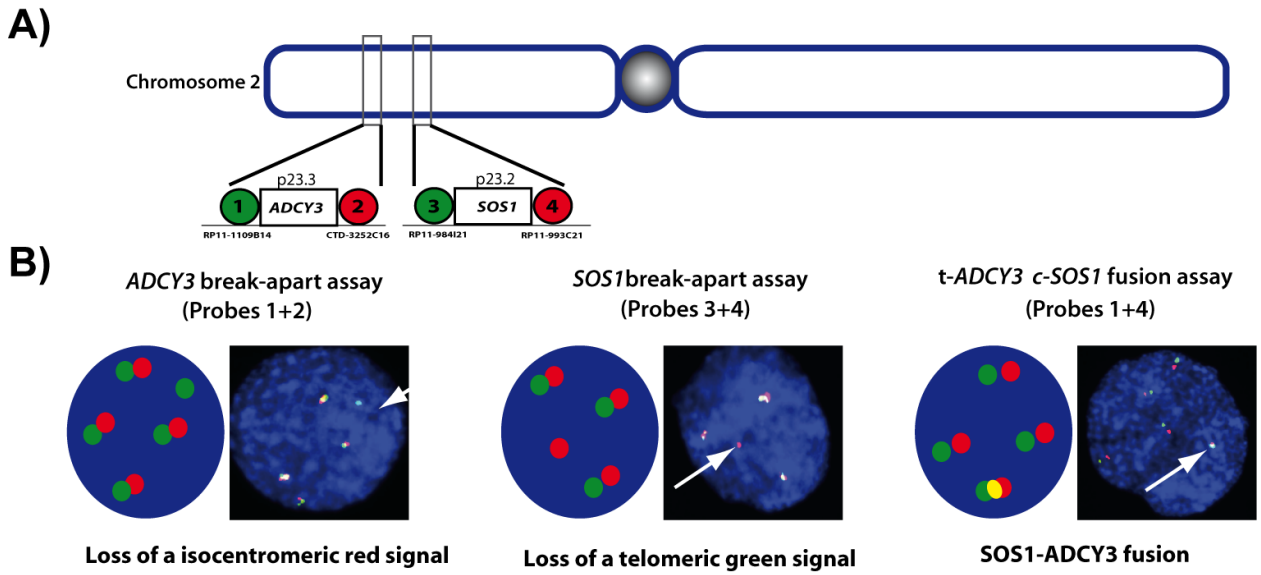

Figure 41 A Schematic representation of the BAC-clone binding sites. **B** Metaphase chromosomes of H3122 cells were stained with green-fluorescent and red-fluorescent BAC probes for *SOS1* and *ADCY3* (data generated by Roopika Menon, Insitute of Pathology, University Bonn, Germany).

signal was used **(Figure 42 A/B)**. Thus, *ALK* and *ADCY3* fusions on different chromosomes would lead to two green signals (one belonging to each gene). In H3122 cells however, only one green signal was observed, suggesting a superposition of the two green signals as a consequence of both events happening in the same chromosome **(Figure 42 B)**.

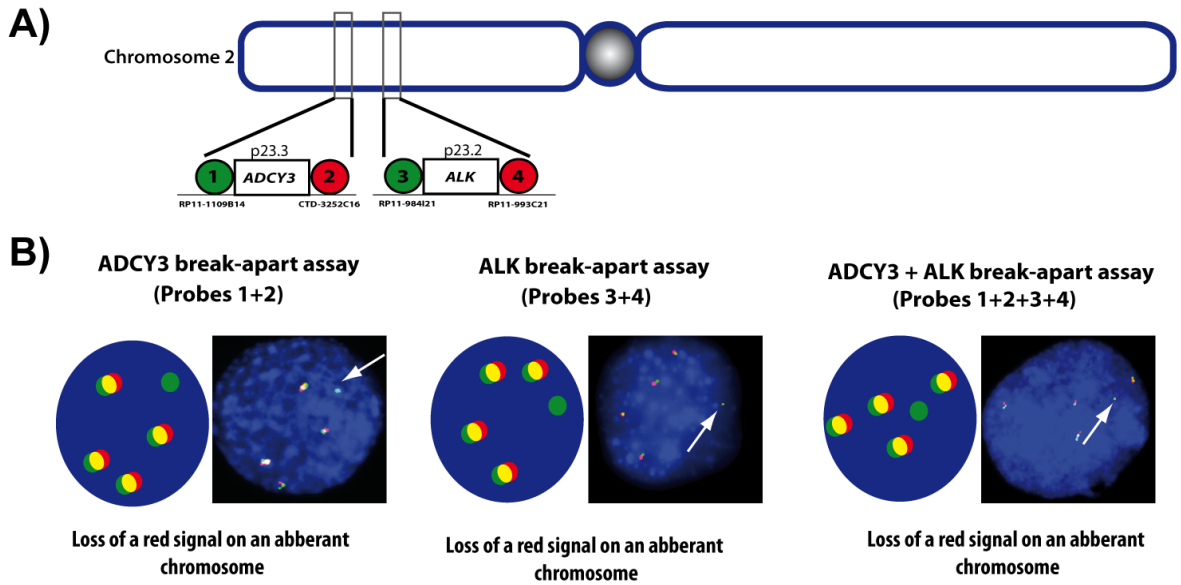

Figure 42 A Schematic representation of the BAC-clone binding sites. **B** Metaphase chromosomes of H3122 cells were stained with green-fluorescent and red-fluorescent BAC probes for *ADCY3* and *ALK* (data generated by Roopika Menon, Insitute of Pathology, University Bonn, Germany).

4.3.3 PKA and MAPK pathway activation in ALK inhibitor resistant H3122 cells

SOS1 encodes for a guanine nucleotide exchange factor of RAS proteins. Hence, SOS1 facilitates the binding of GTP to RAS and thereby the activation of RAS proteins. However, the *SOS1-ADCY3* fusion gene only consists of the first seven exons of *SOS1*, excluding the pleckstrin homology domain and the guanine nucleotide exchange factor domain from the fusion protein. Thus, a functional relevance of SOS1 activity in the fusion protein is highly unlikely **(Figure 43)**. *ADCY3* encodes for a transmembrane protein that catalyzes the formation of ATP to cyclic adenosine monophosphate (cAMP).

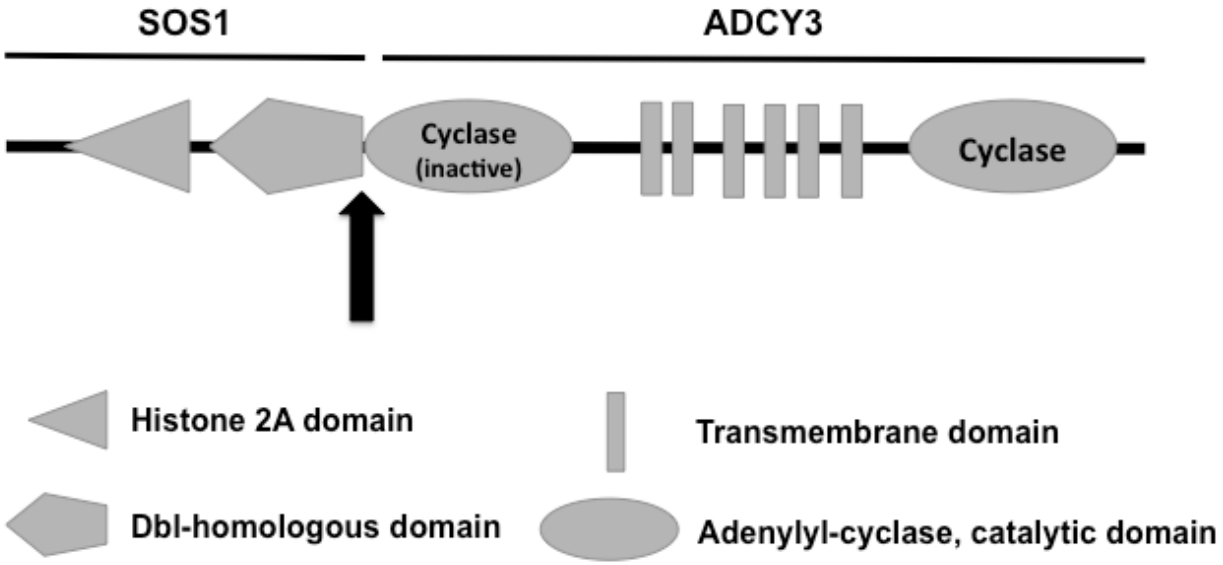

Figure 43 Schematic representation of the SOS1-ADCY3 fusion protein, functional domains for the respective protein fragments are shown, the breakpoint is indicated with a black arrow.

cAMP is a secondary messenger that regulates a diverse set of cellular responses including the activation of protein kinase A (PKA). To analyze if the *SOS1-ADCY3* fusion induces resistance by overexpression at the protein level and increased PKA activation, immunoblotting was performed using an antibody that binds to the N-terminal end of SOS1. Strikingly, all resistant clones tested showed an overexpression of the SOS1-ADCY3 fusion protein, whereas the parental cell line almost exclusively expressed $SOS1^{wt}$. Interestingly, all resistant clones did not show any ALK phosphorylation, even though cells were cultured without drug for 24 hours **(Figure 44**

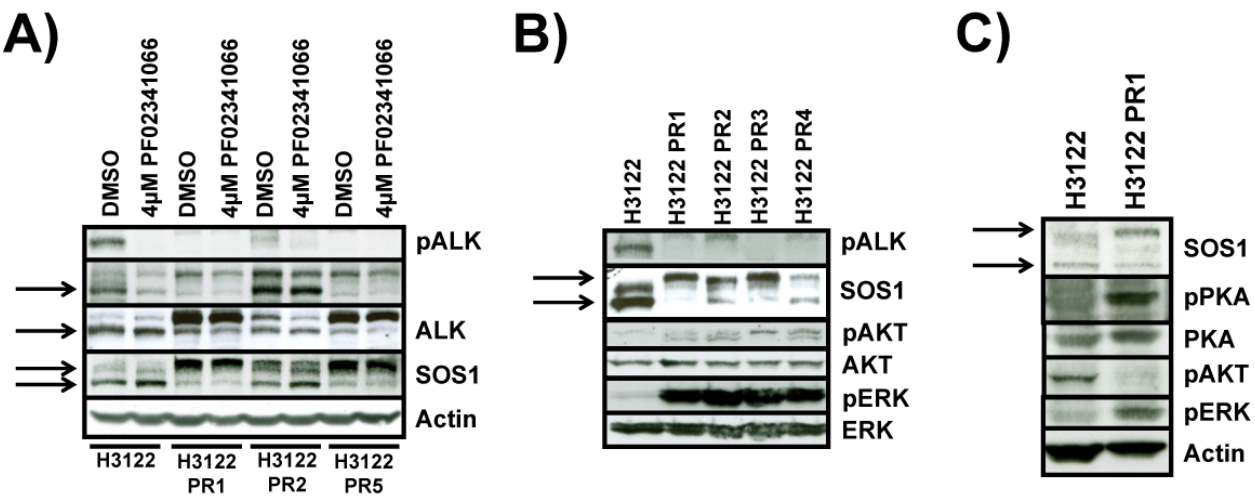

Figure 44 Whole cell lysates of H3122 and ALK inhibitor resistant H3122 clones were stained for pALK, ALK and SOS1 expression (**A**), AKT and ERK phosphorylation (**B**) and PKA activation (**C**).

A). In addition, resistant clones PR1 and PR5 showed a strong signal after staining for total ALK protein, which was at a higher molecular weight than the actual EML4-ALK v1 protein **(Figure 44 A)**. It remains unknown if these bands reflect unspecific staining or a translationally modified EML4-ALK protein. RNA-seq data confirmed no novel ALK fusion transcript on the mRNA level.

Immunostainings for PI3K and MAPK pathway activation showed, that all resistant clones exhibited a dramatic increase in ERK phosphorylation, whereas the phosphorylation of AKT was not increased **(Figure 44 B)**. Thus, overexpression of the SOS1-ADCY3 fusion protein might lead to an activation of the MAPK pathway. It has been described, that increased cAMP levels activate protein kinase A (PKA), inducing the phosphorylation of CREB and stimulation of the MAPK pathway via CRAF activation (Dumaz et al., 2006). Immunoblotting of pPKA in H3122 and PR1 cells showed an increased PKA phosphorylation in H3122 PR1 cells, supporting the hypothesis that this signaling circuit might be responsible for the elevated pERK levels in SOS1-ADCY3 overexpressing cells **(Figure 44 C)**. Staining for phosphorylation of 42 different receptor tyrosine kinases revealed a global reduction in RTK phosphorylation levels after the treatment of sensitive H3122 cells with PF02341066. Interestingly, almost no RTK phosphorylation was observed in the resistant cells, independent of inhibitor treatment **(Figure 45)**.

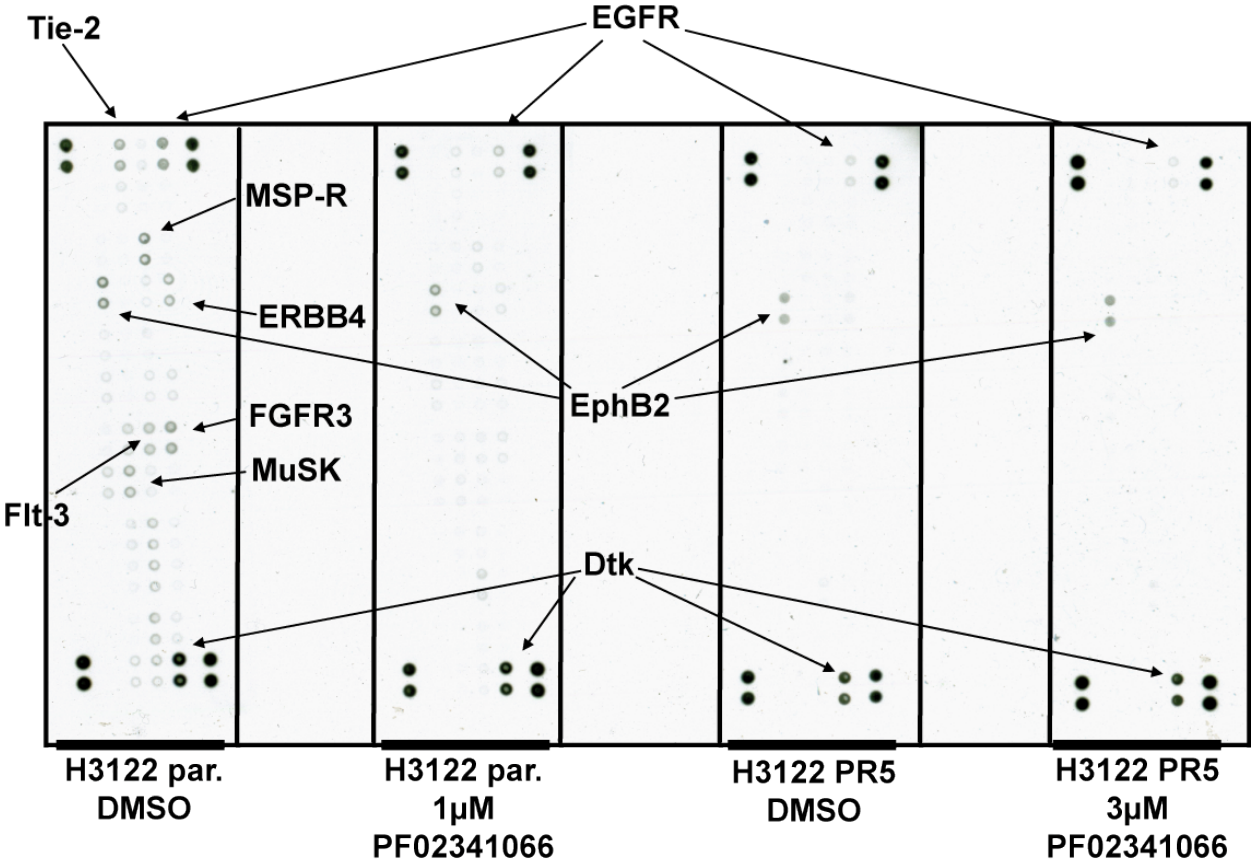

Figure 45 Indicated clones of H3122 cells were treated with DMSO or PF02341066 for 24 hours. After treatment, cells were lysed an incubated with phosphor-receptor tyrosine kinase antibodies spotted nitrocellulose membranes. In duplicate captured RTK levels were visualized using a HRP-conjugated pan phospho-tyrosine antibody. Signals on all four edges are positive controls.

4.3.4 *SOS1-ADCY3* induces tumor formation in a NIH3T3 xenograft model

To examine the oncogenicity of *SOS1-ADCY3,* the fusion gene was amplified from H3122 cDNA, cloned into the retroviral pBabe-puro backbone and expressed in NIH3T3 cells. Interestingly, NIH3T3 cells expressing the *SOS1-ADCY3* fusion

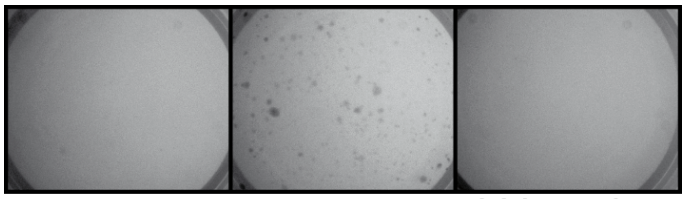

Figure 46 NIH3T3 cells transduced with pBabe empty vector (e.v.), *EML4-ALK* v1 or *SOS1-ADCY3* were plated in soft agar. Pictures were taken after 14 days of incubation.

gene did not form colonies in soft agar **(Figure 46)**. However, after subcutaneous injection of fusion gene expressing NIH3T3 cells into nude mice, tumor formation was observed after 20 days of incubation **(Figure 47)**. It remains to be seen, if extracellular growth factors, interactions with the extracellular matrix or differences in expression levels are responsible for the discrepancy between soft agar and xenograft experiments. Furthermore, ongoing studies will show if these cells also show elevated levels of phosphorylated ERK and might thereby be sensitive to MAPK pathway inhibition.

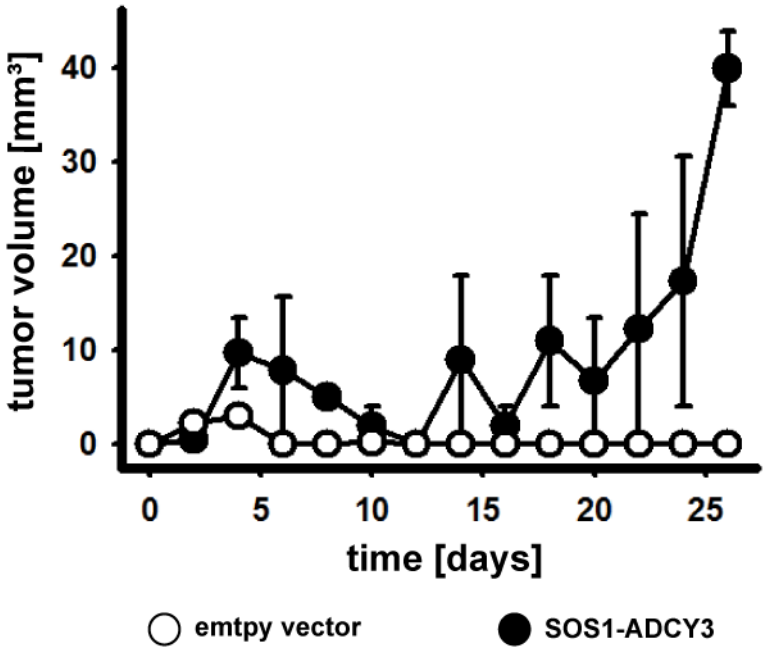

Figure 47 NIH3T3 cells, transduced with pBabe-puro empty vector or *SOS1-ADCY3* were subcutaneously injected into nude mice. Tumor formation was measured on regular bases. Data points represent the average of two tumors on two different mice, error bars indicate SEM (data generated by Jakob Schöttle, Max-Planck-Insitute for neurological research, Cologne, Germany).

5 Discussion

In this study, striking differences in ALK inhibitor sensitivity were shown to be dependent on the expressed *EML4-ALK variant,* the specific resistance mutation and the kinase inhibitor used for treatment.

First, a similar, *EML4-ALK variant* dependent, sensitivity pattern was observed for the two structurally unrelated ALK inhibitors crizotinib and TAE684, showing this effect to be independent of the respective binding mode of the inhibitor **(Figure 9)**. Several mutations in other kinases (e.g. EGFR) have been shown to alter the affinity of ATP to the kinase or the interactions of the kinase with the drug, thereby leading to dramatic changes in drug binding capacities (Greulich et al., 2005; Sharma et al., 2007; Yuza et al., 2007). In the case of *EML4-ALK*, all variants harbor the wild-type kinase domain of ALK, excluding variations in ATP or compound affinity as possible explanation. Furthermore, previous studies have shown comparable levels of kinase activity in different EML4-ALK variants (Choi et al., 2008). In addition to the differential kinase inhibitor sensitivity, the overall fusion protein stability also varied dramatically depending on the ALK fusion partner, underlining the fusion partner and not the ALK kinase domain as the major factor influencing the fusion protein characteristics that were studied **(Figure 18)**. Thus, in contrast to previous findings, the domain composition of the fusion partner and not the size of the fusion protein had a major impact on protein stability (De Sancho et al., 2009). Furthermore, in the case of *EML4-ALK* fusions, almost all variants showed a correlation between ALK kinase inhibitor sensitivity and overall protein stability, indicating that increased protein stability influences the sensitivity to ALK kinase inhibitors. A high turnover of protein might lead to a relatively low fraction of functional fusion proteins that are capable to bind the inhibitor. Thus, lower drug concentrations are needed to achieve a complete target inhibition. The only *EML4-ALK* variant that did not show such a correlation was *EML4-ALK v3b.* In this case, the, compared to *v3a*, 33 additional base pairs from the intronic region of *EML4* are only present in EML4-ALK v3b, making a comparison with other EML4-ALK variants difficult.

In addition to these general differences in protein turnover, ALK kinase inhibitor treatment induced a fusion variant and dose dependent degree of protein degradation **(Figure 16)**. As a type-II inhibitor, crizotinib only binds to, and thereby stabilizes, the

inactive conformation of the kinase. This conformation of the kinase might be intrinsically less stable, leading to the drug-induced degradation of the protein. However, treatment with high doses of TAE684 also induced fusion protein degradation, indicating that other mechanisms may also play a leading role in the kinase inhibitor induced degradation. Inhibition of the proteasome did not rescue this drug induced kinase degradation, suggesting a proteasomal independent degradation mechanism **(Figure 17)**. One possibility could be a folding induced insolubility of the fusion protein after inhibitor binding, thereby forming insoluble aggregates which circumvent immunoblotting analysis and proteasomal degradation (Bonvini et al., 2004; Verhoef et al., 2002).

In line with the findings of differential protein stability, cells expressing different *ALK* fusion genes showed differential sensitivity to HSP90 inhibition. Several groups have shown that *EML4-ALK* expressing cells are highly sensitive towards HSP90 inhibition (Chen et al., 2010; Katayama et al., 2011; Normant et al., 2011; Sasaki et al., 2010a). One reason for this dependency might be the fact that the protein folding properties of the fused proteins are disturbed by the somatically acquired fusion event. In the case of a gene fusion, the forming fusion protein has not developed evolutionarily and might therefore show defects in folding. These defects can be caused by hydrophobic residues at the breakpoint, which point towards the solvent and therefore require chaperonage of HSP90 or other chaperones. The broad spectrum of HSP90 inhibitor sensitivity observed in Ba/F3 cells expressing different *EML4-ALK* variants indicates that the amino acid composition of the breakpoint might dictate the degree of required chaperonage **(Figures 21, 22** and **24)**.

However, this dependency on HSP90 chaperonage does not correlate with sensitivity to ALK kinase inhibition, suggesting an independent mechanism of cytotoxicity. Surprisingly, after a combined treatment with HSP90 and ALK inhibitors, a synergistic effect was observed, clearly linking ALK and HSP90 inhibitor sensitivity in these cells **(Figure 24)** (Peifer et al., 2010). One possible functional link between HSP90 and ALK inhibitors might be the kinase inhibitor induced degradation of ALK **(Figure 16)**. Even though, crizotinib induced EML4-ALK degradation was only observed at higher concentrations of this inhibitor, lower drug concentrations should also induce some

instability of the fusion protein. This destabilization might then be re-stabilized by HSP90 proteins, thereby preventing fusion protein degradation at low drug concentrations. In the combined treatment of ALK and HSP90 inhibitors, this stabilization by HSP90 proteins is blocked, inducing an accelerated degradation of the fusion proteins and subsequent cytotoxicity. The strongest synergy was observed in *EML4-ALK v2* and *KIF5b-ALK* expressing cells, the most ALK inhibitor sensitive *ALK* fusions. However, both fusions were less sensitive to HSP90 inhibition compared to *EML4-ALK v1*, indicating that sensitivity to one of the drugs alone is not indicative for the synergy score after combination treatment. Interestingly, the smaller the ratio between the GI_{50} values of the less potent and the more potent compound, the higher the synergistic effect after combination treatment **(Figure 24, Table 2 page 61 ratio 2)**. Thus, the interplay between these two compounds was maximized, if both compounds had similar GI_{50} values after single drug treatment. This indicates, that a similar level of cytotoxicity is needed for both compounds to maximize the synergistic effect. Supporting this notion, the lowest synergistic effect of all *ALK* fusion genes tested was observed in *EML4-ALK v1* expressing cells, which showed the highest sensitivity towards HSP90 but only intermediate sensitivity to ALK inhibitor treatment **(Figure 24, Table 2 page 61 ratio 2)**. To further increase synergistic effects, the respective drug concentrations might need to be adapted to the respective *ALK* fusion. In the case of *EML4-ALK v1*, crizotinib concentrations that are four- to five-fold higher than 17-DMAG drug concentrations might maximize the synergistic effect. That way, lower concentration of both drugs could be sufficient to induce cytotoxicity in these cells.

In 2005, Radujkovic and colleagues published a study showing synergistic effects after treating *BCR-ABL* expressing cells with a combination of HSP90 and Abl inhibitors. These cells were resistant to treatment with the Abl inhibitor imatinib, but had no mutations in *ABL*. Interestingly, these cells showed a cross-resistance to HSP90 inhibition, which was mediated by a high activity of the p-glycoprotein, an efflux pump with broad substrate specificity. Treatment with HSP90 inhibitors reduces protein levels of p-glycoprotein, thereby explaining the synergistic effect in these cells (Radujkovic et al., 2005). Point mutations in *BCR-ABL* that induced resistance to imatinib however did not alter the sensitivity to HSP90 inhibition, as has been shown for mutated *EML4-ALK*

(Gorre et al., 2002; Katayama et al., 2011; Sasaki et al., 2010a). Thus, point mutations that induce resistance to kinase inhibitors (typically located in close proximity to the ATP-binding pocket) do not seem to have a high impact on the protein stability in these fusion proteins. However, other proteins, like EGFR, have been shown to exhibit an increased sensitivity to HSP90 inhibition in a mutated status (Sawai et al., 2008). This effect has been explained by a shorter half-life of the mutated, and thereby constantly activated form of EGFR. In *ALK* fusion gene expressing cells however, no direct correlation between fusion protein turnover, kinase activity and HSP90 inhibitor sensitivity was observed. One possible explanation might be the intrinsic, coiled-coiled domain mediated, constant kinase activation that may attenuate any additional activation-induced destabilization.

Unfortunately, no *EML4-ALK variant 2* expressing human cell lines are available, to validate the described findings in a human cell line setting. The only commercially available *EML4-ALK* expressing cell lines are H3122 (*variant 1*) and H2228 (*variants 3a/b*). However, it has been published that treatment of H2228 cells with ALK kinase inhibitors leads to a cytostatic effect, but does not induce apoptosis (Koivunen et al., 2008). Thus, the H3122 cell line is the only available cell line responding with an "oncogene addiction" phenotype to ALK kinase inhibition, hampering the analysis of *EML4-ALK* variant specific cytotoxic effects in human cell line models. An artificial human cell line model could be generated by the overexpression of different *EML4-ALK* variants in H3122 cells, followed by silencing of the endogenous fusion gene. However, the ultimate prove that the observed differences in sensitivity translate into the clinic, can exclusively be shown in clinical trials.

The single published crizotinib treated patient cohort consisted of only 31 variant annotated patients, and is thereby too small to confirm the described findings. In this study, only one confirmed *EML4-ALK variant 2* positive patient was included, showing a tumor response rate of 57%. However, tumors expressing *EML4-ALK v1* showed response rates from 33% - 100%, indicating that additional factors influenced the sensitivity of these tumors to crizotinib treatment (Kwak et al., 2010). Currently, *ALK* translocations in clinical trials are almost exclusively detected by FISH analysis (Kwak et al., 2010). By using *ALK* break-apart probes, *ALK* rearrangements are detected

without any information about the respective fusion partner or fusion variant. Thus, fusion variant specific responses cannot be analyzed. In order to enable specific variant calling, diagnostic tests that allow the exact identification of the expressed fusion variant need to be developed. One possibility would be an *EML4-ALK* fusion variant detection by RT-PCR, using RNA extracted from paraffin embedded tumor biopsies. However, this RNA is often degraded, allowing only the transcription of 100 - 150 bp long cDNA fragments. These fragments could then be used to run separate RT-PCRs, with a different forward primer (for each fusion variant) in each reaction. A better alternative would require fresh frozen biopsies for tumor RNA extraction, which, due to the generation of longer cDNA fragments, allow a multiplex RT-PCR approach for fusion variant detection (Takeuchi et al., 2008). Unfortunately, fresh frozen tumor biopsies are often difficult to obtain. In addition, in both RT-PCR approaches unknown fusions cannot be detected. RNA independent approaches would include parallel sequencing of the whole genome, or genomic regions of interest. However, these approaches are relatively expensive and need great expertise in the field of computational biology. Moreover, until now it is not completely clear if the different *EML4-ALK* variants arise on the genomic level or due to exon slippage. Hopefully, future clinical studies will analyze the specific *ALK* variant status and correlate these with tumor response rates. If different *EML4-ALK* variants induce variant specific response rates in the clinic, treatment schedules would need to be adapted accordingly.

In addition to potential up-front resistance mechanisms (e.g. point mutations or, as shown in this study, different fusion variants), acquired resistance diminishes the clinical success of kinase inhibitors. Resistance mechanisms usually re-activate the signaling of the initial “driver mutation” by preventing the drug to bind to its target (*in cis*) or by substitution of the survival pathway initiator to another oncogene (*in trans*). Both of these mechanisms are often difficult to predict and, to take biological signaling circuits into account, can therefore only be analyzed in patients and cell culture or animal models. In fact, these approaches led to the discovery of several ALK kinase inhibitor resistance mutations in *EML4-ALK* expressing cells, hopefully accelerating the development of ALK inhibitors that are capable to inhibit these mutated kinases (Choi et al., 2010; Heuckmann et al., 2011; Katayama et al., 2011; Katayama et al., 2012;

Sasaki et al., 2011; Sasaki et al., 2010a; Zhang et al., 2011). Furthermore, previous studies on other kinase inhibitors have shown, that the identification of *in-trans* resistance mechanisms often allows the development of successful secondary treatment strategies (Emery et al., 2009; Johannessen et al., 2010; Nazarian et al., 2010; Regales et al., 2009; Turke et al., 2010).

In this study, several crizotinib resistance mutations were shown to be highly sensitive to ALK inhibition by the structurally diverse kinase inhibitor TAE684 **(Figures 28 - 29)** (Choi et al., 2010; Katayama et al., 2011; Sasaki et al., 2010a). Unfortunately, TAE684 has not been developed for clinical use and therefore cannot be used to treat tumors harboring one of these mutations. Hopefully, ALK kinase inhibitors based on the scaffold of TAE684 will soon be available to treat of such tumors.

The two described mutagenesis screens identified two novel resistance mutations, which induced a high level of resistance to PF02341066 and TAE684 **(Figures 30 - 35)**. Structural modeling provided the mechanistic explanation for these findings, which are based on the binding mode of each inhibitor to the kinase. To overcome resistance of the L1198P mutation, a different target (e.g. HSP90) or a totally different binding mode, tolerating a highly activated kinase and avoiding the binding to the hinge region, would be needed. However, no allosteric ALK inhibitors have been described so far and it remains to be seen, if third-generation ALK inhibitors will be able to overcome resistance induced by the L1198P mutation (Milkiewicz and Ott, 2010).

Recently, a study was published describing an ENU induced crizotinib resistance screen in *EML4-ALK* expressing Ba/F3 cells. Interestingly, as opposed to the data described here, the most prevalent mutations that were found in this study were L1196M, S1206R and G1269S/C, with no mutations at residue D1203 and only a small fraction of clones with L1198M mutations (Zhang et al., 2011). A possible explanation for the discrepancy between these two studies, are differences in the screening assay. As compared to the present study, Zhang and colleagues expressed *EML4-ALK variant 1* (not *v3a*) in Ba/F3 cells, incubated the ENU/crizotinib treated cells in 96-well plates for monoclonal resistant clones (no polyclonal culture and subsequent deep-sequencing) and treated the cells with crizotinib (not with the racemic mixture PF02341066). It would be interesting to see, if the *EML4-ALK* variant influences the development of specific

resistance mutations after ALK inhibitor treatment. Supporting this notion, all cases reporting the resistance mutation F1174L or L1196M allude to *EML4-ALK variant 1* cell line models or primary tumor samples (Choi et al., 2010; Katayama et al., 2011; Sasaki et al., 2010a; Zhang et al., 2011). Furthermore, two recent studies analyzed crizotinib resistant tumors expressing *EML4-ALK v3a* and detected no F1174L or L1196M mutation (Doebele et al., 2012; Sasaki et al., 2011). An ALK inhibitor resistance screen in neuroblastoma cells, performed by Michael Hölzel at the NKI in the Netherlands, yielded as well the resistance mutation L1198P (Heuckmann et al., 2011). He performed a PCR-based mutagenesis screen for TAE684 resistance in the ALK^{F1174L} expressing SH-SY5Y cell line and found the TAE684 resistance mutations G1123S, G1123D and L1198P. Interestingly, only the L1198P mutation induced resistance to PF02341066 (Heuckmann et al., 2011). The exact resistance mechanism of these G1123S/D mutations is currently unknown, however, these mutations are located in the glycine-rich loop of the kinase, which has been described to be crucial for ATP and ligand binding (Azam et al., 2003; Saraste et al., 1990). Furthermore, a study in thyroid cancer recently described one L1198F and one G1201E transforming mutation in *ALK*, however, no ALK kinase inhibitor sensitivity studies were performed (Murugan and Xing, 2011). Thus, only five-years after the discovery of *EML4-ALK* translocations in lung cancer, a broad spectrum of ALK inhibitor resistance mutations has been described already. A similar spectrum of mutations has been shown to induce resistance to imatinib in *BCR-ABL* expressing cells (Azam et al., 2003; Shah et al., 2002). Interestingly, in *EGFR* mutated lung cancer, resistance to EGFR TKIs is almost exclusively mediated by the gatekeeper mutation (T790M) or *in-trans* resistance mechanisms, highlighting the influence of the kinase inhibitor binding-mode on the development of resistance mutations (Sequist et al., 2011; Sharma et al., 2007).

In addition to resistance mutations within the *ALK* kinase domain, PF02341066 resistant H3122 cells showed an overexpression of the newly discovered SOS1-ADCY3 fusion protein, without any mutations in *EML4-ALK* **(Figure 40, Figure 44)**. Previously, several publications have shown *EGFR* mutations and *EML4-ALK* amplifications as possible resistance mechanisms in *EML4-ALK* positive tumor cells (Doebele et al., 2012; Katayama et al., 2011; Koivunen et al., 2008; Sasaki et al., 2011). In the current study,

no differences in EGFR signaling and no overexpression of *EML4-ALK* were observed, with all SOS1-ADCY3 overexpressing cells showing an ALK inhibitor treatment independent activation of MAPK signaling. This finding is in line with the hypothesis, that resistance mechanisms usually re-activate the signaling pathway of the initial oncogene, which has been shown to be the MAPK pathway in H3122 cells (Katayama et al., 2011; Koivunen et al., 2008; Takezawa et al., 2011). NIH3T3 cells expressing the *SOS1-ADCY3* fusion gene did not form colonies in soft agar, but formed tumors in a xenograft mouse model. The reason for this observation is currently unknown, with growth stimulating factors in the mouse serum or in the subcutaneous extracellular matrix being potential variables that stimulate the growth of these *SOS1-ADCY3* expressing cells only in mice. Another possible explanation might be the expression level of SOS1-ADCY3, with only high levels of fusion protein being capable to induce colony/tumor formation. Thus, only very few of the injected cells are able to form tumors, thereby explaining the delayed tumor formation that was observed in xenografts. However, both hypotheses need further analysis. In contrast to the SOS1-ADCY3 overexpression, Katayama and colleagues identified *EML4-ALK* amplifications and the L1196M mutation in crizotinib resistant H3122 cells. To examine if the *SOS1-ADCY3* fusion is also present in the H3122 cells used in his study, Roopika Menon performed FISH analysis on these cells, confirming the existence of the genomic *SOS1-ADCY3* fusion. It is currently unknown, why some of these cells overexpress the SOS1-ADCY3 fusion, and others develop the L1196M mutation as mechanism of ALK kinase inhibitor resistance.

The current study highlights that the application of ALK inhibitors needs to take the exact genetic background (i.e. the exact fusion variant and potential resistance mutation) as well as the knowledge about compound activities for each resistance mutations into account. Some tumors with acquired (*in-cis*) crizotinib resistance mutations should respond to ALK kinase inhibitors of the diamino-pyrimidine scaffold, whereas other resistance mutation bearing tumors (e.g. L1198P and D1203N) should not respond to any type-I or type-II inhibitor. Conversely, if diamino-pyrimidine inhibitors are used for the treatment of *EML4-ALK* positive tumors, mutations in the glycine-rich loop of the kinase (G1123S/D) might develop, that can then be treated with crizotinib or

analogue drugs. However, all *ALK* fusion gene expressing tumors should be sensitive to HSP90 inhibition, independent of resistance mutation status (Katayama et al., 2011).

In contrast to the development of new drugs, intermittent treatment with high doses of crizotinib might also be a possible treatment option. Several studies have shown that a relatively short duration of oncogene inhibition is sufficient to kill cancer cells (Hiwase et al., 2009; Shah et al., 2008; Snead et al., 2009). In such a scenario, high plasma levels of crizotinib could be achieved for a short period of time, which allow binding to the mutated kinase and subsequent induction of apoptosis in the tumor cell. However, it remains to be seen, if an intermittent treatment is sufficient to reduce the adverse effects that are provoked by sustained off-target inhibition (due to the high drug concentrations) to a tolerable level.

6 Summary

EML4-ALK positive lung cancer can today effectively be treated with the ALK kinase inhibitor crizotinib. However, not only the initial tumor response to crizotinib treatment is heterogeneous, but also several resistance mutations that limit treatment efficiency have been described.

In this study, cells expressing different *EML4-ALK* variants were shown to exhibit differential sensitivity to structurally unrelated ALK kinase inhibitors. Interestingly, these variants also exhibited differential HSP90 inhibitor sensitivity, however, with a varying distribution across the fusion variants. Furthermore, combining ALK and HSP90 inhibitors induced synergistic cytotoxicity in all *ALK* fusion gene expressing cells, arguing for a functional link between HSP90 and the ALK fusion protein. Most likely, this functional interaction is based on the *ALK* fusion partner induced protein instability, which can be enhanced by kinase inhibitors, and attenuated by HSP90 binding.

As opposed to these ALK inhibitor scaffold independent differences in sensitivity, cells expressing the crizotinib resistance mutations L1196M, F1174L or G1269S were highly sensitive to TAE684 treatment. Furthermore, two orthogonal mutagenesis screens identified two novel resistance mutations (L1198P and D1203N), which induced a high level of resistance to crizotinib and TAE684. The L1198P mutation most likely induced resistance to crizotinib by shifting the kinase equilibrium to a more active conformation and consequently hampering the inhibitor binding to the kinase domain. Resistance to TAE684 was most likely induced by mutation induced structural alterations at the hinge region of the kinase, impeding the interactions with the methoxy-group of TAE684. The exact mechanism of resistance induced by D1203N is unclear. Finally, the overexpression of a novel fusion protein in an *EML4-ALK* expressing cell line was described, which could induce ALK inhibitor resistance by MAPK pathway activation.

The described mechanisms of differential sensitivity might explain some of the heterogeneous responses of *EML4-ALK* positive tumors after treatment with crizotinib. Furthermore, these findings demonstrate that the *ALK* genotype as well as the choice of ALK inhibitor highly impacts the therapeutic efficiency and should be taken into account for targeted therapy in *ALK* positive lung cancer and other cancers with *ALK* aberrations.

7 Outlook

Lung cancer is one of the deadliest diseases of mankind. However, intensive research and technical advancement within the last 20 years allow a more optimistic view into the future. The decoding of several important biological processes that are essential for the survival of transformed cells enabled researchers to develop treatments that target these “Achilles heels” of tumor cells. Furthermore, future sequencing efforts will identify additional driver mutations in human tumors that will hopefully be targetable with dugs.

The ability to sequence primary tumor samples and to identify genetic biomarkers for treatment decisions, today allows the use of targeted therapies only on those patients that are expected to respond. Such a combination of sequencing options and the biological understanding of tumor development improved the overall survival of many cancer patients already (Chapman et al., 2011; Druker et al., 2001; Kwak et al., 2010; Mok et al., 2009). Even though these examples are a huge success in the fight against cancer, the genetic drivers of many tumors are not yet known or cannot be targeted today.

However, researchers can make use of a broad spectrum of functional analyses to dissect the biology behind a tumor cell. This study showed once again, that the exact knowledge about the genetic event leading to a certain phenotype, allows an adaptation (i.e. different drug) of treatment. In addition, a general understanding of the biochemical protein characteristics was shown to allow an enhancement in treatment efficiency (i.e. drug combinations). The current knowledge about possible resistance mechanisms in *ALK* already allows the development of second- or third-generation kinase inhibitors, which circumvent the respective resistance mechanism by a different binding mode. Hopefully, such improved drugs will soon be available and will translate the pre-clinical treatment success into the clinic.

Nevertheless, the question remains, if constant adaptations and improvements of cancer care will eventually allow the cure of cancer, or if adaptations in cancer treatment will always initiate the development of novel resistance mechanisms. The latter could be compared to current efforts to contain resistance in viral infections, with virus particles constantly evolving to escape the available treatment. In such a scenario, permanent adaptations in cancer treatment could make cancer become a chronic

disease, with an increase in overall survival, but no cure. A more unfavorable scenario would be, that tumor cells shift their oncogenic signaling to proteins that cannot be targeted, or switch to signaling pathways that are also essential for the survival of non-transformed cells. However, in that case, a careful analysis of potential therapeutic windows for available drugs still might allow the treatment of these tumors.

Hopefully, future scientific advances will not only enhance current techniques (whole genome sequencing, kinase inhibitors etc.), but also allow the development of completely new treatment strategies to address the great demand for effective cancer treatment.

8 References

Alberts, B. (2002). Molecular biology of the cell, 4th edn (New York: Garland Science).

Azam, M., Latek, R. R., and Daley, G. Q. (2003). Mechanisms of autoinhibition and STI-571/imatinib resistance revealed by mutagenesis of BCR-ABL. Cell *112*, 831-843.

Azam, M., Seeliger, M. A., Gray, N. S., Kuriyan, J., and Daley, G. Q. (2008). Activation of tyrosine kinases by mutation of the gatekeeper threonine. Nat Struct Mol Biol *15*, 1109-1118.

Bass, A. J., Watanabe, H., Mermel, C. H., Yu, S., Perner, S., Verhaak, R. G., Kim, S. Y., Wardwell, L., Tamayo, P., Gat-Viks, I.*, et al.* (2009). SOX2 is an amplified lineage-survival oncogene in lung and esophageal squamous cell carcinomas. Nat Genet *41*, 1238-1242.

Beroukhim, R., Mermel, C. H., Porter, D., Wei, G., Raychaudhuri, S., Donovan, J., Barretina, J., Boehm, J. S., Dobson, J., Urashima, M.*, et al.* (2010). The landscape of somatic copy-number alteration across human cancers. Nature *463*, 899-905.

Birch, J. M., Alston, R. D., McNally, R. J., Evans, D. G., Kelsey, A. M., Harris, M., Eden, O. B., and Varley, J. M. (2001). Relative frequency and morphology of cancers in carriers of germline TP53 mutations. Oncogene *20*, 4621-4628.

Bishop, J. M. (1990). Nobel Lecture. Retroviruses and oncogenes II. Biosci Rep *10*, 473-491.

Bonvini, P., Dalla Rosa, H., Vignes, N., and Rosolen, A. (2004). Ubiquitination and proteasomal degradation of nucleophosmin-anaplastic lymphoma kinase induced by 17-allylamino-demethoxygeldanamycin: role of the co-chaperone carboxyl heat shock protein 70-interacting protein. Cancer Res *64*, 3256-3264.

Bossi, R. T., Saccardo, M. B., Ardini, E., Menichincheri, M., Rusconi, L., Magnaghi, P., Orsini, P., Avanzi, N., Borgia, A. L., Nesi, M.*, et al.* (2010). Crystal structures of anaplastic lymphoma kinase in complex with ATP competitive inhibitors. Biochemistry *49*, 6813-6825.

Bradeen, H. A., Eide, C. A., O'Hare, T., Johnson, K. J., Willis, S. G., Lee, F. Y., Druker, B. J., and Deininger, M. W. (2006). Comparison of imatinib mesylate, dasatinib (BMS-354825), and nilotinib (AMN107) in an N-ethyl-N-nitrosourea (ENU)-based mutagenesis screen: high efficacy of drug combinations. Blood *108*, 2332-2338.

Braithwaite, K. L., and Rabbitts, P. H. (1999). Multi-step evolution of lung cancer. Semin Cancer Biol *9*, 255-265.

Brambilla, E., and Gazdar, A. (2009). Pathogenesis of lung cancer signalling pathways: roadmap for therapies. Eur Respir J *33*, 1485-1497.

Bremnes, R. M., Camps, C., and Sirera, R. (2006). Angiogenesis in non-small cell lung cancer: the prognostic impact of neoangiogenesis and the cytokines VEGF and bFGF in tumours and blood. Lung Cancer *51*, 143-158.

Bremnes, R. M., Veve, R., Gabrielson, E., Hirsch, F. R., Baron, A., Bemis, L., Gemmill, R. M., Drabkin, H. A., and Franklin, W. A. (2002). High-throughput tissue microarray analysis used to evaluate biology and prognostic significance of the E-cadherin pathway in non-small-cell lung cancer. J Clin Oncol *20*, 2417-2428.

Butrynski, J. E., D'Adamo, D. R., Hornick, J. L., Dal Cin, P., Antonescu, C. R., Jhanwar, S. C., Ladanyi, M., Capelletti, M., Rodig, S. J., Ramaiya, N.*, et al.* (2010). Crizotinib in ALK-rearranged inflammatory myofibroblastic tumor. N Engl J Med *363*, 1727-1733.

Campbell, P. J., Yachida, S., Mudie, L. J., Stephens, P. J., Pleasance, E. D., Stebbings, L. A., Morsberger, L. A., Latimer, C., McLaren, S., Lin, M. L.*, et al.* (2010). The patterns and dynamics of genomic instability in metastatic pancreatic cancer. Nature *467*, 1109-1113.

Carvalho, A. L., Nishimoto, I. N., Califano, J. A., and Kowalski, L. P. (2005). Trends in incidence and prognosis for head and neck cancer in the United States: a site-specific analysis of the SEER database. Int J Cancer *114*, 806-816.

Chan, W. W., Wise, S. C., Kaufman, M. D., Ahn, Y. M., Ensinger, C. L., Haack, T., Hood, M. M., Jones, J., Lord, J. W., Lu, W. P.*, et al.* (2011). Conformational control inhibition of the BCR-ABL1 tyrosine kinase, including the gatekeeper T315I mutant, by the switch-control inhibitor DCC-2036. Cancer Cell *19*, 556-568.

Chapman, P. B., Hauschild, A., Robert, C., Haanen, J. B., Ascierto, P., Larkin, J., Dummer, R., Garbe, C., Testori, A., Maio, M.*, et al.* (2011). Improved survival with vemurafenib in melanoma with BRAF V600E mutation. N Engl J Med *364*, 2507-2516.

Chen, C. H., and Chen, R. J. (2011). Prevalence of telomerase activity in human cancer. J Formos Med Assoc *110*, 275-289.

Chen, H., Ma, J., Li, W., Eliseenkova, A. V., Xu, C., Neubert, T. A., Miller, W. T., and Mohammadi, M. (2007). A molecular brake in the kinase hinge region regulates the activity of receptor tyrosine kinases. Mol Cell *27*, 717-730.

Chen, Y., Takita, J., Choi, Y. L., Kato, M., Ohira, M., Sanada, M., Wang, L., Soda, M., Kikuchi, A., Igarashi, T.*, et al.* (2008). Oncogenic mutations of ALK kinase in neuroblastoma. Nature *455*, 971-974.

Chen, Z., Sasaki, T., Tan, X., Carretero, J., Shimamura, T., Li, D., Xu, C., Wang, Y., Adelmant, G. O., Capelletti, M.*, et al.* (2010). Inhibition of ALK, PI3K/MEK, and HSP90 in murine lung adenocarcinoma induced by EML4-ALK fusion oncogene. Cancer Res *70*, 9827-9836.

Chiarle, R., Voena, C., Ambrogio, C., Piva, R., and Inghirami, G. (2008). The anaplastic lymphoma kinase in the pathogenesis of cancer. Nat Rev Cancer *8*, 11-23.

Chmielecki, J., Peifer, M., Jia, P., Socci, N. D., Hutchinson, K., Viale, A., Zhao, Z., Thomas, R. K., and Pao, W. (2010). Targeted next-generation sequencing of DNA regions proximal to a conserved GXGXXG signaling motif enables systematic discovery of tyrosine kinase fusions in cancer. Nucleic Acids Res *38*, 6985-6996.

Choi, Y. L., Soda, M., Yamashita, Y., Ueno, T., Takashima, J., Nakajima, T., Yatabe, Y., Takeuchi, K., Hamada, T., Haruta, H.*, et al.* (2010). EML4-ALK mutations in lung cancer that confer resistance to ALK inhibitors. N Engl J Med *363*, 1734-1739.

Choi, Y. L., Takeuchi, K., Soda, M., Inamura, K., Togashi, Y., Hatano, S., Enomoto, M., Hamada, T., Haruta, H., Watanabe, H.*, et al.* (2008). Identification of novel isoforms of the EML4-ALK transforming gene in non-small cell lung cancer. Cancer Res *68*, 4971-4976.

Counter, C. M., Avilion, A. A., LeFeuvre, C. E., Stewart, N. G., Greider, C. W., Harley, C. B., and Bacchetti, S. (1992). Telomere shortening associated with chromosome instability is arrested in immortal cells which express telomerase activity. EMBO J *11*, 1921-1929.

Dalgliesh, G. L., Furge, K., Greenman, C., Chen, L., Bignell, G., Butler, A., Davies, H., Edkins, S., Hardy, C., Latimer, C.*, et al.* (2010). Systematic sequencing of renal carcinoma reveals inactivation of histone modifying genes. Nature *463*, 360-363.

Davis, M. I., Hunt, J. P., Herrgard, S., Ciceri, P., Wodicka, L. M., Pallares, G., Hocker, M., Treiber, D. K., and Zarrinkar, P. P. (2011). Comprehensive analysis of kinase inhibitor selectivity. Nat Biotechnol *29*, 1046-1051.

De Sancho, D., Doshi, U., and Munoz, V. (2009). Protein folding rates and stability: how much is there beyond size? J Am Chem Soc *131*, 2074-2075.

Demetri, G. D., von Mehren, M., Blanke, C. D., Van den Abbeele, A. D., Eisenberg, B., Roberts, P. J., Heinrich, M. C., Tuveson, D. A., Singer, S., Janicek, M.*, et al.* (2002). Efficacy and safety of imatinib mesylate in advanced gastrointestinal stromal tumors. N Engl J Med *347*, 472-480.

Derksen, P. W., Liu, X., Saridin, F., van der Gulden, H., Zevenhoven, J., Evers, B., van Beijnum, J. R., Griffioen, A. W., Vink, J., Krimpenfort, P.*, et al.* (2006). Somatic inactivation of E-cadherin and p53 in mice leads to metastatic lobular mammary carcinoma through induction of anoikis resistance and angiogenesis. Cancer Cell *10*, 437-449.

Di Fiore, P. P., Pierce, J. H., Kraus, M. H., Segatto, O., King, C. R., and Aaronson, S. A. (1987). erbB-2 is a potent oncogene when overexpressed in NIH/3T3 cells. Science *237*, 178-182.

Ding, L., Getz, G., Wheeler, D. A., Mardis, E. R., McLellan, M. D., Cibulskis, K., Sougnez, C., Greulich, H., Muzny, D. M., Morgan, M. B.*, et al.* (2008). Somatic mutations affect key pathways in lung adenocarcinoma. Nature *455*, 1069-1075.

Doebele, R. C., Pilling, A. B., Aisner, D. L., Kutateladze, T. G., Le, A. T., Weickhardt, A. J., Kondo, K. L., Linderman, D. J., Heasley, L. E., Franklin, W. A.*, et al.* (2012). Mechanisms of Resistance to Crizotinib in Patients with ALK Gene Rearranged Non-Small Cell Lung Cancer. Clin Cancer Res *18*, 1472-1482.

Druker, B. J., Guilhot, F., O'Brien, S. G., Gathmann, I., Kantarjian, H., Gattermann, N., Deininger, M. W., Silver, R. T., Goldman, J. M., Stone, R. M.*, et al.* (2006). Five-year follow-up of patients receiving imatinib for chronic myeloid leukemia. N Engl J Med *355*, 2408-2417.

Druker, B. J., Talpaz, M., Resta, D. J., Peng, B., Buchdunger, E., Ford, J. M., Lydon, N. B., Kantarjian, H., Capdeville, R., Ohno-Jones, S., and Sawyers, C. L. (2001). Efficacy and safety of a specific inhibitor of the BCR-ABL tyrosine kinase in chronic myeloid leukemia. N Engl J Med *344*, 1031-1037.

Dumaz, N., Hayward, R., Martin, J., Ogilvie, L., Hedley, D., Curtin, J. A., Bastian, B. C., Springer, C., and Marais, R. (2006). In melanoma, RAS mutations are accompanied by switching signaling from BRAF to CRAF and disrupted cyclic AMP signaling. Cancer Res *66*, 9483-9491.

Emery, C. M., Vijayendran, K. G., Zipser, M. C., Sawyer, A. M., Niu, L., Kim, J. J., Hatton, C., Chopra, R., Oberholzer, P. A., Karpova, M. B.*, et al.* (2009). MEK1 mutations confer resistance to MEK and B-RAF inhibition. Proc Natl Acad Sci U S A *106*, 20411-20416.

Endres, N. F., Engel, K., Das, R., Kovacs, E., and Kuriyan, J. (2011). Regulation of the catalytic activity of the EGF receptor. Curr Opin Struct Biol *21*, 777-784.

Engelman, J. A. (2007). The role of phosphoinositide 3-kinase pathway inhibitors in the treatment of lung cancer. Clin Cancer Res *13*, s4637-4640.

Engelman, J. A., and Janne, P. A. (2008). Mechanisms of acquired resistance to epidermal growth factor receptor tyrosine kinase inhibitors in non-small cell lung cancer. Clin Cancer Res *14*, 2895-2899.

Engelman, J. A., and Settleman, J. (2008). Acquired resistance to tyrosine kinase inhibitors during cancer therapy. Curr Opin Genet Dev *18*, 73-79.

Engelman, J. A., Zejnullahu, K., Mitsudomi, T., Song, Y., Hyland, C., Park, J. O., Lindeman, N., Gale, C. M., Zhao, X., Christensen, J.*, et al.* (2007). MET amplification leads to gefitinib resistance in lung cancer by activating ERBB3 signaling. Science *316*, 1039-1043.

Evans, J. P., Wickremasinghe, R. G., and Hoffbrand, A. V. (1987). Tyrosine protein kinase substrates in Philadelphia-positive human chronic granulocytic leukemia derived cell lines (K562 and BV173): detection by using an immunoblotting technique. Leukemia *1*, 524-525.

Feuk, L., Carson, A. R., and Scherer, S. W. (2006). Structural variation in the human genome. Nat Rev Genet *7*, 85-97.

Fidler, I. J. (2003). The pathogenesis of cancer metastasis: the 'seed and soil' hypothesis revisited. Nat Rev Cancer *3*, 453-458.

Forbes, S. A., Bindal, N., Bamford, S., Cole, C., Kok, C. Y., Beare, D., Jia, M., Shepherd, R., Leung, K., Menzies, A.*, et al.* (2011). COSMIC: mining complete cancer genomes in the Catalogue of Somatic Mutations in Cancer. Nucleic Acids Res *39*, D945-950.

Ford, D., Easton, D. F., Stratton, M., Narod, S., Goldgar, D., Devilee, P., Bishop, D. T., Weber, B., Lenoir, G., Chang-Claude, J.*, et al.* (1998). Genetic heterogeneity and penetrance analysis of the BRCA1 and BRCA2 genes in breast cancer families. The Breast Cancer Linkage Consortium. Am J Hum Genet *62*, 676-689.

Frommolt, P., and Thomas, R. K. (2008). Standardized high-throughput evaluation of cell-based compound screens. BMC Bioinformatics *9*, 475.

Galkin, A. V., Melnick, J. S., Kim, S., Hood, T. L., Li, N., Li, L., Xia, G., Steensma, R., Chopiuk, G., Jiang, J.*, et al.* (2007). Identification of NVP-TAE684, a potent, selective, and efficacious inhibitor of NPM-ALK. Proc Natl Acad Sci U S A *104*, 270-275.

Gambacorti-Passerini, C., Antolini, L., Mahon, F. X., Guilhot, F., Deininger, M., Fava, C., Nagler, A., Della Casa, C. M., Morra, E., Abruzzese, E.*, et al.* (2011). Multicenter independent assessment of outcomes in chronic myeloid leukemia patients treated with imatinib. J Natl Cancer Inst *103*, 553-561.

Gazdar, A. F., and Minna, J. D. (2008). Deregulated EGFR signaling during lung cancer progression: mutations, amplicons, and autocrine loops. Cancer Prev Res (Phila) *1*, 156-160.

George, R. E., Sanda, T., Hanna, M., Frohling, S., Luther, W., 2nd, Zhang, J., Ahn, Y., Zhou, W., London, W. B., McGrady, P.*, et al.* (2008). Activating mutations in ALK provide a therapeutic target in neuroblastoma. Nature *455*, 975-978.

Gleason, B. C., and Hornick, J. L. (2008). Inflammatory myofibroblastic tumours: where are we now? J Clin Pathol *61*, 428-437.

Goldstraw, P., Ball, D., Jett, J. R., Le Chevalier, T., Lim, E., Nicholson, A. G., and Shepherd, F. A. (2011). Non-small-cell lung cancer. Lancet *378*, 1727-1740.

Golub, T. R., Goga, A., Barker, G. F., Afar, D. E., McLaughlin, J., Bohlander, S. K., Rowley, J. D., Witte, O. N., and Gilliland, D. G. (1996). Oligomerization of the ABL tyrosine kinase by the Ets protein TEL in human leukemia. Mol Cell Biol *16*, 4107-4116.

Gorre, M. E., Ellwood-Yen, K., Chiosis, G., Rosen, N., and Sawyers, C. L. (2002). BCR-ABL point mutants isolated from patients with imatinib mesylate-resistant chronic myeloid leukemia remain sensitive to inhibitors of the BCR-ABL chaperone heat shock protein 90. Blood *100*, 3041-3044.

Greider, C. W., and Blackburn, E. H. (1985). Identification of a specific telomere terminal transferase activity in Tetrahymena extracts. Cell *43*, 405-413.

Greulich, H., Chen, T. H., Feng, W., Janne, P. A., Alvarez, J. V., Zappaterra, M., Bulmer, S. E., Frank, D. A., Hahn, W. C., Sellers, W. R., and Meyerson, M. (2005). Oncogenic transformation by inhibitor-sensitive and -resistant EGFR mutants. PLoS Med *2*, e313.

Gustafsson, B. I., Kidd, M., Chan, A., Malfertheiner, M. V., and Modlin, I. M. (2008). Bronchopulmonary neuroendocrine tumors. Cancer *113*, 5-21.

Hanahan, D., and Weinberg, R. A. (2000). The hallmarks of cancer. Cell *100*, 57-70.

Hanahan, D., and Weinberg, R. A. (2011). Hallmarks of cancer: the next generation. Cell *144*, 646-674.

Harris, C. C. (1993). p53: at the crossroads of molecular carcinogenesis and risk assessment. Science *262*, 1980-1981.

Henson, E. S., and Gibson, S. B. (2006). Surviving cell death through epidermal growth factor (EGF) signal transduction pathways: implications for cancer therapy. Cell Signal *18*, 2089-2097.

Herbst, R. S., Heymach, J. V., and Lippman, S. M. (2008). Lung cancer. N Engl J Med *359*, 1367-1380.

Herbst, R. S., Onn, A., and Sandler, A. (2005). Angiogenesis and lung cancer: prognostic and therapeutic implications. J Clin Oncol *23*, 3243-3256.

Hernandez, L., Pinyol, M., Hernandez, S., Bea, S., Pulford, K., Rosenwald, A., Lamant, L., Falini, B., Ott, G., Mason, D. Y.*, et al.* (1999). TRK-fused gene (TFG) is a new partner of ALK in anaplastic large cell lymphoma producing two structurally different TFG-ALK translocations. Blood *94*, 3265-3268.

Heuckmann, J. M., Holzel, M., Sos, M. L., Heynck, S., Balke-Want, H., Koker, M., Peifer, M., Weiss, J., Lovly, C. M., Grutter, C.*, et al.* (2011). ALK mutations conferring differential resistance to structurally diverse ALK inhibitors. Clin Cancer Res *17*, 7394-7401.

Hiwase, D. K., White, D. L., Saunders, V. A., Kumar, S., Melo, J. V., and Hughes, T. P. (2009). Short-term intense Bcr-Abl kinase inhibition with nilotinib is adequate to trigger cell death in BCR-ABL(+) cells. Leukemia *23*, 1205-1206.

Huse, M., and Kuriyan, J. (2002). The conformational plasticity of protein kinases. Cell *109*, 275-282.

Jainchill, J. L., Aaronson, S. A., and Todaro, G. J. (1969). Murine sarcoma and leukemia viruses: assay using clonal lines of contact-inhibited mouse cells. J Virol *4*, 549-553.

Janoueix-Lerosey, I., Lequin, D., Brugieres, L., Ribeiro, A., de Pontual, L., Combaret, V., Raynal, V., Puisieux, A., Schleiermacher, G., Pierron, G.*, et al.* (2008). Somatic and germline activating mutations of the ALK kinase receptor in neuroblastoma. Nature *455*, 967-970.

Jemal, A., Siegel, R., Xu, J., and Ward, E. (2010). Cancer statistics, 2010. CA Cancer J Clin *60*, 277-300.

Jiang, J., Greulich, H., Janne, P. A., Sellers, W. R., Meyerson, M., and Griffin, J. D. (2005). Epidermal growth factor-independent transformation of Ba/F3 cells with cancer-derived epidermal growth factor receptor mutants induces gefitinib-sensitive cell cycle progression. Cancer Res *65*, 8968-8974.

Johannessen, C. M., Boehm, J. S., Kim, S. Y., Thomas, S. R., Wardwell, L., Johnson, L. A., Emery, C. M., Stransky, N., Cogdill, A. P., Barretina, J.*, et al.* (2010). COT drives resistance to RAF inhibition through MAP kinase pathway reactivation. Nature *468*, 968-972.

Jura, N., Zhang, X., Endres, N. F., Seeliger, M. A., Schindler, T., and Kuriyan, J. (2011). Catalytic control in the EGF receptor and its connection to general kinase regulatory mechanisms. Mol Cell *42*, 9-22.

Kancha, R. K., von Bubnoff, N., Peschel, C., and Duyster, J. (2009). Functional analysis of epidermal growth factor receptor (EGFR) mutations and potential implications for EGFR targeted therapy. Clin Cancer Res *15*, 460-467.

Kase, S., Sugio, K., Yamazaki, K., Okamoto, T., Yano, T., and Sugimachi, K. (2000). Expression of E-cadherin and beta-catenin in human non-small cell lung cancer and the clinical significance. Clin Cancer Res *6*, 4789-4796.

Katayama, R., Khan, T. M., Benes, C., Lifshits, E., Ebi, H., Rivera, V. M., Shakespeare, W. C., Iafrate, A. J., Engelman, J. A., and Shaw, A. T. (2011). Therapeutic strategies to overcome crizotinib resistance in non-small cell lung cancers harboring the fusion oncogene EML4-ALK. Proc Natl Acad Sci U S A *108*, 7535-7540.

Katayama, R., Shaw, A. T., Khan, T. M., Mino-Kenudson, M., Solomon, B. J., Halmos, B., Jessop, N., Wain, J. C., Yeo, A. T., Benes, C.*, et al.* (2012). Mechanisms of Acquired Crizotinib Resistance in ALK-Rearranged Lung Cancers. Sci Transl Med.

Khuder, S. A. (2001). Effect of cigarette smoking on major histological types of lung cancer: a meta-analysis. Lung Cancer *31*, 139-148.

Knudson, A. G., Jr. (1971). Mutation and cancer: statistical study of retinoblastoma. Proc Natl Acad Sci U S A *68*, 820-823.

Kobayashi, S., Boggon, T. J., Dayaram, T., Janne, P. A., Kocher, O., Meyerson, M., Johnson, B. E., Eck, M. J., Tenen, D. G., and Halmos, B. (2005). EGFR mutation and resistance of non-small-cell lung cancer to gefitinib. N Engl J Med *352*, 786-792.

Koivunen, J. P., Mermel, C., Zejnullahu, K., Murphy, C., Lifshits, E., Holmes, A. J., Choi, H. G., Kim, J., Chiang, D., Thomas, R.*, et al.* (2008). EML4-ALK fusion gene and efficacy of an ALK kinase inhibitor in lung cancer. Clin Cancer Res *14*, 4275-4283.

Kruse, J. P., and Gu, W. (2009). Modes of p53 regulation. Cell *137*, 609-622.

Kurzrock, R., Shtalrid, M., Talpaz, M., Kloetzer, W. S., and Gutterman, J. U. (1987). Expression of c-abl in Philadelphia-positive acute myelogenous leukemia. Blood *70*, 1584-1588.

Kwak, E. L., Bang, Y. J., Camidge, D. R., Shaw, A. T., Solomon, B., Maki, R. G., Ou, S. H., Dezube, B. J., Janne, P. A., Costa, D. B.*, et al.* (2010). Anaplastic lymphoma kinase inhibition in non-small-cell lung cancer. N Engl J Med *363*, 1693-1703.

Lin, E., Li, L., Guan, Y., Soriano, R., Rivers, C. S., Mohan, S., Pandita, A., Tang, J., and Modrusan, Z. (2009). Exon array profiling detects EML4-ALK fusion in breast, colorectal, and non-small cell lung cancers. Mol Cancer Res *7*, 1466-1476.

Linehan, W. M., Pinto, P. A., Srinivasan, R., Merino, M., Choyke, P., Choyke, L., Coleman, J., Toro, J., Glenn, G., Vocke, C.*, et al.* (2007). Identification of the

genes for kidney cancer: opportunity for disease-specific targeted therapeutics. Clin Cancer Res *13*, 671s-679s.

Liu, Y., and Gray, N. S. (2006). Rational design of inhibitors that bind to inactive kinase conformations. Nat Chem Biol *2*, 358-364.

Lovly, C. M., Heuckmann, J. M., de Stanchina, E., Chen, H., Thomas, R. K., Liang, C., and Pao, W. (2011). Insights into ALK-driven cancers revealed through development of novel ALK tyrosine kinase inhibitors. Cancer Res *71*, 4920-4931.

Lynch, T. J., Bell, D. W., Sordella, R., Gurubhagavatula, S., Okimoto, R. A., Brannigan, B. W., Harris, P. L., Haserlat, S. M., Supko, J. G., Haluska, F. G.*, et al.* (2004). Activating mutations in the epidermal growth factor receptor underlying responsiveness of non-small-cell lung cancer to gefitinib. N Engl J Med *350*, 2129-2139.

MacArthur, M. W., and Thornton, J. M. (1991). Influence of proline residues on protein conformation. J Mol Biol *218*, 397-412.

Mano, H. (2008). Non-solid oncogenes in solid tumors: EML4-ALK fusion genes in lung cancer. Cancer Sci *99*, 2349-2355.

Marx, S. J. (2005). Molecular genetics of multiple endocrine neoplasia types 1 and 2. Nat Rev Cancer *5*, 367-375.

McDermott, U., Iafrate, A. J., Gray, N. S., Shioda, T., Classon, M., Maheswaran, S., Zhou, W., Choi, H. G., Smith, S. L., Dowell, L.*, et al.* (2008). Genomic alterations of anaplastic lymphoma kinase may sensitize tumors to anaplastic lymphoma kinase inhibitors. Cancer Res *68*, 3389-3395.

McWhirter, J. R., Galasso, D. L., and Wang, J. Y. (1993). A coiled-coil oligomerization domain of Bcr is essential for the transforming function of Bcr-Abl oncoproteins. Mol Cell Biol *13*, 7587-7595.

Milkiewicz, K. L., and Ott, G. R. (2010). Inhibitors of anaplastic lymphoma kinase: a patent review. Expert Opin Ther Pat *20*, 1653-1681.

Mok, T. S., Wu, Y. L., Thongprasert, S., Yang, C. H., Chu, D. T., Saijo, N., Sunpaweravong, P., Han, B., Margono, B., Ichinose, Y.*, et al.* (2009). Gefitinib or carboplatin-paclitaxel in pulmonary adenocarcinoma. N Engl J Med *361*, 947-957.

Morris, S. W., Kirstein, M. N., Valentine, M. B., Dittmer, K. G., Shapiro, D. N., Saltman, D. L., and Look, A. T. (1994). Fusion of a kinase gene, ALK, to a nucleolar protein gene, NPM, in non-Hodgkin's lymphoma. Science *263*, 1281-1284.

Mosse, Y. P., Laudenslager, M., Longo, L., Cole, K. A., Wood, A., Attiyeh, E. F., Laquaglia, M. J., Sennett, R., Lynch, J. E., Perri, P.*, et al.* (2008). Identification of

ALK as a major familial neuroblastoma predisposition gene. Nature *455*, 930-935.

Murugan, A. K., and Xing, M. (2011). Anaplastic thyroid cancers harbor novel oncogenic mutations of the ALK gene. Cancer Res *71*, 4403-4411.

Nazarian, R., Shi, H., Wang, Q., Kong, X., Koya, R. C., Lee, H., Chen, Z., Lee, M. K., Attar, N., Sazegar, H.*, et al.* (2010). Melanomas acquire resistance to B-RAF(V600E) inhibition by RTK or N-RAS upregulation. Nature *468*, 973-977.

Nevins, J. R. (2001). The Rb/E2F pathway and cancer. Hum Mol Genet *10*, 699-703.

Noguchi, M. (2010). Stepwise progression of pulmonary adenocarcinoma--clinical and molecular implications. Cancer Metastasis Rev *29*, 15-21.

Normant, E., Paez, G., West, K. A., Lim, A. R., Slocum, K. L., Tunkey, C., McDougall, J., Wylie, A. A., Robison, K., Caliri, K.*, et al.* (2011). The Hsp90 inhibitor IPI-504 rapidly lowers EML4-ALK levels and induces tumor regression in ALK-driven NSCLC models. Oncogene *30*, 2581-2586.

Nowell, P. C., and Hungerford, D. A. (1960). Chromosome studies on normal and leukemic human leukocytes. J Natl Cancer Inst *25*, 85-109.

O'Hare, T., Shakespeare, W. C., Zhu, X., Eide, C. A., Rivera, V. M., Wang, F., Adrian, L. T., Zhou, T., Huang, W. S., Xu, Q.*, et al.* (2009). AP24534, a pan-BCR-ABL inhibitor for chronic myeloid leukemia, potently inhibits the T315I mutant and overcomes mutation-based resistance. Cancer Cell *16*, 401-412.

Paez, J. G., Janne, P. A., Lee, J. C., Tracy, S., Greulich, H., Gabriel, S., Herman, P., Kaye, F. J., Lindeman, N., Boggon, T. J.*, et al.* (2004). EGFR mutations in lung cancer: correlation with clinical response to gefitinib therapy. Science *304*, 1497-1500.

Paez-Ribes, M., Allen, E., Hudock, J., Takeda, T., Okuyama, H., Vinals, F., Inoue, M., Bergers, G., Hanahan, D., and Casanovas, O. (2009). Antiangiogenic therapy elicits malignant progression of tumors to increased local invasion and distant metastasis. Cancer Cell *15*, 220-231.

Palanisamy, N., Ateeq, B., Kalyana-Sundaram, S., Pflueger, D., Ramnarayanan, K., Shankar, S., Han, B., Cao, Q., Cao, X., Suleman, K.*, et al.* (2010). Rearrangements of the RAF kinase pathway in prostate cancer, gastric cancer and melanoma. Nat Med *16*, 793-798.

Palmer, R. H., Vernersson, E., Grabbe, C., and Hallberg, B. (2009). Anaplastic lymphoma kinase: signalling in development and disease. Biochem J *420*, 345-361.

Pao, W., Miller, V., Zakowski, M., Doherty, J., Politi, K., Sarkaria, I., Singh, B., Heelan, R., Rusch, V., Fulton, L.*, et al.* (2004). EGF receptor gene mutations are common in lung cancers from "never smokers" and are associated with sensitivity of tumors to gefitinib and erlotinib. Proc Natl Acad Sci U S A *101*, 13306-13311.

Pao, W., Miller, V. A., Politi, K. A., Riely, G. J., Somwar, R., Zakowski, M. F., Kris, M. G., and Varmus, H. (2005a). Acquired resistance of lung adenocarcinomas to gefitinib or erlotinib is associated with a second mutation in the EGFR kinase domain. PLoS Med *2*, e73.

Pao, W., Wang, T. Y., Riely, G. J., Miller, V. A., Pan, Q., Ladanyi, M., Zakowski, M. F., Heelan, R. T., Kris, M. G., and Varmus, H. E. (2005b). KRAS mutations and primary resistance of lung adenocarcinomas to gefitinib or erlotinib. PLoS Med *2*, e17.

Peifer, M., Fernández-Cuesta, L., and al., e. (under review). Small cell lung cancer: identification of relevant mutated genes in a highly mutated genome by integrative genome analyses.

Peifer, M., Weiss, J., Sos, M. L., Koker, M., Heynck, S., Netzer, C., Fischer, S., Rode, H., Rauh, D., Rahnenfuhrer, J., and Thomas, R. K. (2010). Analysis of compound synergy in high-throughput cellular screens by population-based lifetime modeling. PLoS One *5*, e8919.

Petersen, I. (2011). The morphological and molecular diagnosis of lung cancer. Dtsch Arztebl Int *108*, 525-531.

Piccaluga, P. P., Rondoni, M., Paolini, S., Rosti, G., Martinelli, G., and Baccarani, M. (2007). Imatinib mesylate in the treatment of hematologic malignancies. Expert Opin Biol Ther *7*, 1597-1611.

Pleasance, E. D., Cheetham, R. K., Stephens, P. J., McBride, D. J., Humphray, S. J., Greenman, C. D., Varela, I., Lin, M. L., Ordonez, G. R., Bignell, G. R.*, et al.* (2010). A comprehensive catalogue of somatic mutations from a human cancer genome. Nature *463*, 191-196.

Pollmann, M., Parwaresch, R., Adam-Klages, S., Kruse, M. L., Buck, F., and Heidebrecht, H. J. (2006). Human EML4, a novel member of the EMAP family, is essential for microtubule formation. Exp Cell Res *312*, 3241-3251.

Poulikakos, P. I., Persaud, Y., Janakiraman, M., Kong, X., Ng, C., Moriceau, G., Shi, H., Atefi, M., Titz, B., Gabay, M. T.*, et al.* (2011). RAF inhibitor resistance is mediated by dimerization of aberrantly spliced BRAF(V600E). Nature *480*, 387-390.

Radujkovic, A., Schad, M., Topaly, J., Veldwijk, M. R., Laufs, S., Schultheis, B. S., Jauch, A., Melo, J. V., Fruehauf, S., and Zeller, W. J. (2005). Synergistic activity

of imatinib and 17-AAG in imatinib-resistant CML cells overexpressing BCR-ABL--Inhibition of P-glycoprotein function by 17-AAG. Leukemia *19*, 1198-1206.

Regales, L., Gong, Y., Shen, R., de Stanchina, E., Vivanco, I., Goel, A., Koutcher, J. A., Spassova, M., Ouerfelli, O., Mellinghoff, I. K*., et al.* (2009). Dual targeting of EGFR can overcome a major drug resistance mutation in mouse models of EGFR mutant lung cancer. J Clin Invest *119*, 3000-3010.

Rous, P. (1983). Landmark article (JAMA 1911;56:198). Transmission of a malignant new growth by means of a cell-free filtrate. By Peyton Rous. JAMA *250*, 1445-1449.

Saraste, M., Sibbald, P. R., and Wittinghofer, A. (1990). The P-loop--a common motif in ATP- and GTP-binding proteins. Trends Biochem Sci *15*, 430-434.

Saretzki, G., Petersen, S., Petersen, I., Kolble, K., and von Zglinicki, T. (2002). hTERT gene dosage correlates with telomerase activity in human lung cancer cell lines. Cancer Lett *176*, 81-91.

Sasaki, T., Koivunen, J., Ogino, A., Yanagita, M., Nikiforow, S., Zheng, W., Lathan, C., Marcoux, J. P., Du, J., Okuda, K*., et al.* (2011). A novel ALK secondary mutation and EGFR signaling cause resistance to ALK kinase inhibitors. Cancer Res *71*, 6051-6060.

Sasaki, T., Okuda, K., Zheng, W., Butrynski, J., Capelletti, M., Wang, L., Gray, N. S., Wilner, K., Christensen, J. G., Demetri, G*., et al.* (2010a). The neuroblastoma-associated F1174L ALK mutation causes resistance to an ALK kinase inhibitor in ALK-translocated cancers. Cancer Res *70*, 10038-10043.

Sasaki, T., Rodig, S. J., Chirieac, L. R., and Janne, P. A. (2010b). The biology and treatment of EML4-ALK non-small cell lung cancer. Eur J Cancer *46*, 1773-1780.

Sawai, A., Chandarlapaty, S., Greulich, H., Gonen, M., Ye, Q., Arteaga, C. L., Sellers, W., Rosen, N., and Solit, D. B. (2008). Inhibition of Hsp90 down-regulates mutant epidermal growth factor receptor (EGFR) expression and sensitizes EGFR mutant tumors to paclitaxel. Cancer Res *68*, 589-596.

Schlessinger, J. (2002). Ligand-induced, receptor-mediated dimerization and activation of EGF receptor. Cell *110*, 669-672.

Schlessinger, J., and Lemmon, M. A. (2003). SH2 and PTB domains in tyrosine kinase signaling. Sci STKE *2003*, RE12.

Senger, D. R., Galli, S. J., Dvorak, A. M., Perruzzi, C. A., Harvey, V. S., and Dvorak, H. F. (1983). Tumor cells secrete a vascular permeability factor that promotes accumulation of ascites fluid. Science *219*, 983-985.

Sennino, B., Ishiguro-Oonuma, T., Wei, Y., Naylor, R., Williamson, C., Bhagwandin, V., Tabruyn, S., You, W., Chapman, H., Christensen, J.*, et al.* (2012). Suppression of Tumor Invasion and Metastasis by Concurrent Inhibition of c-Met and VEGF Signaling in Pancreatic Neuroendocrine Tumors. Cancer Discovery.

Sequist, L. V., Waltman, B. A., Dias-Santagata, D., Digumarthy, S., Turke, A. B., Fidias, P., Bergethon, K., Shaw, A. T., Gettinger, S., Cosper, A. K.*, et al.* (2011). Genotypic and histological evolution of lung cancers acquiring resistance to EGFR inhibitors. Sci Transl Med *3*, 75ra26.

Shah, N. P., Kasap, C., Weier, C., Balbas, M., Nicoll, J. M., Bleickardt, E., Nicaise, C., and Sawyers, C. L. (2008). Transient potent BCR-ABL inhibition is sufficient to commit chronic myeloid leukemia cells irreversibly to apoptosis. Cancer Cell *14*, 485-493.

Shah, N. P., Nicoll, J. M., Nagar, B., Gorre, M. E., Paquette, R. L., Kuriyan, J., and Sawyers, C. L. (2002). Multiple BCR-ABL kinase domain mutations confer polyclonal resistance to the tyrosine kinase inhibitor imatinib (STI571) in chronic phase and blast crisis chronic myeloid leukemia. Cancer Cell *2*, 117-125.

Shah, N. P., Tran, C., Lee, F. Y., Chen, P., Norris, D., and Sawyers, C. L. (2004). Overriding imatinib resistance with a novel ABL kinase inhibitor. Science *305*, 399-401.

Sharma, S. V., Bell, D. W., Settleman, J., and Haber, D. A. (2007). Epidermal growth factor receptor mutations in lung cancer. Nat Rev Cancer *7*, 169-181.

Sharma, S. V., Haber, D. A., and Settleman, J. (2010). Cell line-based platforms to evaluate the therapeutic efficacy of candidate anticancer agents. Nat Rev Cancer *10*, 241-253.

Shimizu, T., Tolcher, A. W., Papadopoulos, K. P., Beeram, M., Rasco, D., Smith, L. S., Gunn, S., Smetzer, L., Mays, T. A., Kaiser, B.*, et al.* (2012). The clinical effect of the dual-targeting strategy involving PI3K/AKT/mTOR and RAS/MEK/ERK pathways in patients with advanced cancer. Clin Cancer Res.

Smith, K. M., Yacobi, R., and Van Etten, R. A. (2003). Autoinhibition of Bcr-Abl through its SH3 domain. Mol Cell *12*, 27-37.

Snead, J. L., O'Hare, T., Adrian, L. T., Eide, C. A., Lange, T., Druker, B. J., and Deininger, M. W. (2009). Acute dasatinib exposure commits Bcr-Abl-dependent cells to apoptosis. Blood *114*, 3459-3463.

Soda, M., Choi, Y. L., Enomoto, M., Takada, S., Yamashita, Y., Ishikawa, S., Fujiwara, S., Watanabe, H., Kurashina, K., Hatanaka, H.*, et al.* (2007). Identification of the transforming EML4-ALK fusion gene in non-small-cell lung cancer. Nature *448*, 561-566.

Soda, M., Takada, S., Takeuchi, K., Choi, Y. L., Enomoto, M., Ueno, T., Haruta, H., Hamada, T., Yamashita, Y., Ishikawa, Y.*, et al.* (2008). A mouse model for EML4-ALK-positive lung cancer. Proc Natl Acad Sci U S A *105*, 19893-19897.

Solomon, B., Varella-Garcia, M., and Camidge, D. R. (2009). ALK gene rearrangements: a new therapeutic target in a molecularly defined subset of non-small cell lung cancer. J Thorac Oncol *4*, 1450-1454.

Soria, J. C., Mok, T. S., Cappuzzo, F., and Janne, P. A. (2011). EGFR-mutated oncogene-addicted non-small cell lung cancer: Current trends and future prospects. Cancer Treat Rev.

Sos, M. L., Fischer, S., Ullrich, R., Peifer, M., Heuckmann, J. M., Koker, M., Heynck, S., Stuckrath, I., Weiss, J., Fischer, F.*, et al.* (2009a). Identifying genotype-dependent efficacy of single and combined PI3K- and MAPK-pathway inhibition in cancer. Proc Natl Acad Sci U S A *106*, 18351-18356.

Sos, M. L., Koker, M., Weir, B. A., Heynck, S., Rabinovsky, R., Zander, T., Seeger, J. M., Weiss, J., Fischer, F., Frommolt, P.*, et al.* (2009b). PTEN loss contributes to erlotinib resistance in EGFR-mutant lung cancer by activation of Akt and EGFR. Cancer Res *69*, 3256-3261.

Sporn, M. B., and Todaro, G. J. (1980). Autocrine secretion and malignant transformation of cells. N Engl J Med *303*, 878-880.

Stefanou, D., Batistatou, A., Arkoumani, E., Ntzani, E., and Agnantis, N. J. (2004). Expression of vascular endothelial growth factor (VEGF) and association with microvessel density in small-cell and non-small-cell lung carcinomas. Histol Histopathol *19*, 37-42.

Sudarsanam, S., and Johnson, D. E. (2010). Functional consequences of mTOR inhibition. Curr Opin Drug Discov Devel *13*, 31-40.

Sugawara, E., Togashi, Y., Kuroda, N., Sakata, S., Hatano, S., Asaka, R., Yuasa, T., Yonese, J., Kitagawa, M., Mano, H.*, et al.* (2012). Identification of anaplastic lymphoma kinase fusions in renal cancer: Large-scale immunohistochemical screening by the intercalated antibody-enhanced polymer method. Cancer.

Sun, S., Schiller, J. H., and Gazdar, A. F. (2007). Lung cancer in never smokers--a different disease. Nat Rev Cancer *7*, 778-790.

Sun, Y., Ren, Y., Fang, Z., Li, C., Fang, R., Gao, B., Han, X., Tian, W., Pao, W., Chen, H., and Ji, H. (2010). Lung adenocarcinoma from East Asian never-smokers is a disease largely defined by targetable oncogenic mutant kinases. J Clin Oncol *28*, 4616-4620.

Takeuchi, K., Choi, Y. L., Soda, M., Inamura, K., Togashi, Y., Hatano, S., Enomoto, M., Takada, S., Yamashita, Y., Satoh, Y.*, et al.* (2008). Multiplex reverse

transcription-PCR screening for EML4-ALK fusion transcripts. Clin Cancer Res *14*, 6618-6624.

Takeuchi, K., Choi, Y. L., Togashi, Y., Soda, M., Hatano, S., Inamura, K., Takada, S., Ueno, T., Yamashita, Y., Satoh, Y.*, et al.* (2009). KIF5B-ALK, a novel fusion oncokinase identified by an immunohistochemistry-based diagnostic system for ALK-positive lung cancer. Clin Cancer Res *15*, 3143-3149.

Takeuchi, K., Soda, M., Togashi, Y., Suzuki, R., Sakata, S., Hatano, S., Asaka, R., Hamanaka, W., Ninomiya, H., Uehara, H.*, et al.* (2012). RET, ROS1 and ALK fusions in lung cancer. Nat Med *18*, 378-381.

Takezawa, K., Okamoto, I., Nishio, K., Janne, P. A., and Nakagawa, K. (2011). Role of ERK-BIM and STAT3-survivin signaling pathways in ALK inhibitor-induced apoptosis in EML4-ALK-positive lung cancer. Clin Cancer Res *17*, 2140-2148.

TCGA (2008). Comprehensive genomic characterization defines human glioblastoma genes and core pathways. Nature *455*, 1061-1068.

Thomas, M., Huang, W. S., Wen, D., Zhu, X., Wang, Y., Metcalf, C. A., Liu, S., Chen, I., Romero, J., Zou, D.*, et al.* (2011). Discovery of 5-(arenethynyl) hetero-monocyclic derivatives as potent inhibitors of BCR-ABL including the T315I gatekeeper mutant. Bioorg Med Chem Lett *21*, 3743-3748.

Thomas, R. K., Nickerson, E., Simons, J. F., Janne, P. A., Tengs, T., Yuza, Y., Garraway, L. A., LaFramboise, T., Lee, J. C., Shah, K.*, et al.* (2006). Sensitive mutation detection in heterogeneous cancer specimens by massively parallel picoliter reactor sequencing. Nat Med *12*, 852-855.

Thompson, D., Duedal, S., Kirner, J., McGuffog, L., Last, J., Reiman, A., Byrd, P., Taylor, M., and Easton, D. F. (2005). Cancer risks and mortality in heterozygous ATM mutation carriers. J Natl Cancer Inst *97*, 813-822.

Timofeevski, S. L., McTigue, M. A., Ryan, K., Cui, J., Zou, H. Y., Zhu, J. X., Chau, F., Alton, G., Karlicek, S., Christensen, J. G., and Murray, B. W. (2009). Enzymatic characterization of c-Met receptor tyrosine kinase oncogenic mutants and kinetic studies with aminopyridine and triazolopyrazine inhibitors. Biochemistry *48*, 5339-5349.

Todaro, G. J., and Green, H. (1963). Quantitative studies of the growth of mouse embryo cells in culture and their development into established lines. J Cell Biol *17*, 299-313.

Togashi, Y., Soda, M., Sakata, S., Sugawara, E., Hatano, S., Asaka, R., Nakajima, T., Mano, H., and Takeuchi, K. (2012). KLC1-ALK: a novel fusion in lung cancer identified using a formalin-fixed paraffin-embedded tissue only. PLoS One *7*, e31323.

Travis, W. D., and WHO (2004). Pathology and genetics of tumours of the lung, pleura, thymus and heart, (Lyon: IARC Press).

Turke, A. B., Zejnullahu, K., Wu, Y. L., Song, Y., Dias-Santagata, D., Lifshits, E., Toschi, L., Rogers, A., Mok, T., Sequist, L.*, et al.* (2010). Preexistence and clonal selection of MET amplification in EGFR mutant NSCLC. Cancer Cell *17*, 77-88.

Varela, I., Tarpey, P., Raine, K., Huang, D., Ong, C. K., Stephens, P., Davies, H., Jones, D., Lin, M. L., Teague, J.*, et al.* (2011). Exome sequencing identifies frequent mutation of the SWI/SNF complex gene PBRM1 in renal carcinoma. Nature *469*, 539-542.

Varmus, H. E. (1990). Nobel lecture. Retroviruses and oncogenes. I. Biosci Rep *10*, 413-430.

Vasen, H. F., Stormorken, A., Menko, F. H., Nagengast, F. M., Kleibeuker, J. H., Griffioen, G., Taal, B. G., Moller, P., and Wijnen, J. T. (2001). MSH2 mutation carriers are at higher risk of cancer than MLH1 mutation carriers: a study of hereditary nonpolyposis colorectal cancer families. J Clin Oncol *19*, 4074-4080.

Vecchiarelli-Federico, L. M., Cervi, D., Haeri, M., Li, Y., Nagy, A., and Ben-David, Y. (2010). Vascular endothelial growth factor--a positive and negative regulator of tumor growth. Cancer Res *70*, 863-867.

Verhoef, L. G., Lindsten, K., Masucci, M. G., and Dantuma, N. P. (2002). Aggregate formation inhibits proteasomal degradation of polyglutamine proteins. Hum Mol Genet *11*, 2689-2700.

Wakeling, A. E., Guy, S. P., Woodburn, J. R., Ashton, S. E., Curry, B. J., Barker, A. J., and Gibson, K. H. (2002). ZD1839 (Iressa): an orally active inhibitor of epidermal growth factor signaling with potential for cancer therapy. Cancer Res *62*, 5749-5754.

Weinberg, R. A. (2007). The biology of cancer, (New York: Garland Science).

Weiss, J., Sos, M. L., Seidel, D., Peifer, M., Zander, T., Heuckmann, J. M., Ullrich, R. T., Menon, R., Maier, S., Soltermann, A.*, et al.* (2010). Frequent and focal FGFR1 amplification associates with therapeutically tractable FGFR1 dependency in squamous cell lung cancer. Sci Transl Med *2*, 62ra93.

Xu, C., and Min, J. (2011). Structure and function of WD40 domain proteins. Protein Cell *2*, 202-214.

Yan, H., Parsons, D. W., Jin, G., McLendon, R., Rasheed, B. A., Yuan, W., Kos, I., Batinic-Haberle, I., Jones, S., Riggins, G. J.*, et al.* (2009). IDH1 and IDH2 mutations in gliomas. N Engl J Med *360*, 765-773.

Yeang, C. H., McCormick, F., and Levine, A. (2008). Combinatorial patterns of somatic gene mutations in cancer. FASEB J *22*, 2605-2622.

Yuan, A., Yu, C. J., Chen, W. J., Lin, F. Y., Kuo, S. H., Luh, K. T., and Yang, P. C. (2000). Correlation of total VEGF mRNA and protein expression with histologic type, tumor angiogenesis, patient survival and timing of relapse in non-small-cell lung cancer. Int J Cancer *89*, 475-483.

Yuan, T. L., and Cantley, L. C. (2008). PI3K pathway alterations in cancer: variations on a theme. Oncogene *27*, 5497-5510.

Yun, C. H., Mengwasser, K. E., Toms, A. V., Woo, M. S., Greulich, H., Wong, K. K., Meyerson, M., and Eck, M. J. (2008). The T790M mutation in EGFR kinase causes drug resistance by increasing the affinity for ATP. Proc Natl Acad Sci U S A *105*, 2070-2075.

Yuza, Y., Glatt, K. A., Jiang, J., Greulich, H., Minami, Y., Woo, M. S., Shimamura, T., Shapiro, G., Lee, J. C., Ji, H.*, et al.* (2007). Allele-dependent variation in the relative cellular potency of distinct EGFR inhibitors. Cancer Biol Ther *6*, 661-667.

Zerbino, D. R., and Birney, E. (2008). Velvet: algorithms for de novo short read assembly using de Bruijn graphs. Genome Res *18*, 821-829.

Zerbino, D. R., and Schulz, M. (unplublished data).

Zhang, A., Zheng, C., Lindvall, C., Hou, M., Ekedahl, J., Lewensohn, R., Yan, Z., Yang, X., Henriksson, M., Blennow, E.*, et al.* (2000). Frequent amplification of the telomerase reverse transcriptase gene in human tumors. Cancer Res *60*, 6230-6235.

Zhang, S., Wang, F., Keats, J., Zhu, X., Ning, Y., Wardwell, S. D., Moran, L., Mohemmad, Q. K., Anjum, R., Wang, Y.*, et al.* (2011). Crizotinib-resistant mutants of EML4-ALK identified through an accelerated mutagenesis screen. Chem Biol Drug Des *78*, 999-1005.

Zhou, W., Ercan, D., Chen, L., Yun, C. H., Li, D., Capelletti, M., Cortot, A. B., Chirieac, L., Iacob, R. E., Padera, R.*, et al.* (2009). Novel mutant-selective EGFR kinase inhibitors against EGFR T790M. Nature *462*, 1070-1074.

Internet sources

FDA news release, August 26 2011;
http://www.fda.gov/NewsEvents/Newsroom/PressAnnouncements/ucm269856.htm;
U.S. Food and Drug Administration; May 2012

http://globocan.iarc.fr/; Globocan 2008; May 2012

http://www.cancer.gov/cancertopics/types/lung; National Cancer Institute; May 2012

http://www.cancerstaging.org/; American Joint Committee in Cancer; May 2012

http://www.dkfz.de/de/krebsatlas/gesamt/mort_2.html; Deutsches
Krebsforschungszentrum; May 2012

http://www.dkfz.de/de/krebsatlas/gesamt/mort_6.html; Deutsches
Krebsforschungszentrum; May 2012

http://www.who.int/tobacco/research/cancer/en/; World Health Organization; May 2012

IARC TP53 database; http://www-p53.iarc.fr/; May 2012

Simple Modular Architecture Research Tool; http://smart.embl-heidelberg.de/; May 2012

www.cancer.org; American Cancer Society; May 2012

9 Acknowledgment

First I would like to thank Roman Thomas for giving me the opportunity to conduct my dissertation in his laboratory at the Max-Planck-Institute for neurological research in Cologne. Furthermore, I would like to thank him for introducing me into the field of cancer research and the inspiration for future endeavors.

I would also like to thank Prof. Ralf Küppers from the University Duisburg-Essen for being my examiner and for his help during the compilation of this work.

In addition, I would like to thank Lynnette Fernandez-Cuesta for her help regarding the SOS1-ADCY3 project, especially for performing the RNA-seq analysis and taking care of the FISH analysis.

I would also like to thank Martin Sos, Hyatt Balke-Want, Florian Malchers, Danila Seidel, Martin Peifer, Steffi Heynck, Thomas Zander, Jakob Schöttle and all the other members of the Thomas laboratory for scientific help, emotional support as well as stimulating discussions regarding life sciences and private life.
Furthermore, I thank Daniel Rauh, Christian Grütter, Zhizhou Fang and Roopika Menon for performing structural modeling, lectures on kinase activation and for performing the FISH analyses.

Last but not least, I would like to thank Laura Oberbusch, my family and my friends for their patience, support and understanding.

I would like to thank all people who made this work possible!

10 Publications

Heuckmann JM, Balke-Want H, Malchers F, Peifer M, Sos ML, Koker M, Meder L, Lovly CM, Heukamp LC, William Pao W, Thomas RK. Differential protein stability and ALK inhibitor sensitivity of EML4-ALK fusion variants. Clin Cancer Res. under review

Peifer M, Fernández-Cuesta L, Seidel D, Leenders F, Sun R, Sos ML, Zander T, Menon R, Koker M, Dahmen I, Müller C, Altmüller J, Plenker D, Baessmann I, Becker C, de Wilde D, Vandesompele J, Böhm D, Ansén S, Gabler F, Wilkening I, **Heuckmann JM**, et al. Small cell lung cancer: identification of relevant mutated genes in a highly mutated genome by integrative genome analyses. Nature Genetics. under review

Heuckmann JM, Hölzel M, Sos ML, Heynck S, Balke-Want H, Koker M, Peifer M, Weiss J, Lovly CM, Grütter C, Rauh D, Pao W, Thomas RK. ALK mutations conferring differential resistance to structurally diverse ALK inhibitors. Clin Cancer Res. 2011 Dec 1;17(23):7394-401. Epub 2011 Sep 26. PubMed PMID: 21948233.

Lovly CM, **Heuckmann JM**, de Stanchina E, Chen H, Thomas RK, Liang C, Pao W. Insights into ALK-driven cancers revealed through development of novel ALK tyrosine kinase inhibitors. Cancer Res. 2011 Jul 15;71(14):4920-31. Epub 2011 May 25. PubMed PMID: 21613408; PubMed Central PMCID: PMC3138877.

Hammerman PS, Sos ML, Ramos AH, Xu C, Dutt A, Zhou W, Brace LE, Woods BA, Lin W, Zhang J, Deng X, Lim SM, Heynck S, Peifer M, Simard JR, Lawrence MS, Onofrio RC, Salvesen HB, Seidel D, Zander T, **Heuckmann JM**, et al. Mutations in the DDR2 kinase gene identify a novel therapeutic target in squamous cell lung cancer. Cancer Discov. 2011 Apr 3;1(1):78-89. PubMed PMID: 22328973; PubMed Central PMCID: PMC3274752.

Weiss J, Sos ML, Seidel D, Peifer M, Zander T, **Heuckmann JM**, et al. Frequent and focal FGFR1 amplification associates with therapeutically tractable FGFR1 dependency in squamous cell lung cancer. Sci Transl Med. 2010 Dec 15;2(62):62ra93. Erratum in: Sci Transl Med. 2011 Jan 19;3(66):66er2. PubMed PMID: 21160078.

Sos ML, Rode HB, Heynck S, Peifer M, Fischer F, Klüter S, Pawar VG, Reuter C, **Heuckmann JM**, Weiss J, Ruddigkeit L, Rabiller M, Koker M, Simard JR, Getlik M, Yuza Y, Chen TH, Greulich H, Thomas RK, Rauh D. Chemogenomic profiling provides insights into the limited activity of irreversible EGFR Inhibitors in tumor cells expressing the T790M EGFR resistance mutation. Cancer Res. 2010 Feb 1;70(3):868-74. Epub 2010 Jan 26. PubMed PMID: 20103621.

Sos ML, Fischer S, Ullrich R, Peifer M, **Heuckmann JM**, Koker M, Heynck S, Stückrath I, Weiss J, Fischer F, Michel K, Goel A, Regales L, Politi KA, Perera S, Getlik M, Heukamp LC, Ansén S, Zander T, Beroukhim R, Kashkar H, Shokat KM, Sellers WR, Rauh D, Orr C, Hoeflich KP, Friedman L, Wong KK, Pao W, Thomas RK. Identifying genotype-dependent efficacy of single and combined PI3K- and MAPK-pathway inhibition in cancer. Proc Natl Acad Sci U S A. 2009 Oct 27;106(43):18351-6. Epub 2009 Oct 5. PubMed PMID: 19805051; PubMed Central PMCID: PMC2757399.

Muñoz IM, Hain K, Déclais AC, Gardiner M, Toh GW, Sanchez-Pulido L, **Heuckmann JM**, Toth R, Macartney T, Eppink B, Kanaar R, Ponting CP, Lilley DM, Rouse J. Coordination of structure-specific nucleases by human SLX4/BTBD12 is required for DNA repair. Mol Cell. 2009 Jul 10;35(1):116-27. PubMed PMID: 19595721.

Klehr M, Koehl U, Mühlenhoff M, Tawadros S, Fischer T, Schomäcker K, **Heuckmann JM**, Bochennek K, Jensen M. The novel chimeric anti-NCAM (neural cell adhesion molecule) antibody ch.MK1 displays antitumor activity in SCID mice but does not activate complement-dependent cytolysis (CDC). J Immunother. 2009 Jun;32(5):442-51. PubMed PMID: 19609236.

Curriculum Vitae

Der Lebenslauf ist in der Online-Version aus Gründen des Datenschutzes nicht enthalten

Erklärung:

Hiermit erkläre ich, gem. § 6 Abs. 2, f der Promotionsordnung der Math.-Nat. Fakultäten zur Erlangung der Dr. rer. nat., dass ich das Arbeitsgebiet, dem das Thema „Different EML4-ALK fusion variants and novel ALK resistance mutations induce differential sensitivity to ALK inhibitors“ zuzuordnen ist, in Forschung und Lehre vertrete und den Antrag von Johannes Heuckmann befürworte.

Essen, den _____ _____

(Prof. Ralf Küppers)

Erklärung:

Hiermit erkläre ich, gem. § 7 Abs. 2, c und e der Promotionsordnung der Math.-Nat. Fakultäten zur Erlangung des Dr. rer. nat., dass ich die vorliegende Dissertation selbständig verfasst und mich keiner anderen als der angegebenen Hilfsmittel bedient habe und alle wörtlich oder inhaltlich übernommenen Stellen als solche gekennzeichnet habe.

Essen, den _____ _____

(Johannes Heuckmann)

Erklärung:

Hiermit erkläre ich, gem. § 7 Abs. 2, d und f der Promotionsordnung der Math.-Nat. Fakultäten zur Erlangung des Dr. rer. nat., dass ich keine anderen Promotionen bzw. Promotionsversuche in der Vergangenheit durchgeführt habe, dass diese Arbeit von keiner anderen Fakultät abgelehnt worden ist, und dass ich die Dissertation nur in diesem Verfahren einreiche.

Essen, den _____ _____

(Johannes Heuckmann)